The middle Miocene Leitha Mountains carbonate platform (Vienna Basin, Austria) – a palaeoenvironmental archive at the margin of the tropical reef belt

by

Bak. rer. nat. Mag. rer. nat. Thomas Wiedl

A thesis submitted to the Institute of Earth Sciences
Karl-Franzens University of Graz

In partial fulfilment of the requirements for the degree of
Doctor of Natural Sciences (Dr. rer. nat.)

Graz, October 2015

Supervisor

O. Univ.-Prof. Dr. phil. Werner Piller
University of Graz
Institute of Earth Sciences
Heinrichstraße 26
8010 Graz
Austria

Co-supervisor

Priv. Doz. Mag. Dr. Mathias Harzhauser
Head of Department
Geological-Paleontological Department
Natural History Museum Vienna
Burgring 7
1010 Wien
Austria

Contents

Preface

The present PhD-thesis deals with studies on middle to upper Badenian (Langhian to Serravallian) deposits of a coralline algal dominated carbonate platform in the southern Vienna Basin. The scientific objectives of the studies are focussed on major topics as follows:

- The identification of carbonate facies types represented on the Leitha Platform and interpretations of palaeoenvironmental and palaeoclimatic conditions based on various organism groups (e.g., corals, coralline algae, molluscs, echinoids, foraminifers).
- A review of spatial distribution of the different carbonate facies on the platform and the attempt to use this information to reconstruct sedimentary regimes on various sites on the platform.
- The stratigraphic distribution of the various facies and conclusions about the temporal evolution and sedimentation processes.
- Possible relations between tectonics, relative sea-level changes, changing palaeooceanographic settings and shifts in depositional regimes on the platform.
- Insights in the main palaeoenvironmental factors and their role in the modulation of the ecospace on the carbonate platform.

The present thesis summarizes the results of the project and is divided into five chapters:

Chapter I provides a brief introduction to the Leitha Platform, its position in the Vienna Basin and its tectonic and geological setting.
Chapters 2-4 consist of three scientific articles which are already published in peer-reviewed international journals:
Chapter II: Wiedl, T., Harzhauser, M., Piller, W.E., 2012. Facies and synsedimentary tectonics on a Badenian carbonate platform in the southern Vienna Basin (Austria, Central Paratethys). Facies 58, 523–548.
Chapter III: Wiedl, T., Harzhauser, M., Kroh, A., Ćorić, S., Piller, W.E., 2013. Ecospace variability along a carbonate platform at the northern boundary of the

Miocene reef belt (Upper Langhian, Austria) Palaeogeography, Palaeoclimatology, Palaeoecology 370:232–246.

Chapter IV: Wiedl, T., Harzhauser, M., Kroh, A., Ćorić, S., Piller, W.E., 2014. From biologically to hydrodynamically controlled carbonate production by tectonically induced palaeogeographic rearrangement (Middle Miocene, Pannonian Basin). Facies 60:865-881.

The final **chapter V** presents the summary and conclusions of this project.

Acknowledgements

At this point I would like to express my sincere thanks to a number of people that have supported the present thesis. I am grateful to my supervisors Werner E. Piller and Mathias Harzhauser (NHM) for their guidance with discussions, constructive comments, critical reviews and field excursions. I want to thank Dr. Andreas Kroh and Dr. Stjepan Ćorić who contributed data in ecology and stratigraphy to the present work. Special thanks for the access to the active limestone quarries go to the raw material- and quarry manager Dipl.-Ing. Ralf Baehr-Mörsen of the Lafarge-Perlmooser AG and to Dr. Peter Hoffmann-Ostenhof, Dipl. Ing. Peter Karlich and Ing. Manfred Lang of the Mühlendorfer Kreidefabrik Margit Hoffmann-Ostenhof KG. Many thanks go to Dr. Markus Reuter (University of Graz), Dr. Ulrike Exner (University of Vienna) and Dr. Harald Fritz (University of Graz) for constructive discussions. For determination of bivalve remains I would like to thank Dr. Oleg Mandic (Natural History Museum Vienna) and for determination of foraminifers Dr. Patrick Grunert (University of Graz). Special thanks go to Gerhard Wanzenböck (Bad Vöslau) for insights in his impressive collection of fossils and precise information on their provenience as well as to Hans Schwengersbauer (Mannersdorf museum of local history) for reports of decades of mining activity. Finally, I want to thank Dr. Steven J. Weiss (University of Graz) for improving the English of my manuscripts.

Chapter I

Introduction to the study area

1.1 The Leitha platform in the southern Vienna Basin

Carbonate platforms are mirrors of paleoenvironmental changes concerning climate, temperature, nutrient availability and water energy (Wright and Burchette 1998). Contrary to open oceanic areas, the precipitation of carbonates within epicontinental basins is much more influenced by regional factors, such as relative sea-level, weathering rates and fluvial runoff (Pomar et al. 2004). An example for such a shallow epicontinental sea was the Paratethys Sea, which was recognised as a paleogeographic entity already by Laskarev (1924) (Fig. 1.1). It was formed during the Late Eocene and Early Oligocene due to the rising archipelago including the Alps, Dinarids, Hellenids, Pontids, and the Anatolian Massif, which acted as geographic barriers (Rögl 1998). Its paleogeographic and geotectonic evolution is well studied (Rögl and Steininger 1983; Rögl 1998, 1999; Popov et al. 2004) and the stratigraphic correlation with the international stages was strongly enhanced during the last years (Piller et al. 2007; Lirer et al. 2009, de Leeuw et al. 2010). One of the best studied basins within the former Paratethys realm is the Vienna Basin. Throughout the middle Miocene, it was structured by several

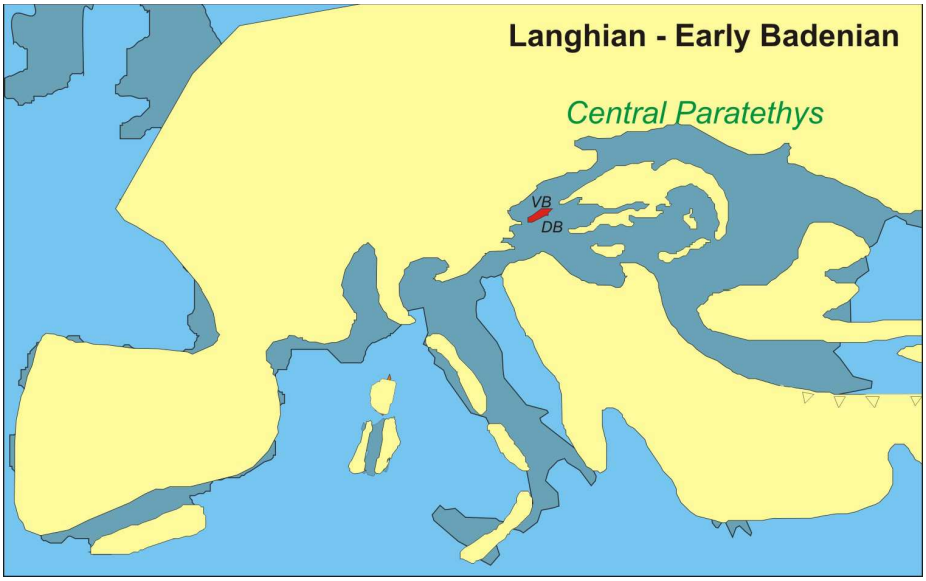

Fig. 1.1 Palaeogeographic situation during the Langhian (early Badenian/Tarkhanian) with positions of the Vienna Basin (VB) and Danube Basin (DB) within the Central Paratethyan Sea (after Rögl 1998). The Leitha Platform is highlighted in red.

topographic highs that formed islands, shoals and small platforms with extensive carbonate production (e.g., Dullo 1983; Riegl and Piller 2000; Schmid et al. 2001; Harzhauser and Piller 2010; Wiedl et al. 2013).

One of these structures is represented by the Leitha Mountains in the southern part of the Vienna Basin (Fig. 1.2). This small platform was studied since the 19th century due to the economic importance of the so-called Leitha Limestone (sensu Keferstein 1828) as building stone (e.g. Čžjžek 1852, Karrer and Fuchs 1868, Reuss 1871). This chain of hills spans 35 km from southwest to northeast with a maximum width of 17 km. During the middle Miocene, however, the structure was significantly wider as suggested by 3-D seismic surveys, which document subsided blocks along the NW side extending several kilometres into the Vienna Basin (Strauss et al. 2006). Then, the carbonate platform was a shallow subtidal ramp sloping into the basin (Piller and Vavra 1991, Piller et al. 1996) with a pre-Cenozoic basement of predominantly Central Alpine Crystalline (Tollmann 1964) and Central Alpine Permian-Mesozoic units (Kröll and Wessely 1993).

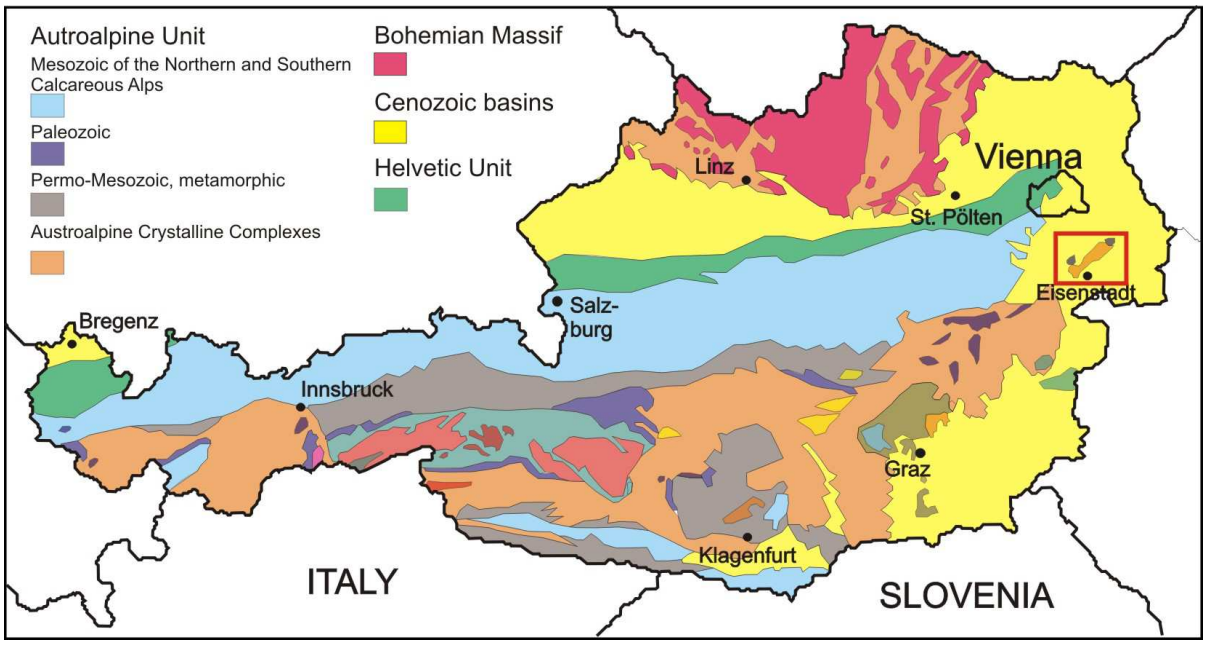

Fig. 1.2 Geological map of Austria after Egger et al. (1999). The Leitha Platform (highlighted by a rectangle) is located in the SE of Vienna.

The main constituents of the Leitha Limestone (Fig. 1.3) are coralline red algae, whereas corals formed only small carpets in relatively low-energy environments (Riegl and Piller 2000, Wiedl et al. 2012, 2013). These red algal limestones along with marls and clays are widespread in the entire Central Paratethys during the

middle Miocene Badenian stage (Papp et al. 1978; Piller et al. 1991; Studencki 1988).

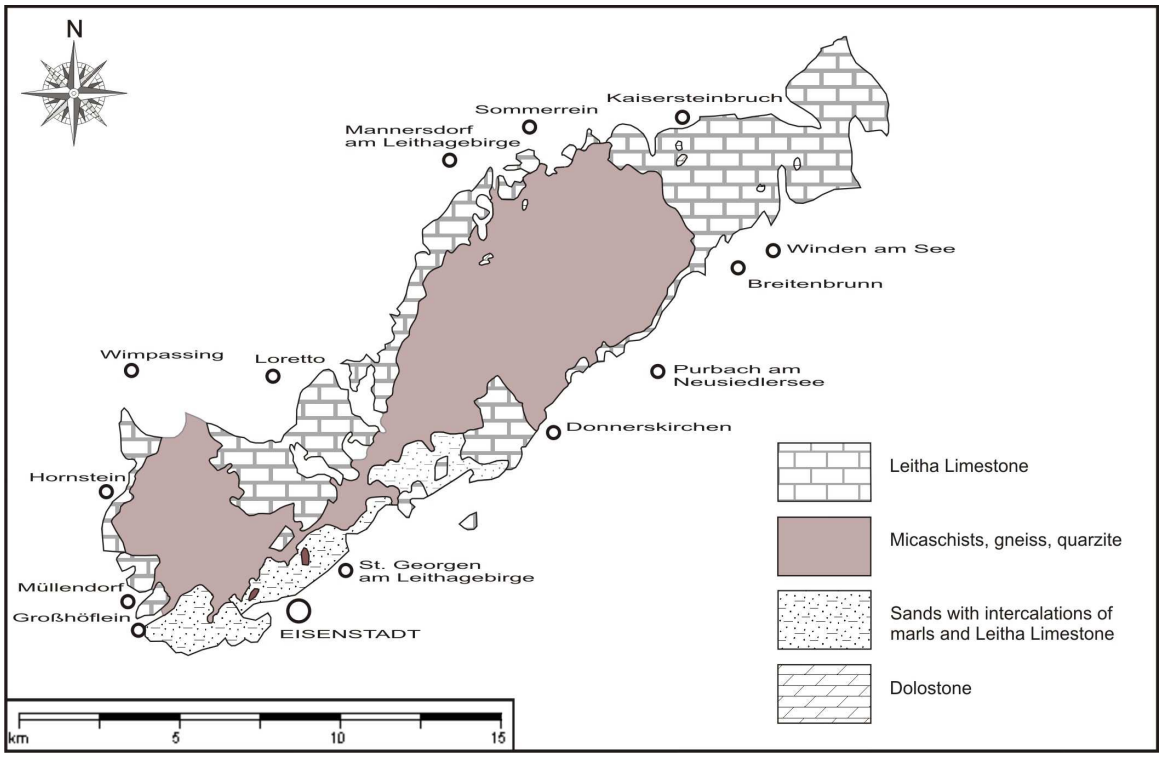

Fig. 1.3 Geological map illustrating the distribution of the Leitha Limestone on the Leitha Mountains (after Fuchs and Grill 1984).

A key section for limestones of the regional Central Paratethyan Badenian stage is the Fenk quarry NNW of Grosshöflein (Burgenland province, N 47°50'42.65", E16° 28'36.04"), defined as type locality for the Leitha Limestone (Steininger and Papp 1978). It represents a 20-m-thick sequence of frame-building coral carpets and non-framebuilding biostromal coral communities (Riegl and Piller 2000). The macro- and microfacies of the Leitha Limestone was discussed in several publications (Dullo 1983; Tollmann 1985; Piller and Vavra 1991; Piller et al. 1996 and Rohatsch 1996; Wiedl et al. 2012, 2013).

1.2 Tectonic and geological setting of the study area

The evolution of the Vienna Basin started with the development of a complex pull-apart basin along the junction of the Eastern Alps and the Western Carpathians (Royden 1985). The basin evolution shows a complex interplay of compression, strike-slip movements and extension, related to compression and lateral extrusion

within the Eastern Alps (Ratschbacher et al. 1991; Decker and Peresson 1996). Subsidence rates often changed and show intervals of increased rates especially during the middle Badenian (Lankreijer et al. 1995, Wagreich and Schmid 2002) with highest subsidence rates observed in the early Badenian (~ 14.5 – 14.2 Ma) with up to 1000 m/Ma in the southern part and around 700 m/Ma in the central part of the Vienna Basin (Hölzel et al. 2008). During the Badenian the Leitha Mountains formed a topographic high or island giving rise to a carbonate platform (Tollmann 1955; Dullo 1983, Riegl and Piller 2000; Schmid et al. 2001; Strauss et al. 2006; Harzhauser and Piller 2010). The basement of the Leitha Mountains is characterized by East Alpine units covered by Badenian and Sarmatian limestones (Herrmann et al. 1993).

1.3 Stratigraphy

The Badenian stage (which corresponds with the Langhian and the lower part of the Serravallian) and other regional chronostratigraphic stages of the Central Paratethyan Miocene (Fig. 1.3) were defined as the geodynamically controlled paleogeographic and biogeographic differentiation of the Eurasian ecosystems and landscapes which caused major difficulties in correlations with international chronostratigraphic stages (see Piller et al. 2007 for discussion). The base of the Badenian is equivalent or close to the base of the Langhian and was defined with the first occurrence of *Praeorbulina* (Papp and Cicha 1978). A correlation of the Badenian sediments to the global sea level cycles TB 2.3–2.5 of Haq et al. (1988) was proposed by Kreutzer (1986), Weissenbäck (1996) and Strauss et al. (2006).
An internal subdivision of the Badenian stage was proposed by Grill (1941, 1943) based on significant changes in the foraminifers assemblages in drillings in the Vienna Basin. Later, this subdivision was applied for large parts of the Paratethys (Papp and Turnovsky 1953; Papp 1963; Turnovsky 1963; Papp et al. 1973, 1978; Cicha 1998; Kováč et al 2004; Rögl et al. 2008). Hence, the lower Badenian comprises the “Lower and Upper Lagenidae Zones”, the middle Badenian corresponds to the “*Spiroplectammina* Zone” (also termed zone of agglutinated foraminifera) and the upper Badenian is represented by the “*Bulimina*/*Bolivina* Zone” (also termed *Bulimina*-*Rotalia* Zone) (Grill 1941; Piller et al. 2007; Rögl et al. 2008; Hohenegger et al. 2009). In fact, this biozonation reflects only ecostratigraphic

sequences (Piller et al. 1991) and the proposed evolutionary lineages (Papp and Turnowsky 1953) are rather successions of ecotypes (Haunold 1995). The proposed internal subdivision of the Badenian stage was supported by seismic studies in the northern (Kovác et al. 2004) and southern Vienna Basin (Strauss et al. 2006). Close to the Leitha Mountains a SW-NE trending seismic section from a survey in Moosbrunn shows that the basin sequences can be correlated to surface outcrops and wells in the area of Stotzing and Mannersdorf (Strauss et al. 2006). A topographic high in the basin (Mannersdorf Horst) offered similar conditions as both flanks of the Leitha Mountains with corallinacean limestones and coral carpets did (Strauss et al. 2006).

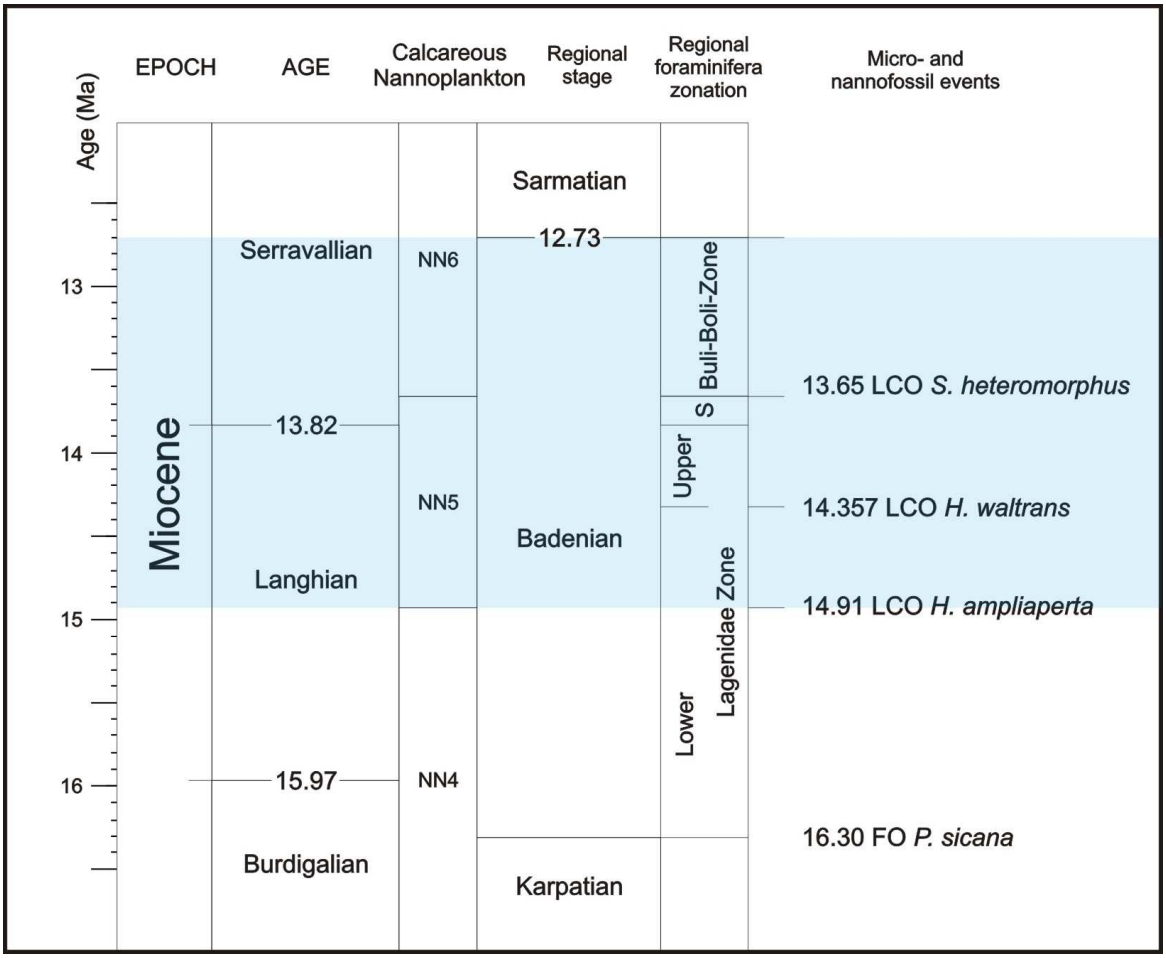

Fig. 1.4 Stratigraphic table modified after Hohenegger and Wagreich (2012) including Badenian geochronology and biozonations of calcareous nannoplankton and Central Paratethyan foraminifera zonations (S: *Spiroplectammina* Zone, Buli-Boli: *Bulimina–Bolivina* Zone, FO: First Occurrence, LCO: Last Common Occurrence). The studied sections are located within nannoplankton zones NN5 and NN6 (highlighted in blue).

1.4 References

Cicha I, Rögl F, Rupp C, Ctyroká J (1998) Oligocene–Miocene foraminifera of the Central Paratethys. Abhandlungen der Senckenbergischen Naturforschenden Gesellschaft 549:1–325

Čžjžek J (1852) Geologische Verhandlung der Umgebung von Hamburg, des Leithagebirges und der Ruster Berge. Jahrb Geol R A 3:35–55

Decker K, Peresson H (1996) Tertiary kinematics in the Alpine-Carpathian-Pannonian system: links between thrusting, transform faulting and crustal extension. In: Wessely G, Liebl W (eds) Oil and gas in Alpidic thrusts and basins of Central and Eastern Europe. Eur Assoc Geosci Eng Spec Publ 5:69–77

De Leeuw A, Mandic O, Vranjković A, Pavelić D, Harzhauser H, Krijgsman W, Kuiper KF (2010) Chronology and integrated stratigraphy of the Miocene Sinj Basin (Dinaride Lake System, Croatia), Palaeogeogr Palaeocl Palaeoec 292, pp 155–167

Dullo WC (1983) Diagenesis of fossils of the Miocene Leitha Limestone of the Paratethys, Austria: An Example for faunal modifications due to changing diagenetic environments. Facies 8:1–112

Egger H, Krenmayr HG, Mandl GW, Matura A, Nowotny A, Pascher G, Pestal G, Pistotnik J, Rochenschaub M, Schnabel W (1999) Geologische Übersichtskarte der Republik Österreich 1: 1500000. Geol. Bundesanst., Wien.

Fuchs W, Grill R (1984) Geologische Karte von Wien und Umgebung 1:200.000. Geol. B.-A., 1 Karte, 2 Tafeln, Wien.

Grill R (1941) Stratigraphische Untersuchungen mit Hilfe von Mikrofaunen im Wiener Becken und den benachbarten Molasseanteilen. Oel und Kohle 31:595–602

Grill R (1943) Über mikropaläontologische Gliederungsmöglichkeiten im Miozän des Wiener Beckens. Mitt Reichsanst Bodenforsch 6:33–44

Haq BU, Hardenbol J, Vail PV (1988) Mesozoic and Cenozoic chronostratigraphy and cycles of sea-level change. In: Wilgus CK, Hastings BS, Kendall CGSC, Posamentier HW, Ross CA, Van Wagoner JC (eds), Sea-level changes: an integrated approach. SEPM Spec Pub 42:71–108

Harzhauser M, Piller WE (2010) Molluscs as a major part of subtropical shallow-water carbonate production - an example from a Middle Miocene oolite shoal (Upper Serravallian, Austria). Sp Publ Int 42:185–200

Haunold TG (1995) Zur Taxonomie, Systematik und stratigraphischen Bedeutung uvigerinider Foraminiferen im Neogen des Wiener Beckens und benachbarter Gebiete – 40 Jahre nach Papp & Turnovsky (1953). Jb Geol B A 138(1):67-87

Herrmann P, Pascher GA, Pistotnik J (1993) Geologische Karte der Republik Österreich 1.50.000, Blatt 78 Rust. Geol B A, Wien

Hohenegger J, Ćorić S, Khatun M, Pervesler P, Rögl F, Rupp C, Selge A, Uchmann A, Wagreich M (2009) Cyclostratigraphic dating in the Lower Badenian (Middle Miocene) of the Vienna Basin (Austria): the Baden-Sooss core. Int J Earth Sci 98:915–930.

Hohenegger J, Wagreich M (2012) Time calibration of sedimentary sections based on isolation cycles using combined cross-correlation: dating the gone Badenian stratotype (Middle Miocene, Paratethys, Vienna Basin, Austria) as an example. Int J Earth Sci (Geol Rundsch) 101:339–349

Hölzel M, Wagreich M, Faber R, Strauss P (2008) Regional Subsidence analysis in the Vienna basin (Austria) - Austrian Journal of Earth Sciences 101:88–98

Karrer F, Fuchs T (1868): Geologische Studien in den Tertiärbildungen des Wiener Beckens. Jahrb KK Geol RA 18(2):269–286

Keferstein C (1828): Beobachtungen und Ansichten über die geognostischen Verhältnisse der nördlichen Kalk-Alpenkette in Österreich-Bayern. – Teutschland geognostisch-geologisch dargestellt 5(3):1–425

Kováč M, Barath I, Harzhauser M, Hlavaty I, Hudackova, N (2004) Miocene depositional systems and sequence stratigraphy of theVienna Basin. Cour Forsch-Inst Senckenberg 246:187–212

Kreutzer N (1986) Die Ablagerungssequenzen der miozänen Badener Serie im Feld Matzen und im zentralen Wiener Becken. Erdöl-Erdgas-Kohle 102:492–503

Kröll AW, Wessely G (1993) Strukturkarte Basis der tertiären Beckenfüllung. Geologische Themenkarte der Republik Österreich. Wiener Becken und angrenzende Gebiete 1: 200.000. Geol Surv Austria, Vienna

Lankreijer A, Kovac M, Cloetingh S, Pitonak P, Hloska M, Biermann C (1995) Quantitative subsidence analysis and forward modelling of the Vienna and Danube basins: thin-skinned versus thick-skinned extension. Tectonophysics 252:433-451

Laskarev VN (1924) Sur les equivalentes du Sarmatien supérieur en Serbie. Zborník Cvijic, pp 73–85

Lirer F, Harzhauser M, Pelosi N, Piller WE, Schmid HP, Sprovieri M (2009) Astronomically forced teleconnection between Paratethyan and Mediterranean sediments during the Middle and Late Miocene Palaeogeogr Palaeocl Palaeoec 275:1–13

Hohenegger J, Ćorić S, Khatun M, Pervesler P, Rögl F, Rupp C, Selge A, Uchman A, Wagreich M (2009) Cyclostratigraphic dating in the Lower Badenian (Middle Miocene) of the Vienna Basin (Austria): the Baden-Sooss core. Int J Earth Sci (Geol Rundsch) 98:915–930

Papp A (1963) Die biostratigraphische Gliederung des Neogens im Wiener Becken. Mitt Geol Ges Wien 56:225–317

Papp A, Cicha I (1978) Definition der Zeiteinheit M – Badenien. In: Papp A, Cicha I, Senes J, Steininger F (eds): M4 – Badenien (Moravien, Wielicien, Kosovien). Chronostratigraphie und Neostratotypen. Miozän der Zentralen Paratethys: Slowakische Akademie der Wissenschaften, Bratislava, pp 47-48

Papp A, Cicha I, Senes J, Steininger F (1978) M4 – Badenien (Moravien, Wielicien, Kosovien). Chronostratigraphie und Neostratotypen. Miozän der Zentralen Paratethys: Slowakische Akademie der Wissenschaften, Bratislava, 594 pp

Papp A, Krobot W, Hladecek K (1973) Zur Gliederung des Neogens im Zentralen Wiener Becken. Mitt. Ges Geol Bergbaustud Österr 22:191–199

Papp A, Turnovsky K (1953) Die Entwicklung der Uvigerinen im Vindobon (Helvet und Torton) des Wiener Beckens. Jahrbuch der Geologischen Bundesanstalt 96:117–142

Piller WE, Decker K, Haas M (1996) Sedimentologie und Beckendynamik des Wiener Beckens: Sediment 96, 11. Sedimentologentreffen, Exkursion guide, Geologische Bundesanstalt, Wien, 41 pp

Piller WE, Harzhauser M, Mandic O (2007) Miocene Central Paratethys stratigraphy–current status and future directions. Stratigraphy 4:151–168

Piller W, Kleemann K, Friebe JG (1991) Middle Miocene reefs and related facies in eastern Austria. In: Excursion B4 Guidebook of the VI International Symposium on Fossil Cnidaria including Archaeocyatha and Porifera, International Association for the Study of Fossil Cnidaria and Porifera, 47 pp

Piller WE, Vavra N (1991) Das Tertiär im Wiener und Eisenstädter Becken. In: Roetzel R, Nagel D (eds): Exkursionen im Tertiär Österreichs, Österreichische Paläontologische Gesellschaft, Wien, pp 169–216

Plan L, Pavuza R, Seemann R (2006) Der Nasse Schacht bei Mannersdorf am Leithagebirge, NÖ (2911/21) – eine thermal beeinflusste Höhle am Ostrand des Wiener Beckens. Die Höhle 57:30–46

Pomar L, Brandano M, Westphal H (2004) Environmental factors influencing skeletal grain sediment associations: a critical review of Miocene examples from the western Mediterranean 51:627–651

Popov SV, Rögl F, Rozanov AY, Steininger FF, Shcherba IG, Kováč M (2004) Lithological–Paleogeographic maps of Paratethys. 10 Maps Late Eocene to Pliocene. Cour Forsch-Inst Senckenberg 250:1–46

Ratschbacher L, Frisch W, Linzer HG, Merle O (1991) Lateral extrusion in the Eastern Alps. Tectonics 10:257–271

Riegl B, Piller WE (2000) Biostromal coral facies — A Miocene example from the Leitha Limestone (Austria) and its actualistic interpretation. Palaios 15:399–413

Reuss AE (1871) Die fossilen Korallen des österreichisch−ungarischen Miocäns. Denkschriften der Kaiserlichen Akademie der Wissenschaften, Mathematisch−naturwissenschaftliche Classe 31:197–270

Rögl F (1998) Paleogeographic considerations for Mediterranean and Paratethys seaways (Oligocene to Miocene). Ann Naturhist Mus Wien 99(A):279–310

Rögl F (1999).Mediterranean and Paratethys. Facts and hypotheses of an Oligocene to Miocene paleogeography (short overview). Geologica Carpathica 50:339–349

Rögl, F., Ćorić, S., Harzhauser, M., Jimenez-Moreno, G., Kroh, A., Schultz, O., Wessely, G. & Zorn, I., 2008. The Middle Miocene Badenian Stratotype at Baden-Sooss (Lower Austria). Geologica Carpathica, 59: 367 – 374.

Rögl F, Steininger FF (1983) Vom Zerfall der Tethys zu Mediterran und Paratethys. Ann Naturhist Mus Wien 85(A):135–163

Rohatsch A (1996) Ökologische Aspekte bei Foraminiferenfaunen der kalkigen Randfazies des Wiener Beckens. Mitt Ges Geol Bergbaustud Österr 39/40:55–63

Royden LH (1985) The Vienna basin: a thin-skinned pull-apart basin. In Biddle KT, Christie-Blick N (Eds) Strike-Slip Deformation, Basin Formation, and Sedimentation. SEPM Spec Publ 37:319–338

Schmid HP, Harzhauser M, Kroh A (2001) Hypoxic events on a Middle Miocene carbonate platform of the Central Paratethys (Austria, Badenian, 14 Ma). Ann Naturhist Mus Wien 102(A):1–50

Steininger FF and Papp A (1978) Faziostratotypus: Gross Höflein NNW, Steinbruch „Fenk“, Burgenland, Österreich. In: Papp A, Cicha I, Seneš J, Steininger FF (eds): Chronostratigraphie und Neostratotypen, Miozän der Zentralen Paratethys. Bd. VI. M4 Badenien (Moravien, Wielicien, Kosovien) Slowakische Akademie der Wissenschaften, Bratislava, pp 194–203

Strauss P, Harzhauser M, Hinsch R, Wagreich M (2006) Sequence stratigraphy in a classic pull-apart basin (Neogene, Vienna Basin). A 3D seismic based integrated approach. Geol Carpath 57:185–197

Studencki W (1988): Facies and sedimentary environment of the Pinczow limestones (Middle Miocene; Holy cross mountains, central Poland). Facies 18:1–26

Tollmann, A., 1955. Das Neogen am Nordwestrand der Eisenstädter Bucht. Wissenschaftliche Arbeiten aus dem Burgenland 10, 1–74.

Tollmann A (1964): Exkursion II/6. Semmering-Grauwackenzone. Mitt Geol Ges Wien 57:193–203

Tollmann A (1985) Geologie von Österreich, Band 2. Deuticke, Wien, 710 pp

Turnovsky K (1963) Zonengliederung mit Foraminiferenfaunen und Ökologie im Neogen des Wiener Beckens. Mitt Geol Ges Wien 56(1):211–224

Wagreich M, Schmid HP (2002) Backstripping dip-slip fault histories: apparent slip rates for the Miocene of the Vienna Basin. Terra Nova 14:163–168

Weissenbäck M (1996) Lower to Middle Miocene sedimentation model of the central Vienna Basin. In: Wessely G, Liebl W (Eds), Oil and Gas in alpidic thrustbelts and basins of the Central and Eastern Europe. EAGE Spec Publ 5:355–363

Wiedl, T., Harzhauser, M., Kroh, A., Ćorić, S., Piller, W.E., 2013. Ecospace variability along a carbonate platform at the northern boundary of the Miocene reef belt (Upper Langhian, Austria) Palaeogeography, Palaeoclimatology, Palaeoecology 370:232–246

Wiedl, T., Harzhauser, M., Piller, W.E., 2012. Facies and synsedimentary tectonics on a Badenian carbonate platform in the southern Vienna Basin (Austria, Central Paratethys). Facies 58, 523–548.

Wright VP, Burchette TP (1998) Carbonate ramps: an introduction. In: Wright VP, Burchette TP (eds) Carbonate Ramps. Geological Society, London, Spec Publ 149:1-5

Chapter II

Facies and synsedimentary tectonics on a Badenian carbonate platform in the southern Vienna Basin (Austria, Central Paratethys)

Thomas Wiedl[1], Mathias Harzhauser[2], Werner E. Piller[1]

[1] Institute of Earth Sciences, Geology and Paleontology, University of Graz, Heinrichstrasse 26, 8010 Graz, Austria, thomas.wiedl@uni-graz.at, werner.piller@uni-graz.at
[2] Natural History Museum Vienna, Burgring 7, 1010 Vienna, Austria, mathias.harzhauser@nhm-wien.ac.at

2.1 Abstract

The Mannersdorf quarries at the north-eastern edge of the Leitha Mountains (Lower Austria) preserve a record of pre-, syn- and post-tectonical phases of a Badenian carbonate platform in the Vienna Basin. The pre-tectonic phase is reported by a marine transgression with the development of a coastal slope scree and subsequent prograding of a Gilbert-type fan delta, overlain by very heterogeneous corallinacean limestones. A fault divides the study area into two independent tectonic blocks which have been logged and subjected to detailed investigation and sampling. The corallinacean limestones of the first block indicate shallow water environments (i.e., seagrass meadows) and gradual transitions from shallower to deeper environments, while the second block shows an unconformity which is linked to a rapid facies change from relatively deeper environments (i.e., indicated by the abundance of in situ *Pholadomya*) to shallow waters (indicated by corals). Contrary to coral-bearing limestones of the same age at the south-western part of the Leitha Mountains, corals are generally rare in the limestones of the Mannersdorf quarries, which represent mostly deeper environments with conspicuous differences in faunal associations. The onlap of limestones on a tectonic-caused flexure indicates syn-tectonical movements. Palaeostress analyses verify a normal-fault reactivated as a dextral strike-slip fault. The temporal character of this fault is indicated by a post-tectonical phase with a marine transgression, a burial of the fault and neptunian dyke development.

2.2 Introduction

The Vienna Basin between the Eastern Alps and the Western Carpathians is one of the most studied basins – in terms of both structural and sedimentary geology (e.g. Royden 1985; Wessely 1988; Fodor 1995; Decker 1996; Strauss et al. 2006). The ca. 200 x 50 km large basin lies primarily within Austria, but extends into the Czech Republic and Slovakia (Wessely 2006). Its developmental history began with the formation of a pull-apart basin along the junction of the Eastern Alps and the Western Carpathians (Royden 1985). Interactive processes of compression, strike-slip movements and extension, related to compression and lateral extrusion led to its present-day appearance (Ratschbacher et al. 1991; Fodor 1995; Decker and Peresson 1996). The main extension activity occurred during the Middle Miocene, similar to the onset of extension in the Danube Basin (Ratschbacher et al. 1990). Basin subsidence led to fault tectonics at basin margins (Wessely 1983) and to synsedimentary filling of the newly formed accommodation space, especially during the Middle to Late Miocene (Wessely 2006). For this period, synsedimentary or buried faults are documented for the Vienna Basin (Seifert 1992; Fodor 1995). Subsidence rates often changed during basinal development and show intervals of increased rates especially during the Early Badenian (Lankreijer et al. 1995; Wagreich and Schmid 2002; Hohenegger and Wagreich 2011) with the highest rates of subsidence reaching 1000 m/Ma in the south and around 700 m/Ma in the central part of the basin (Hölzel et al. 2008).

Throughout the Middle Miocene, the Vienna Basin was structured by several topographic highs that formed islands, shoals, and small platforms with extensive carbonate production (e.g. Dullo 1983; Riegl and Piller 2000; Schmid et al. 2001; Harzhauser and Piller 2010). One of these structures is represented by the Leitha Mountains in the southern part of the basin (Fig. 2.1). During the Middle Miocene the Leitha Mountains represented a shallow carbonate platform (Schmid et al. 2001). The basement is formed by pre-Cenozoic rocks, predominantly Central Alpine Crystalline units (Tollmann 1964) and Central Alpine Permian-Mesozoic units (Kröll and Wessely 1993) covered by Langhian and Serravallian limestones (corresponding with the Central Paratethyan Badenian and Sarmatian stages, see Fig. 2.1 and Piller et al. 2007 for discussion) (Herrmann et al. 1993). Shallow-water carbonate rocks,

widely known as Leitha Limestones (sensu Keferstein 1828), are widespread in the entire Central Paratethys during the Middle Miocene Badenian stage (Papp et al. 1978; Studencki 1988; Piller et al. 1991). The most dominant limestone constituents are coralline algae but locally corals formed small patch reefs and carpets (Riegl and Piller 2000). Within the Paratethyan realm during Miocene time the Vienna Basin was strongly influenced by the Alpine orogeny (Steininger and Rögl 1984). The Badenian, which was the acme of the Miocene carbonate production in the Central Paratethys (Harzhauser and Piller 2007), was also a time of increased tectonic activity in the Vienna Basin (Wessely 2006). Accordingly, synsedimentary tectonics were documented in lost quarries near Hof am Leithagebirge (Schaffer 1908, Häusler et al. 2010). However, tectonic effects on the carbonate sedimentation regime in this area have not been documented.

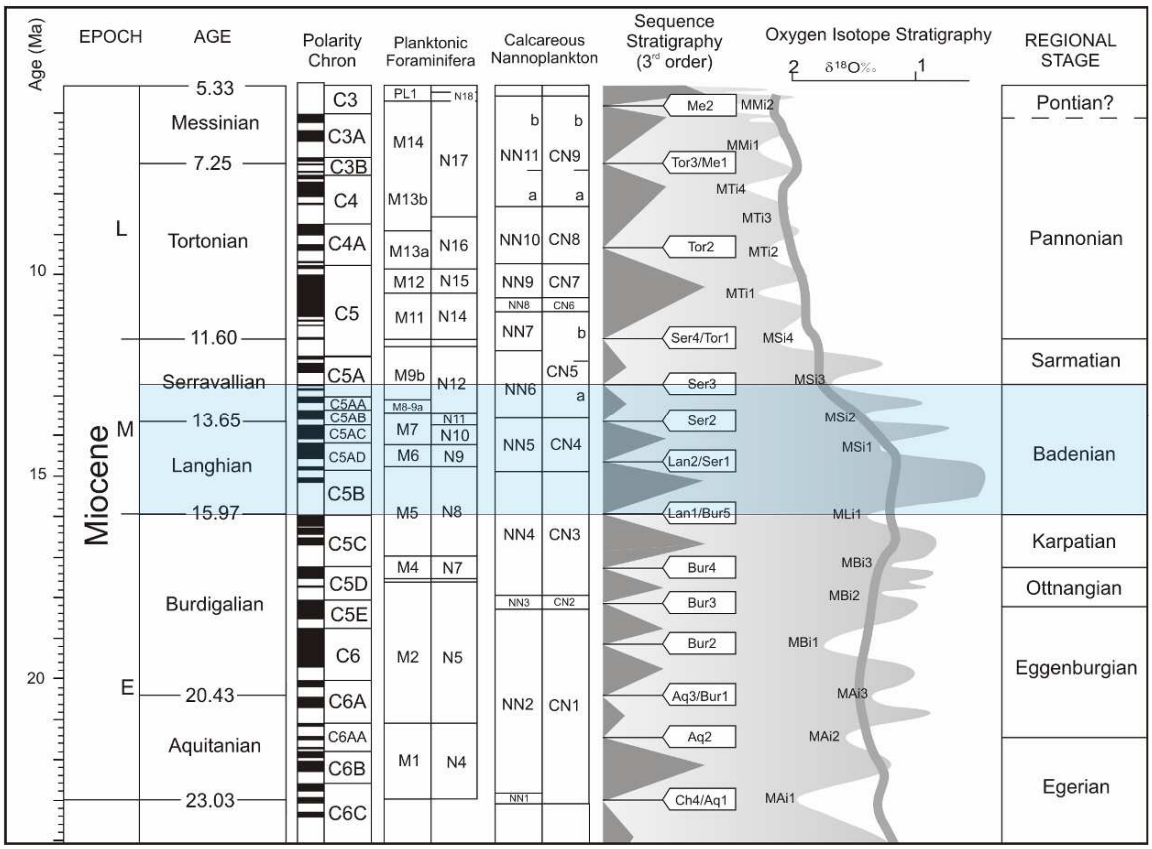

Fig. 2.1 Stratigraphic table after Piller et al. (2007) including Miocene geochronology, geomagnetic polarity chrons, and biozonations of planktonic foraminifers and calcareous nannoplankton. Sequence stratigraphy and sea-level curve, and oxygen isotope stratigraphy are correlated to regional chronostratigraphy of the Central Paratethys. The studied time interval (Badenian) is highlighted in blue colour.

In the present study we describe an up to 80-m-thick carbonate succession from the largest active quarry in the Leitha Mountains at Mannersdorf (Lower Austria). The

quarry is divided by a fault system into two tectonic blocks. Field observations and microfacies analyses demonstrate tectonically active and inactive phases as well as their influence on relative sea-level changes. The vertical and horizontal development of micro- and macrofacies within the succession also allows to interpret the temporal and spatial evolution of that part of the carbonate platform.

2.2.1 Study area

The investigated outcrops are located within the active quarry system of the Lafarge-Perlmooser AG close to the village Mannersdorf in Lower Austria (Fig. 2.2). The

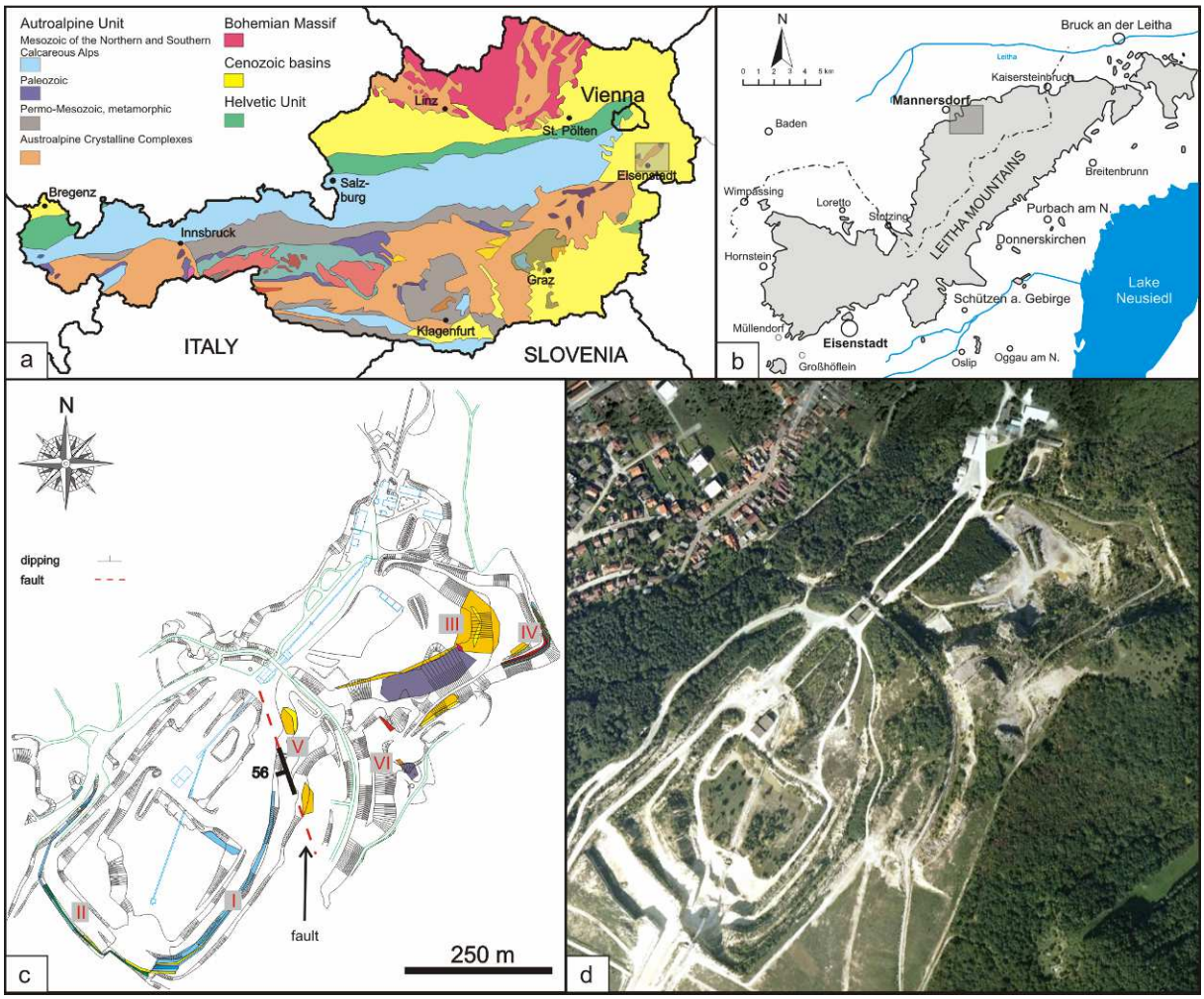

Fig. 2.2 Location of the study area and indication of transects. a Geological map of Austria, simplified after Egger et al. 1999. b Geographic map (inset in a) of the Leitha Mountains spanning the border region of Lower Austria and Burgenland provinces. c Detailed map of inset in b of the Mannersdorf quarry system of Lafarge-Perlmooser AG (courtesy of Dipl.-Ing. Baehr-Mörsen) indicating the studied facies zonations (colours indicate facies types, cf. illustration in Fig. 3). Roman numbers indicate positions of the phototransects; fault dip is given by a symbol and a numerical value; the fault is marked by a red line. d Satellite image of the study area (C)2011 Google corresponding to Fig. 1c.

geology of the Leitha Mountains close to Mannersdorf is characterized by an East Alpine basement, primarily composed of Middle Triassic dolostone and Semmering Quartzite, covered by Badenian Leitha Limestones (Herrmann et al. 1993). The Mannersdorf quarries were only cursorily mentioned in the literature (Fuchs 1894; Schaffer 1908; Sohs 1963; Rohatsch 1997, 2008; Fencl 2005). Some of the described sections no longer exist due to intensive mining activity over many decades. A basic concept of the typical succession was proposed by Harzhauser and Piller (2004) for the nearby Baxa Quarry (ca. 1 km distance), which is characterized by Triassic dolostones overlain by Badenian and Sarmatian carbonates. Hydrothermal influence and hypogenic speleogenesis, which locally affects the Leitha Limestones, were described for a cave south of the Baxa Quarry (Plan et al. 2006).

2.3 Material and methods

Two sections, representative for the facies development of each tectonic block, have been logged and subjected to detailed investigation and sampling. The thickness of each bed was measured and oriented rock samples were collected for thin-section analyses. Due to 3-10 m high vertical walls the reconstruction is based on a series of overlapping sub-sections (exact positions are indicated in Fig. 2.2). This enables the study of composite sections of almost 80 and 40 m thickness, respectively. For a detailed mapping of facies and faunal content and lateral facies-changes, photomosaics were prepared. For microfacies analyses, 47 thin-sections (5x5 cm) have been prepared. Carbonate nomenclature follows Dunham (1962) and Embry and Klovan (1971). The classification of siliciclastic sediments is based on terms of Wentworth (1922). Nomenclature of corallinacean growth forms follows Woelkerling et al. (1993). Field data of 26 slickensides and lineations were analyzed and plotted with Win-Tensor 3.0.0. of the TENSOR program (cf. Delvaux and Sperner 2003).

2.4 Section description

Both sections are characterized by bedded limestones dominated by coralline algae debris. However, the corallinacean limestones differ in their faunal associations in each section. Additionally, the base of section II shows the transition from dolomitic

basement to dolostone breccias and cross-bedded gravels overlain by corallinacean limestones. Skeletons with a primary calcite mineralogy, such as oysters, pectinids, and echinoids, are well preserved, while aragonitic biota are always dissolved or replaced by calcite. For example, corals occur as voids or sediment-filled corallites, while aragonitic bivalves are found as steinkerns or casts. Details (thickness, lithology, faunal content) of each bed, including results of thin-section analyses, are listed in Tab. 1.

2.4.1 Section I

The succession starts with massive corallinacean limestones (bed 1 and 2) characterized by a macrofauna of various bivalves (oysters, pectinids, cardiids), gastropods (Conidae, Trochidae, *Cerithium*, *Xenophora*, *Turritella*) and rare echinoids. Toward the top of bed 1 a fining-upward trend is visible. The similar macrofauna of bed 2 (Fig. 2.4a) is additionally characterised by large *Gigantopecten nodosiformis* (de Serres in Pusch, 1837), *Glycymeris deshayesi* (Mayer, 1868) and *Thalassinoides* burrows. The transition between both beds (ca. 2 m) is not exposed. Ca. 100 m to the SSW, a lateral change within bed 2 from massive to a more porous marly limestone is visible and single in situ *Pinna tetragona* (Brocchi, 1814) occur in the upper part. There follows a massive corallinacean limestone (bed 3; Fig 2.4b) which pinches out to the NNE. It contains common molluscs as debris of oysters and pectinids or steinkerns of *Glycymeris deshayesi* and casts of *Periglypta miocaenica* (Michelotti, 1847). Articulated and disarticulated shells of *Gigantopecten nodosiformis* occur parallel to the bedding plane and form coquinas. Following the bed ca. 130 m to the SW it changes to a well sorted corallinacean limestone. The marl content is variable and increases to the top of the bed where bioturbation is very common. Bivalve steinkerns are frequent; loosely dispersed *Gigantopecten nodosiformis* shells are intensely bored by sponges. Bed 4, which is onlapping on bed 3, starts with a distinct coquina of disarticulated shells of *Gigantopecten nodosiformis*. In the lower part it is characterised by high marl content; the upper part gradually passes into a well-cemented limestone. Articulated *Glycymeris deshayesi* and *Periglypta miocaenica* are common throughout the bed. The following bed (5, Fig. 2.4c) is dominated by a soft, marly limestone with a macrofauna dominated by celleporiform bryozoans at the base, which occasionally encrust corallinaceans. Close to the boundary to bed 6, large and thick-branched rhodoliths (up to 7 cm in diameter) float

within corallinacean debris. A 1-cm-thick intercalation of terrigenous silt (5a) separates bed 5 from the following bed (6) which contains common *Glans subrudista* (Friedberg, 1934), *Ctena decussata* (Costa, 1829), *Gigantopecten nodosiformis*, *Glycymeris deshayesi* and cardiids along with in situ *Pinna tetragona*. Fragments of branched *Porites* occur as well. Ca. 80 m to the W small irregularly distributed quartz fine-sand lenses (up to ca. 0.5 m long and ca. 0.3 m thick) are intercalated within the bed. The bed is terminated by a 1-2 cm-thick silty clay bed, which is locally overlain by 1-3 cm of quartz fine-sand. The following bed (bed 7; Fig. 2.4c) is characterized by marly limestone containing many poorly preserved bivalves and gastropods (a few mm in sizes) and clusters of *Amphistegina* mass occurrences are typical. In situ shells of *Pinna tetragona* are distributed throughout the bed but form a distinct horizon with densely spaced specimens (Fig. 2.8h) in the upper part of the bed where *Thalassinoides* burrows are also common. *Gigantopecten nodosiformis*, *Aequipecten malvinae* (du Bois de Montpereux, 1831), *Ctena decussata* and *Codakia* are typical bivalves. The bed is terminated by a thin silt-layer (bed 7a). A well-cemented corallinacean limestone (bed 8) follows, similar to bed 7, containing *Pinna tetragona* fragments. The bed is again terminated by a thin silty clay bed (8a). The following bed (bed 9; Fig. 2.4c), which is again terminated by a thin silty clay (bed 9a) is characterized by in situ *Pinna tetragona*, especially at the base. *Thalassinoides* burrows and cardiids are very common; disarticulated shells of *Gigantopecten nodosiformis* are found in the entire bed. There is a change to a massive limestone (Fig. 2.4c) which contains abundant *Periglypta miocaenica*, especially in the basal part along with *Glycymeris deshayesi*, whilst *Pinna tetragona* occurs only at the base. A fining-upward trend is documented by development of fine-grained limestones at the top. Ca. 100 m to the N the bed becomes more porous. It is followed by two beds (11 and 12) which are characterized by poorly cemented corallinacean limestones with common shells of *Gigantopecten nodosiformis* (e.g., at the base of bed 11, commonly affected by sponge borings) and *Glycymeris deshayesi*. *Pinna tetragona* rarely occurs in situ (bed 12). Bed 11 can be clearly discriminated from bed 12 by its soft chalky appearance. Bed 12 is overlain by a corallinacean limestone (bed 13), characterized by numerous *Amphistegina* in the lower part which are disappearing abruptly after ca. 7 m. Bryozoans and serpulids (horizon of ca. 25 cm) are common 6 m above the base. The amount of *Amphistegina* increases toward the top. The same bed pinches out to ca. 500 m to the ENE directly onlapping onto the dolostone. It is

represented by two horizons consisting of corallinacean limestones characterized by mass occurrences of *Amphistegina*. Section I is terminated by a massive corallinacean limestone, similar to bed 1 in its faunal content.

2.4.2 Section II

The base of section II (Figs. 2.3, 2.4d) is made up of a dark-grey massive dolostone, which crops out only in the northern part of the Mannersdorf quarry area with a total height of ca. 30 m in unconformable contact to overlying beds. With a gap of ca. 2 m above the dolostone, section II starts with a white silt layer (bed 1) followed by a succession of three monomictic dolostone breccia beds, onlapping on the dolostone. The lowest breccia (bed 2) consists of subangular components up to 20 cm while the components of the middle layer (bed 3) are smaller (5-7 cm) and the bed shows a fining-upward trend with increasing amounts of silty sand in the topmost 5-8 cm. The uppermost breccia layer (bed 4), displays a fining-upward trend as well, ranging from components of 3-5 cm in diameter in the basal 30 cm to components of 1-2 cm in size in the upper part. The components at the base are better rounded than those of the lower and middle breccia bed and show bioerosion of *Entobia*. The transition from the onlapping breccias to the gravels (bed 5) is covered by soil. About 15 m of [non-cemented] gravel (Fig. 2.4d) are exposed, which develop foresets in the upper part of bed 5 with a dip of ca. 20° to the NW. The gravel is well rounded but poorly sorted with alternating coarse and fine layers. It is terminated by a ca. 20-cm-thick iron-crust containing well rounded quartz pebbles. The crust is overlain by 10 to 15 cm of calcareous quartz-fine-sandstone (bed 6). Above follows a marly corallinacean limestone (bed 7) dominated by fragments of corallinaceans with laminar growth forms. Well rounded quartz pebbles are common in the lower part and above there is about 7 m of gravels (bed 8) that show clear foresets in the lower part. Sand content increases continuously to the top reaching up to 50%; sorting of the gravel also increases. Ca. 5 m above the corallinacean limestone bed, a fine-sand layer (bed 9) is developed. Also some local fine-sand lenses with 0.1-0.5 m length and 1-2 cm thickness are dispersed within the gravel, e.g. directly below the corallinacean limestone (bed C1), which terminates the gravel. Ca. 400 m further SW the gravels crop out (B1), directly followed by corallinacean limestones containing dolostone cobbles with dimensions of up to 14 cm. The boundary between gravel (Fig. 2.5b) and limestones is mostly an unconformity (also cropping out ca. 400 m in the SW)

but conformable contacts are also present (e.g., ca. 160 m in the S and ca. 260 m in the SW). It shows a dome-shaped topography (cupolas) with diameters of ca. 30 cm. Mudstone and partly wackestone horizons with variable thickness (1-15 cm) are locally developed between the corallinacean limestones and the gravel. Internally the wackestones are laminated containing bryozoan and corallinacean debris and scattered *Amphistegina*. A differently developed boundary can be found ca. 150 m in the SSW where the gravel (bed E0) is followed by a calcareous middle- to fine-grained sandstone (bed E1), yellowish mudstones to wackestones with packstone areas covered by calcareous fine-sandstone E2, calcareous fine-grained sandstones (bed E3) with clusters of quartz pebbles and corallinacean limestones (bed E4). The first limestone bed above the gravel (C1, B3 and E4, see Fig. 2.3) consists of corallinacean limestones with common encrusting corallinaceans. Well rounded scattered quartz and dolostone pebbles, some cm in diameter, can also be detected, especially in the lower part of the bed. Close to the dolostone (ca. 90 m to the SW) well rounded dolostone cobbles (up to 14 cm diameter) with sponge borings occur. In B3, the corallinaceans occasionally bind quartz grains. *Acervulina*-corallinacean macroids are common as well as laminar rhodoliths of the same size. The contact of bed C1 to bed C2 is not exposed. The outcropping bed consists of a corallinacean limestone. Steinkerns (10-15 cm) of *Pholadomya alpina* (Matheron, 1842) and *Periglypta miocaenica* are very common, along with shell debris of ostreids. In southern direction, debris of delicate (ca. 3 mm) branched corals (probably *Stylocora*) occurs. Branched and celleporiform bryozoans commonly occur, occasionally encrusted by corallinaceans forming thick branched rhodoliths. The mass occurrence of *Amphistegina* and the prominence of thin encrusting corallinaceans in layer C2 distinguishes it very clearly from the following bed. Bed C3 (Fig. 2.5a), which is characterized by a high marly content, locally shows mass occurrences of branched and celleporiform bryozoans. Up-section, the bed becomes more porous and grades into a clay layer (ca. 5 mm in thickness). *Modiolus*, cardiids, pycnodont oysters and *Aequipecten malvinae* are typical bivalves. In contrast, the following bed (C4; Fig. 2.5a) shows mass occurrences of *Amphistegina* and *Panopea menardi* (Deshayes, 1828) which can be found in life position at the base. Fragments of bivalves are common; at the top well preserved shells of *Hyotissa hyotis* (Linnaeus, 1758) occur. Up-section a highly bioturbated and poorly sorted corallinacean limestone follows (bed C5; Fig. 2.5a), which is nearly identical to bed C3. The contact to bed C6 is

unconformable (Fig. 2.5a). Bed C6 (Fig. 2.5a) is a massive, densely packed, prominently exposed corallinacean limestone containing debris of delicate (ca. 3 mm) branched corals. It is overlain by a poorly cemented corallinacean limestone (C7; Fig. 2.5a) which contains many nodular rhodoliths (∅ 3-10 cm) which are densely packed or occasionally float in a matrix of corallinacean debris. Celleporiform bryozoans are commonly encrusted by corallinaceans or *Acervulina*. The top of the section (C8; Fig. 2.5a) is formed by a massive corallinacean limestone which contains common thin-branched (ca. 1 cm) *Porites* and debris of delicate branched (ca. 3 mm) corals at the base. Bivalves and gastropods are common in this bed, as are *Amphistegina* and *Acervulina*.

Section	Bed	Thickness	Lithology	Fossil content
I	1	6.2 m	Massive corallinacean rudstone with packstone matrix or locally diffuse packstone areas dominated by debris (∅ 2-5 mm) of fruticose (c) and encrusting corallinaceans (r) growth forms; nodular rhodoliths (∅ 3 cm, r)	Bivalves: cardiids (c), ostreids (c), pectinids (c); gastropods: Conidae (r), Trochidae (r), *Cerithium* (c), *Xenophora* (r), *Turritella* (c); echinoids: cidariids (r), *Clypeaster* (r); celleporiform bryozoans (r, < 5 mm); *Thalassinoides* (∅ 1-2 cm, c); foraminifers: *Amphistegina* (r), textulariids (r)
	2	11 m	Massive, poorly sorted corallinacean rudstone with packstone matrix dominated by debris (∅ 2-5 mm) of fruticose (c) and thin encrusting growth forms (r); nodular rhodoliths (∅ 3 cm, s); *Acervulina* (r)	Bivalves: *Gigantopecten nodosiformis* (c), *Glycymeris deshayesi* (c), *Pinna tetragona* (s); gastropods: Conidae (c), rissoids (m), trochids (c); celleporiform bryozoans (< 5 mm, r); echinoids: *Clypeaster* (r), disarticulated cidariids (c); foraminifers: *Planostegina* (r), *Amphistegina* (r), textulariids (r); *Thalassinoides* (∅ 1-2 cm, c)
	3	2.15 m	Massive corallinacean rudstone with packstone matrix dominated by debris (∅ 4-5 mm) of fruticose (c) and encrusting (r) growth forms; *Acervulina*-corallinacean macroids (∅ 2-3 cm, c); spheroidal to ellipsoidal rhodoliths (∅ 5-7 cm, r)	Bivalves: *Gigantopecten nodosiformis* (m), *Glycymeris deshayesi* (c), *Periglypta miocaenica* (c), pycnodont oysters (r); gastropod steinkerns (< 5 mm, r); branched and celleporiform (∅ 3-4 cm, r) bryozoans; foraminifers: *Amphistegina* (c), biserial textulariids (r), miliolids (r), globigerinids (s)
	4	8.1 m	Corallinacean rudstone with packstone matrix	Bivalves: *Gigantopecten nodosiformis* (c), ostreids (c),

			dominated by debris (∅ 2-3 mm) of fruticose growth forms	*Glycymeris deshayesi* (c), *Periglypta miocaenica* (c); echinoid spines (c); foraminifers: *Elphidium* (c), *Amphistegina* (r), textulariids (r)
	5	6.7 m	Soft, marly corallinacean rudstone to floatstone with packstone matrix dominated by debris (∅ 4 mm) of fruticose (c) and thin encrusting (r) growth forms; locally rhodoliths (∅ 7 cm, c)	Bivalves: shell fragments (< 3mm, c); serpulids (r); locally celleporiform bryozoans (∅ 1-2 cm, c); foraminifers: *Amphistegina* (c), biserial textulariids (r), miliolids (*Triloculina*, r), globigerinids (s); rare and poorly preserved nannoplankton: *Coccolithus pelagicus* (Wallich, 1877) Schiller 1930, *Coronocyclus nitescens* (Kamptner, 1963, Bramlette and Wilcoxon, 1967)
	5a	1 cm	Dark silty clay	-
	6	1.7 m	Corallinacean rudstone with packstone to wackestone matrix dominated by debris (∅ 2-5 mm) of fruticose (c) and thin encrusting (c) growth forms; locally fine-quartz-sand lenses (0.5 x 0.3 m)	Bivalves: *Glans subrudista* (c), *Ctena decussata* (c), *Gigantopecten nodosiformis* (c), *Glycymeris deshayesi* (c), cardiids (c), *Pinna tetragona* (m); coral: *Porites* (m); foraminifers: *Amphistegina* (c), biserial textulariids (c), miliolids (s)
	6a	1-2 cm	Dark silty clay	-
	7	5.1 m	Marly corallinacean rudstone with wackestone matrix dominated by debris (∅ 2-4 mm) of thin	Bivalves: shell fragments (< 3mm, c), *Pinna tetragona* (m), *Gigantopecten nodosiformis* (c), *Aequipecten malvinae* (r),

			encrusting (c) and fruticose growth forms (c); spheroidal to ellipsoidal rhodoliths (ca. 5 cm, s)	*Ctena decussata* (c), *Codakia* (c); gastropods: steinkerns (< 5mm, c); celleporiform bryozoans (∅ 1-2 cm, r); foraminifers: *Amphistegina* (m), biserial textulariids (r), miliolids (s), globigerinids (r); *Thalassinoides* (∅ 1-2 cm, c)
	7a	0.3-0.5 cm	Dark silty clay	-
	8	28 cm	Well-cemented corallinacean rudstones with packstone matrix dominated by debris (ca. 400-700 µm thick) of thin encrusting (c) and rare fruticose (r) growth forms	Bivalve: *Pinna tetragona* (r); foraminifer: *Amphistegina* (c); echinoid debris and spines (r); serpulids (r); *Thalassinoides* (∅ 1-2 cm, c); celleporiform bryozoans (r)
	8a	0.5 cm	Dark silty clay	-
	9	1.4 m	Corallinacean rudstone with packstone matrix dominated by debris (∅ 1-2 mm) of thin encrusting (c) and fruticose (r) growth forms	Bivalves: *Pinna tetragona* (m), cardiids (c), *Gigantopecten nodosiformis* (c); celleporiform bryozoans (r); *Thalassinoides* (∅ 1-2 cm, c)
	9a	1 cm	Dark silty clay	-
	10	7.5 m	Massive corallinacean rudstone to floatstones dominated by debris (∅ 2-3 mm) of fruticose (c) and encrusting (r) growth forms	Bivalves: *Periglypta miocaenica* (c), *Glycymeris deshayesi* (c), *Pinna tetragona* (c); celleporiform bryozoans (r); echinoid debris (r); fish: spariid teeth (r); foraminifers: *Amphistegina* (r), textulariids (r), miliolids (s)

	11	4.1 m	Well sorted, poorly cemented soft chalky corallinacean rudstone of debris (∅ 5 mm) with packstone matrix consisting of fragments (∅ 1-2 mm) of fruticose (c) and thin encrusting (r) growth forms	Bivalves: *Gigantopecten nodosiformis* (c), *Glycymeris deshayesi* (c); gastropods: *Turritella* (r), Conidae (c); foraminifer: *Amphistegina* (r)
	12	5.5 m	Corallinacean rudstones to floatstones with packstone matrix dominated by debris (∅ 1-4 mm) of thin encrusting growth forms	Bivalves: *Glycymeris deshayesi* (c), *Pinna tetragona* (r), *Gigantopecten nodosiformis* (c); bryozoans: branching (r); foraminifers: *Amphistegina* (r), textulariids (r)
	13	11.5 m	Corallinacean rudstones to packstones dominated by debris (∅ 1-4 mm) of thin encrusting (c) and fruticose (c) growth forms; 500 m to the ENE: poorly cemented corallinacean rudstones dominated by debris (∅ 2-6 mm) of encrusting (c) and fruticose (r) growth forms; *Acervulina* (r)	Gastropods: *Cerithiopsis* (c), *Trochus* (c); bivalves: *Gigantopecten nodosiformis* (c), *Spondylus* (s); echinoid: *Arabacina* cf. *macrophyma* (c); serpulids (c); bryozoans: celleporiform (∅ 3 cm, c), branched (c); foraminifers: *Amphistegina* (m), *Planostegina* (r), textulariids (c), miliolids (r); *Thalassinoides* (∅ 1-2 cm, c)
	14	4.4 m	Light massive corallinacean rudstone with wacke- to grainstone matrix dominated by debris (∅ 0.5-2 mm) of fruticose (c) and thin encrusting (r) growth forms	Bivalve: *Gigantopecten nodosiformis* (c); bryozoans (r); echinoid debris (r); foraminifers: *Amphistegina* (r), textulariids (r), miliolids (r)
II	0	ca. 30 m	Dark-grey massive dolostone	-

	1	1.5 m	White silt	-
	2	0.5 m	Monomictic dolostone breccia of subangular components (up to 20 cm diameter) and silty sand	-
	3	0.6 m	Monomictic dolostone breccia of subangular components (5-7 cm) and silty sand	-
	4	1.1 m	Monomictic dolostone breccia of subangular components (1-5 cm) and silty sand	Entobia (r)
	5	ca. 15 m	Non-cemented, well rounded but poorly sorted gravel consisting of granite-, quartz- and dolostone-pebbles with alternating coarse (grain size: 5-7 cm) and fine layers (grain size: 1-2 cm) containing quartz-fine-sand	-
	6	0.1-0.15 m	Calcareous quartz-fine-sandstone	-
	7	0.6-0.8 m	Marly corallinacean rudstone with packstone matrix dominated by debris (∅ 4-5 mm) of laminar (c) and fruticose (r) growth forms; well rounded quartz components (∅ 1-1.5 cm, c); rhodoliths (∅ 2-3 cm, r) and *Acervulina*-	Echinoids: debris (c)

			corallinacean macroids (∅ 3-4 cm, r)	
	8	7 m	Non-cemented, well rounded but poorly sorted gravel consisting of granite-, quartz- and dolostone-pebbles (∅ 1-7 cm) and quartz-fine-sand (up to 50 in amount)	-
	9	0.4-0.6 m	Quartz-fine-sand	-
	C1	1.5 m	Corallinacean rudstones to floatstones with mud- to wackestone matrix dominated by debris (∅ 4-6 mm) of encrusting corallinaceans (c): well rounded quartz and dolostone pebbles (2-3 cm), locally well rounded dolostone cobbles (∅ up to 14 cm); *Acervulina*-corallinacean macroids (∅ 4-7 cm, c), laminar rhodoliths (∅ <10 cm, c)	Bivalves: pectinids debris (< 5 cm, r), ostreid fragments (r), steinkerns (1-2 cm, c); echinoids: *Echinolampas barchinensis* (r); foraminifer: *Amphistegina* (r); biserial textulariids (r), miliolids (r), globigerinids (s); bryozoans: celleporiforms (r)
	C2	2.4 m	Grey-brown corallinacean rudstone to floatstone with packstone matrix dominated by debris (∅ 0.5-2 mm) of thin encrusting corallinaceans (c) and fruticose growth forms (r)	Bivalves: *Pholadomya alpina* (c), *Periglypta miocaenica* (c), ostreid debris; branched and celleporiform bryozoans (0.5-1.5 cm, c); corals: delicate (ca. 3 mm) branched corals (probably *Stylocora*, r); foraminifers: *Amphistegina* (m), *Planostegina* (r), biserial textulariids (c)

	C3	1.2 m	Poorly sorted marly corallinacean rudstones to floatstones with packstone matrix dominated by debris (∅ 1-2 mm) of fruticose (c) growth forms containing *Acervulina* (r); at the top clay horizon (5 mm thickness)	Bryozoans: branched (∅ 1-2 mm, m), celleporiform (1-2 mm, m); bivalves: *Modiolus* (c), cardiids (c), pycnodont oysters (r), *Aequipecten malvinae* (c); foraminifers: *Amphistegina* (r), *Planostegina* (r), biserial textulariids (c), *Triloculina* (r), globigerinids (r)
	C4	2.1 m	Densely packed corallinacean rudstones, floatstones and packstones dominated by debris (∅ 1-3 mm) of fruticose growth forms	Bivalves: *Panopea menardi* (c), *Gigantopecten nodosiformis* (c), *Aequipecten malvinae* (c); *Hyotissa hyotis* (c), debris of pycnodont oysters (c); echinoid remains (c); *Thalassinoides* (∅ 1-2 cm, c); foraminifers: *Amphistegina* (m), textulariids (c), miliolids (r)
	C5	2.4 m	Porous corallinacean rudstone to floatstone with packstone matrix dominated by debris (∅ 2-4 mm) of fruticose (c) and thin encrusting (r) growth forms; *Acervulina* (r)	Bivalves: pycnodont oysters (c), *Aequipecten malvinae* (c), *Gigantopecten nodosiformis* (s); branched and celleporiform bryozoans (c); cirriped: *Pyrgoma multicostatum* (Seguenza, 1873; s); foraminifers: *Amphistegina* (c), *Sphaerogypsina* (r), biserial textulariids (c); *Thalassinoides* (∅ 1-2 cm, m)
	C6	1.2 m	Massive, densely packed corallinacean rudstone with packstone matrix dominated by debris (∅ 3-10 mm) of fruticose (c) and encrusting (r) growth forms and *Acervulina* (r); nodular rhodoliths (∅ 3 cm, s)	Corals: delicate branched (probably *Stylocora*, c); foraminifers: biserial textulariids (c), miliolids (r), *Amphistegina* (r)

	C7	3.1 m	Poorly sorted corallinacean rudstone with packstone matrix dominated by debris (∅ 2-8 mm) of fruticose and thin encrusting growth forms containing nodular rhodoliths (∅ 3-10 cm, c); *Acervulina* (r)	Bivalve: *Gigantopecten nodosiformis* (c); celleporiform bryozoans (c); echinoid debris (c); foraminifers: *Amphistegina* (r), *Triloculina* (r)
	C8	6.5 m	Massive corallinacean rudstone with packstone matrix dominated by debris (∅ 3-5 mm) of fruticose (c) and encrusting (c) growth forms; *Acervulina* (c)	Corals: *Porites* (c), delicate branched (probably *Stylocora*, c); gastropod and bivalve debris (< 1 mm, c), steinkerns (< 5 mm, c), *Cardium* (c); foraminifers: *Amphistegina* (c), textulariids (r), miliolids (r)
II	B1	0.3 m	Non-cemented, well rounded but poorly sorted gravel consisting of granite-, quartz- and dolostone-pebbles (∅ 1-7 cm) and quartz-fine-sand	-
	B2	5 cm	Laminated mud- to wackestone	Bryozoans and corallinacean debris (c); *Amphistegina* (r)
	B3	1.5 m	Corallinacean rudstones to floatstones with mud- to wackestone matrix dominated by debris (∅ 0.5-1.5 cm) of laminated corallinaceans and rare well rounded quartz and dolostone pebbles (∅ 2-3 cm); *Acervulina*-corallinacean macroids (∅ 4-7 cm); laminar	Branched bryozoans (r); foraminifers: *Amphistegina* (r), biserial textulariids (r), miliolids (r), globigerinids (s)

			rhodoliths (∅ 4-7 cm)	
II	E0	0.4 m	Non-cemented, well rounded but poorly sorted gravel consisting of granite-, quartz- and dolostone-pebbles (∅ 1-7 cm) and quartz-fine-sand	-
	E1	0.2 m	Calcareous middle- to fine-grained quartz-sandstone	-
	E2	0.4 m	Yellowish mudstone to wackestone with packstone areas dominated by corallinacean debris (< 1 mm diameter) grading into a calcareous quartz-fine-sandstone; *Avervulina* (r)	Bivalves: shell fragments (< 500 µm, c); bryozoans: celleporiform (r), branched (r); echinoid debris (r); foraminifer: *Amphistegina* (r)
	E3	0.1 m	Calcareous fine-grained quartz-sandstone and local clusters of quartz pebbles	-
	E4	1.2 m	Corallinacean rudstones to floatstones dominated by debris (∅ 2-4 mm) of laminated corallinaceans; *Acervulina*-corallinacean macroids (∅ 2-3 cm, c)	Bivalves: ostreid fragments, steinkerns (2-3 cm); echinoids debris (r); foraminifers: *Amphistegina* (r), biserial textulariids (r), miliolids (r), globigerinids (s); bryozoans: branched (r)

Tab. 1 Thickness, lithology, microfacies and faunal content of each bed. Abbreviations: s: single; r: rare; c: common; m: mass occurrence.

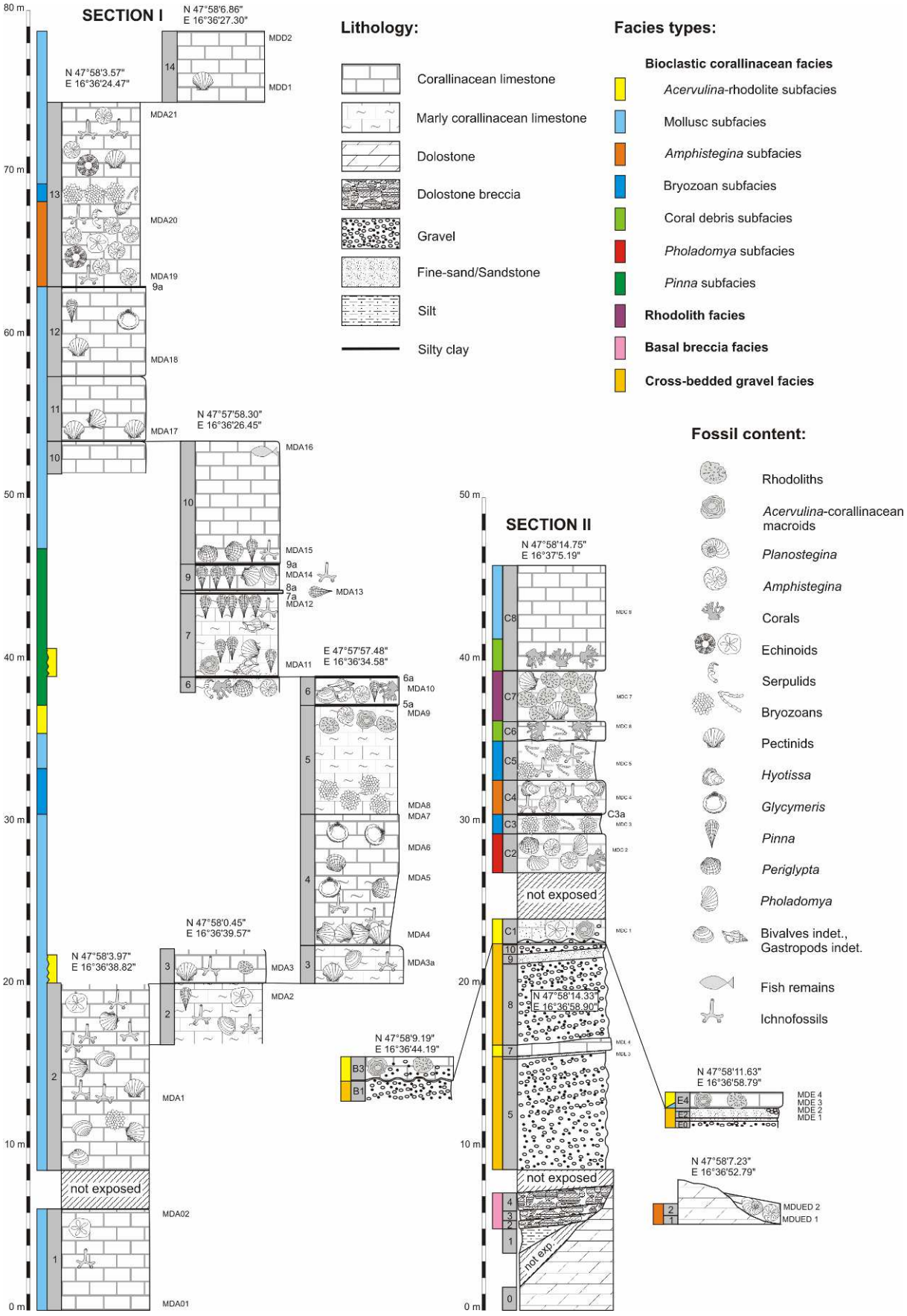

Fig. 2.3 Lithologic columns of sections I and II including sample numbers and GPS coordinates. Colours represent facies types.

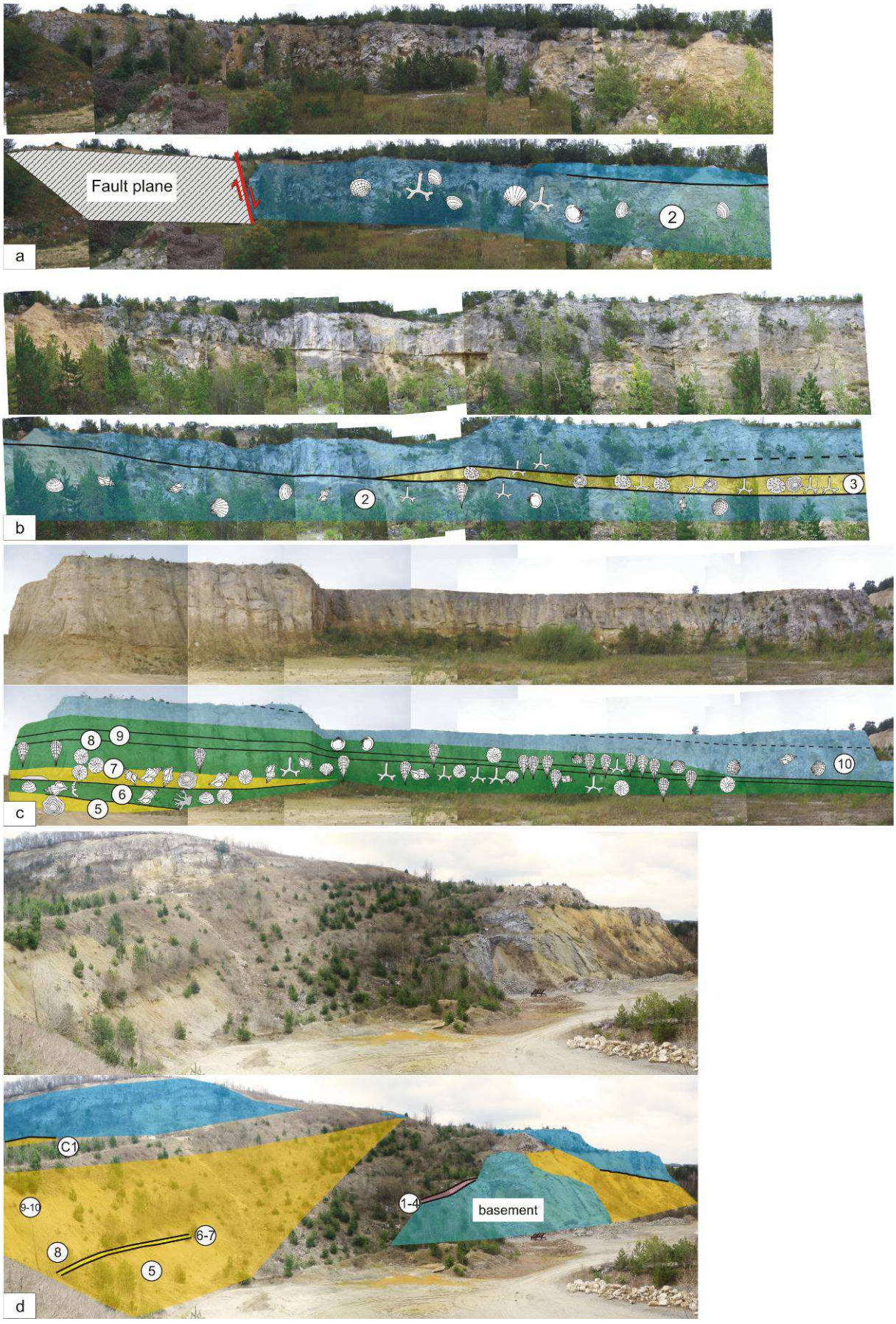
Fault plane
2
a
2
3
b
8
9
7
6
5
10
c
C1
9-10
8
6-7
5
1-4
basement
d

Figs. 2.4-5 Phototransects with bed numbers documenting facies zonations (highlighted in colours) and fossils (legends follow Fig. 2.3). Section I is represented by Figs. 2.4a-c, section II by Fig. 2.4d and Figs. 2.5a-c. Positions of phototransects are marked in Fig. 2.2.

Fig. 2.4 a Phototransect I - Part 1, NNE-SSW oriented. A fault plane is illustrated by a shaded field. The hanging wall at the right is represented by bed 2. b Phototransect I - Part 2, NNE-SSW oriented. Bed 3 (yellow) onlaps on bed 2 which shows a flexure with a height of ca. 5 m. c Phototransect II, ESE-WNW oriented. Horizontal bedding with a lateral facies change from the *Pinna* subfacies to the mollusc subfacies. d Phototransect III, N-S oriented. The basement (dolostone) is overlain by a breccia (1-4). It is followed by cross-bedded gravels (5, 8-10) with a corallinacean limestone intercalation (6-7). At the top corallinacean limestones (C1) are developed.

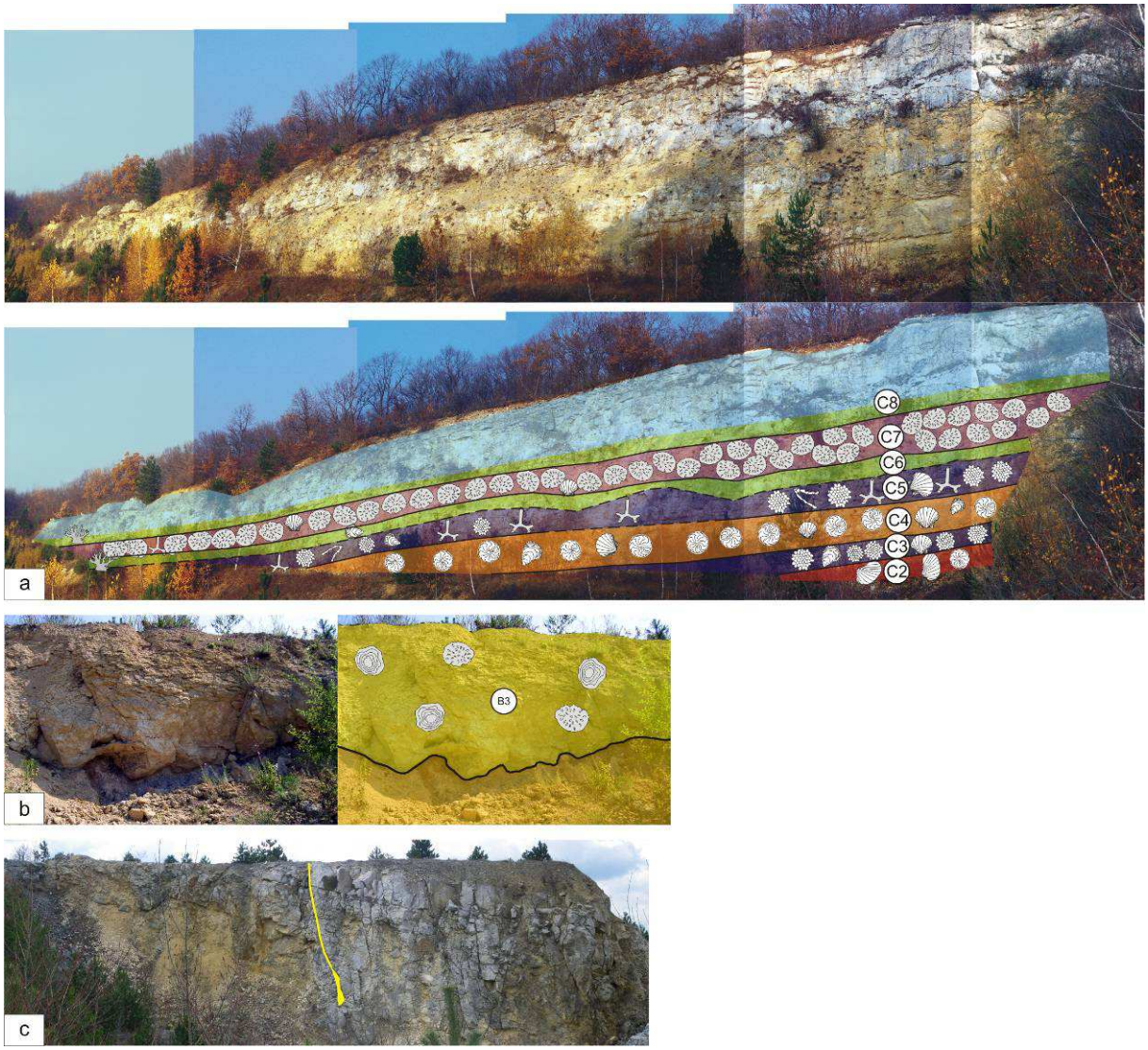

Fig. 2.5 a Phototransect IV, NNW-SSE oriented. Corallinacean limestones show horizontal bedding. Between bed C5 and C6 an unconformity is present. b Phototransect V, NNW-SSE oriented. Unconformity between gravel (base) and corallinacean limestone (top). c Phototransect VI, NW-SE oriented. Jointset fillings highlighted in yellow.

2.4.3 Tectonics

A fault (indicated in Figs. 2.2, 2.4a) divides the quarry area into two blocks; the south-western block acts as a hanging wall. A vertical displacement of the blocks of at least 20 m can be estimated. The fault plane has a mean dip angle of 56° with a mean dip direction of 251°. The surface is smoothly polished; locally the footwall is covered by a few cm thick flowstone. Two types of slickensides are present, the first slip-line gives a mean value of 53°/258° (plunge/azimuth); the second a mean value of 25°/333°. Close to the fault plane, bed 2 shows a slight flexure with a height of ca. 5 m at the deepest point (Fig. 2.4b). The first slip-line indicates ENE-WSW extension, the second, younger lineation documents a reactivation as a dextral strike-slip fault (Figs. 2.6a-b). Orientations of the principal stress axes (dip angle/dip direction) are given by σ1 (79/042, 90/000), σ2 (05/160, 00/090) and σ3 (10/251, 00/000). Within section II, close to the fault (N 47°58'10.07", E 16°36'52.48"), the limestone beds C2-

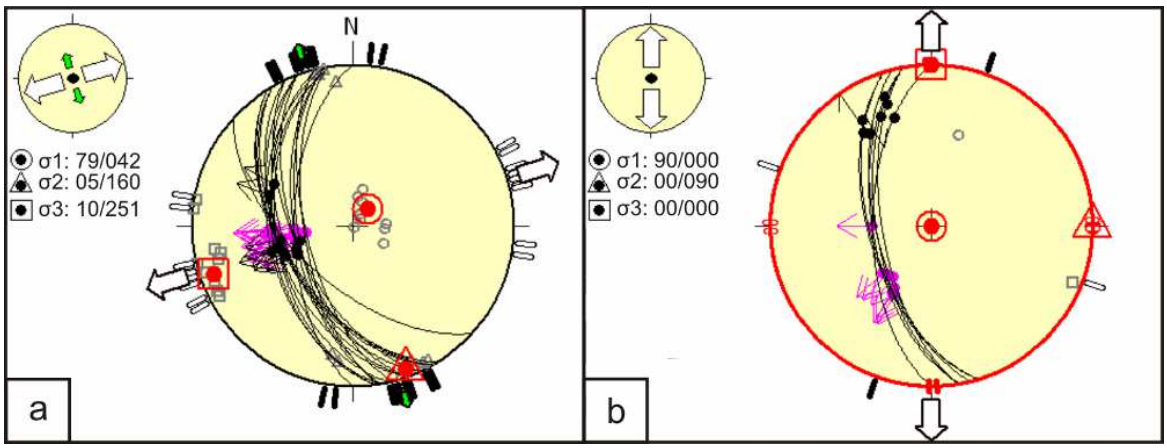

Fig. 2.6 Stereographic representation of the fault and its palaeostress orientations. The fault plane is shown as cyclographic trace with associated slip lines; normal fault is given by a dot with outward arrow for normal faulting. Stress inversion results are represented by σ1 (dot surrounded by circle), σ2 (triangle) and σ3 (square). The small circle on the upper left corner of the figures symbolizes the vertical stress (σv), in this case representing extensional regimes (σ1≈σv). Green arrow: σ2 is subhorizontal; white arrow: σ3 is subhorizontal; outward arrow: extensional deviatoric stress. The fault represents two differently oriented extensions. a ENE-WSW trending extension (slip-line 1). b N-S trending extension (slip-line 2).

C4 are pervaded by a closely spaced vertical jointset with 10-100 cm wide, open fractures (Figs. 2.5c, 2.9c). The joints are filled with well cemented thin-layered (mm thick) marly packstones to wacke- and mudstones. The layers show repeated fining-upward sequences (ca. 1-2 cm). Corallinacean debris is common; *Amphistegina*,

echinoid spines and *Planostegina* are rare. Also reworked limestone clasts (ca. 2 mm), consisting of grainstones with mollusc and corallinacean fragments, commonly occur (Fig. 2.9d).

2.5 Facies analysis and interpretation

10 facies types, including subfacies types, have been distinguished based on lithological and palaeontological characters. The spatial relationship between the facies is indicated in Fig. 2.10.

2.5.1 Basal breccia facies

The basal breccia facies (Figs. 2.7a-b) consists of a monomictic dolostone breccia. Components are subangular and between 1 and 20 cm. Fining-upward sequences are developed in this facies, which is seen in beds 2-4 of section II. The matrix is a silty fine-sand. Towards the top of the fining-upward sequence the amount of matrix is increasing. *Gastrochaenolites* (clavate borings) and *Entobia* (chambers with small channels) within the dolostone clasts are common. The facies directly follows above the dolostone and is overlain by the cross-bedded gravel facies.

Interpretation - The subangular components indicate very short transport within a turbulent water body. A marine environment is evident due to the occurrence of borings, which are referred to the bivalve *Lithophaga* and to clionid sponges. The facies is interpreted as coastal slope scree with breccias in a few metres water depth originating from the rocky shore formed by a dolostone cliff.

2.5.2 Cross-bedded gravel facies

The cross-bedded gravel facies (Figs. 2.7c-d) is exposed in section II and consists of well rounded but poorly sorted polymict gravel (1-7 cm) composed of metamorphic and pegmatitic rocks (Fencl 2005). They are supported by fine-grained quartz-sand reaching 50-70% and occasionally clay up to 25%. Quartz fine-sand layers or dispersed fine-sand lenses of variable thickness (cm to dm) are intercalated within the gravels. The whole succession shows cross-bedding with a dip of ca. 20° to the

NW. Within this facies a limestone bed of the *Acervulina*-rhodolith facies is intercalated, the latter also terminates the cross-bedded gravel facies.

Interpretation -The gravels, which derive from Lower Austroalpine tectonic units (Fencl 2005), are poorly sorted but well rounded with a high fine-sand content. The high degree of roundness indicates a long transport and/or subsequent coastal reworking. The exact provenience of the gravels is still unclear; the source area may be the basement of the Leitha Mountains itself, as part of the Semmering Quartzite (Tollmann 1976). River transport but also marine reworking by coastal breakers in a deltaic system has been discussed by Sohs (1963) and Fencl (2005) and the cross-beddings have been interpreted as foresets (Fencl 2005) originating from a prograding river delta. Marine reworking may be indicated in the uppermost part of the gravel successions, where clear foresets are missing. The dip of the foresets (ca. 20°) indicates a steep alluvial cone of relatively small radius; such characteristics point to a fan delta (cf. McPherson et al. 1987) most likely of Gilbert-type (Postma 1990). The limestone bed within the gravels reports an interruption of river progradation and a slight deepening, maybe during a marine transgression or temporal change in river discharge. In a similar depositional setting, corallinacean limestones formed above a drowned Gilbert-type delta in a water depth of 10-20 m (García-García et al. 2006).

2.5.3 Bioclastic corallinacean facies

In this study the bioclastic corallinacean facies is a unit subsuming sediments predominantly composed of unattached coralline algal branches, rhodoliths and their detritus and is therefore very similar to maërl described from many modern environments (e.g. Cabioch 1968; Keegan 1974; Adey 1986; Steneck 1986; Freiwald et al. 1991; Freiwald 1994). It is neutral in terms of represented coralline algal species, however, it is similar to the *Lithothamnium* facies of Bosence (1976) although *Lithothamnion* is not dominating, and is not defined by certain grain sizes as for example the algal gravel facies (Schlanger and Johnson 1969). The facies comprises packstones, rudstones, and floatstones consisting of angular and sub-rounded corallinacean clasts of fruticose or encrusting growth forms. The corallinaceans are represented by *Lithothamnion*, *Spongites*, *Mesophyllum*, *Lithophyllum*, and *Sporolithon*. Occasionally rhodoliths or *Acervulina*-corallinacean

macroids occur. Bivalves and gastropods occur in variable amounts, as well as regular and irregular echinoids and bryozoans which are represented by celleporiform, branching or crustose growth forms. Foraminifers are represented by rotaliids, such as *Amphistegina*, *Planostegina*, *Asterigerina*, and common cibicidoids, biserial textulariids, miliolids (e.g., *Triloculina*), and rarely globigerinids. The heterogeneity of this facies allows the definition of subfacies types that can be discriminated by the abundance of certain biogenic components and textural differences. Similar Recent sediments occur e.g., in rather low-energy and clear waters of the Mediterranean Sea down to 40 m (Rasser 2000 and further references therein), and in very shallow (less than 10 m) environments e.g., the Gulf of California (Schlanger and Johnson 1969; Halfar et al. 2004).

2.5.4 *Acervulina*-rhodolith subfacies

The *Acervulina*-rhodolith subfacies (Figs. 2.7e-f) is represented by rudstones and floatstones with a packstone matrix and exhibits sub-rounded corallinacean debris (2-5 mm), *Acervulina*-corallinacean macroids (3-5 cm), and laminar spheroidal to ellipsoidal rhodoliths (5-7 cm) with warty surface. The bioclasts of the packstone matrix are poorly sorted consisting of fine-grained debris of corallinaceans, molluscs, and foraminifers. Corallinaceans are dominated by fruticose and encrusting growth forms; thin encrusting growth forms are common. Foraminifers are represented by rotaliids (e.g. *Amphistegina*), biserial textulariids, miliolids, and rare globigerinids. Rare celleporiform bryozoans are commonly encrusted by corallinaceans. Fragments of echinoids rarely occur. The *Acervulina*-rhodolith subfacies is developed in sections I (beds 3, 5, 7) and section II (beds C1, B3 and E4). The facies is also intercalated within the cross-bedded gravel facies and associated with the mollusc subfacies and the *Pinna* subfacies.

Interpretation - The *Avervulina*-rhodolith subfacies shows similarities with the mollusc subfacies but exhibits a high amount of *Acervulina*-corallinacean macroids. It is similar to the bioclastic rhodolith debris facies of Dullo (1983). Also corallinacean rudstones and rhodolith floatstones from the Burdigalian of the Latium-Abruzzi Platform (Brandano and Piller 2010) or Eocene limestones of the Maritime Alps, where *Acervulina*-corallinacean macroids and rhodoliths occur together (Varrone and D'Atri 2007) are similar to this facies.

Pebble- to cobble-sized macroids of *Acervulina inhaerens* (Schultze, 1854), together with corallinaceans are reported from Pacific fore-reef to island shelf areas from approximately 50 to 150 m depth (Iryu et al. 1995) and also from 60 to 100 m depth (Bassi et al. 2011). In the Northern Red Sea *Acervulina inhaerens* occurs from 5-50 m but is dominant below 40 m (Rasser and Piller 1997). Also fossil acervulinid macroids are indicative of environments around 40-50 m (cf. Hottinger 1983; Reid and Macintyre 1988; Prager and Ginsburg 1989; Varrone and D'Atri 2007). Settings with higher water energy for formation of acervulinid macroids are discussed in Perrin (1994) and Varrone and D'Atri (2007).

Although common occurrences of *Acervulina* often indicate deeper water, their dependence on symbionts restricts them to clear water conditions (Hottinger 1983). The occurrence of *Acervulina* in section II (always directly above the gravels) may be caused by turbid water conditions, in which they outcompete corallinaceans (Bosellini and Papazzoni 2003) and make a considerably shallower water depth very likely. The intercalation of this facies within the cross-bedded gravel facies suggests a water depth of 10-20 m (see above).

Corallinacean limestones characterized by this facies, locally show unconformities at the contact to the cross-bedded gravels (Fig. 2.5b). The limestones show influence of freshwater diagenesis, which is indicated by completely dissolved and newly formed crystals that build a mosaic destroying former structures. Such phenomena are influenced by the freshwater phreatic zone (e.g. Dullo 1983). The limestones show dome-shaped topographies (cupolas) at the bottom side of the bed. These structures in combination with freshwater diagenesis of the limestone bed indicate groundwater influence and very likely a hypogenic speleogenesis with hydrothermal influence (Klimcouk 2007). Hydrothermal influence in interaction with hypogenic speleogenesis has already been documented for a cave south of the Baxa Quarry (Plan et al. 2006). The gravels of the Mannersdorf quarry area in that way acted as aquifer. Interspace between gravels and limestones probably vanished due to compaction load. Iron-crusts, which occur in section II, are occasionally of synsedimentary or postsedimentary origin formed along fluid diffusion passages associated with microbial processes (Baskar et al. 2008), occasionally under hydrothermal influence (Konhauser and Ferris 1996).

2.5.5 Mollusc subfacies

The mollusc subfacies (Figs. 2.7g-h) comprises rudstones and floatstones which are characterized by high amounts of various molluscs. The corallinaceans are dominated by corallinacean debris with fruticose growth forms (2-5 mm). Occasionally fragments (200-400 µm) of thin encrusting growth forms are abundant. Mollusc shells are commonly encrusted and often strongly bioeroded before or after encrustation (Fig. 2.7g). The borings are frequently filled with peloids (Fig 2.7g). Aragonitic shells are often dissolved and replaced by sparite. Small thin-shelled bivalves are common in this facies. Foraminifers are represented by rotaliids (*Amphistegina*, *Planostegina*), biserial textulariids, miliolids (e.g., *Triloculina*), and rare globigerinids. Bryozoans (100-200 µm) are rare. The facies is characterized by strong bioturbation; occasionally *Thalassinoides* burrows are preserved. Bivalves are represented by ostreids (e.g. *Hyotissa hyotis* and *Ostrea*), pectinids (*Gigantopecten nodosiformis*), cardiids (*Cardium*), venerids (*Periglypta miocaenica*), glycymeridids (*Glycymeris deshayesi*) and lucinids (*Codakia*). Pectinids are usually disarticulated and randomly distributed, locally they form distinct coquinas. In most cases they are highly bioeroded by sponges and bivalves. Bivalves are commonly articulated and preserved in situ. Gastropods are mainly represented by steinkerns of *Conus*, *Trochus*, *Cerithium*, *Xenophora*, and *Turritella*. Cidarids are usually fragmented, whilst irregular echinoids are well preserved. Cirripedians, polychaetes and fish teeth occur in negligible amounts. The mollusc subfacies characterizes beds 1-5 and 10-14 in section I and beds E4, and the upper part of C8 in section II. The facies is associated with the *Acervulina*-rhodolith subfacies and the bryozoan subfacies.

Interpretation - The facies is equivalent to the bioclastic algal mollusc facies of Dullo (1983) and to the branching algae facies of Studencki (1988, 1999) with its diversified molluscan assemblage. Also the branch-dominated facies of Basso et al. (2008) is similar to this facies. The packstone areas have strong similarities to the bioclastic algal debris facies of Dullo (1983) and the algal branch packstone facies and algal debris wackestone facies of Bosence and Pedley (1979). The packstone areas, consisting of fine-grained bioclastic algal debris, indicate locally high bioturbation (Bosence and Pedley 1982).

Zuschin and Hohenegger (1998), Zuschin et al. (2009) and Janssen et al. (2011) describe comparable mollusc assemblages from the modern Red Sea. There,

turritellids are widely distributed on soft and hard substrates, muddy sediments, and on the reef slope down to 40 m; cerithiids show distinct habitat preferences and occur in water depths between 1 and 40 m with common occurrences between 5 and 30 m whilst xenophorids are common in depths between 40 and 50 m (Janssen et al. 2011). Trochids are abundant in samples from seagrass meadows, reef slopes and sands between coral patches in depths around 5 to 20 m (Zuschin et al. 2009).

Glycymeris is documented from sands between coral patches in depth of ca. 10 m (Zuschin and Hohenegger 1998). Glycymerids and *Periglypta* are also reported from present-day sand bottoms at 10-30 m depth from the Florida Keys (Mikkelsen and Bieler 2008).

The mollusc subfacies is often associated with the *Acervulina*-rhodolith subfacies and the bryozoan subfacies in section I. A similar association has been described by Studencki (1999), who mentions a linkage to the relatively deeper algal-bryozoan facies. The mollusc subfacies very likely represents a shallow transition zone between shallower regimes (*Acervulina*-rhodolith subfacies, see above) and relatively deeper water leading to the bryozoan subfacies (see below). Aside from subtropic faunal elements, modern analogues are coralline algal deposits in the bays of Naples and Pozzuoli in the Mediterranean area (Toscano et al. 2006).

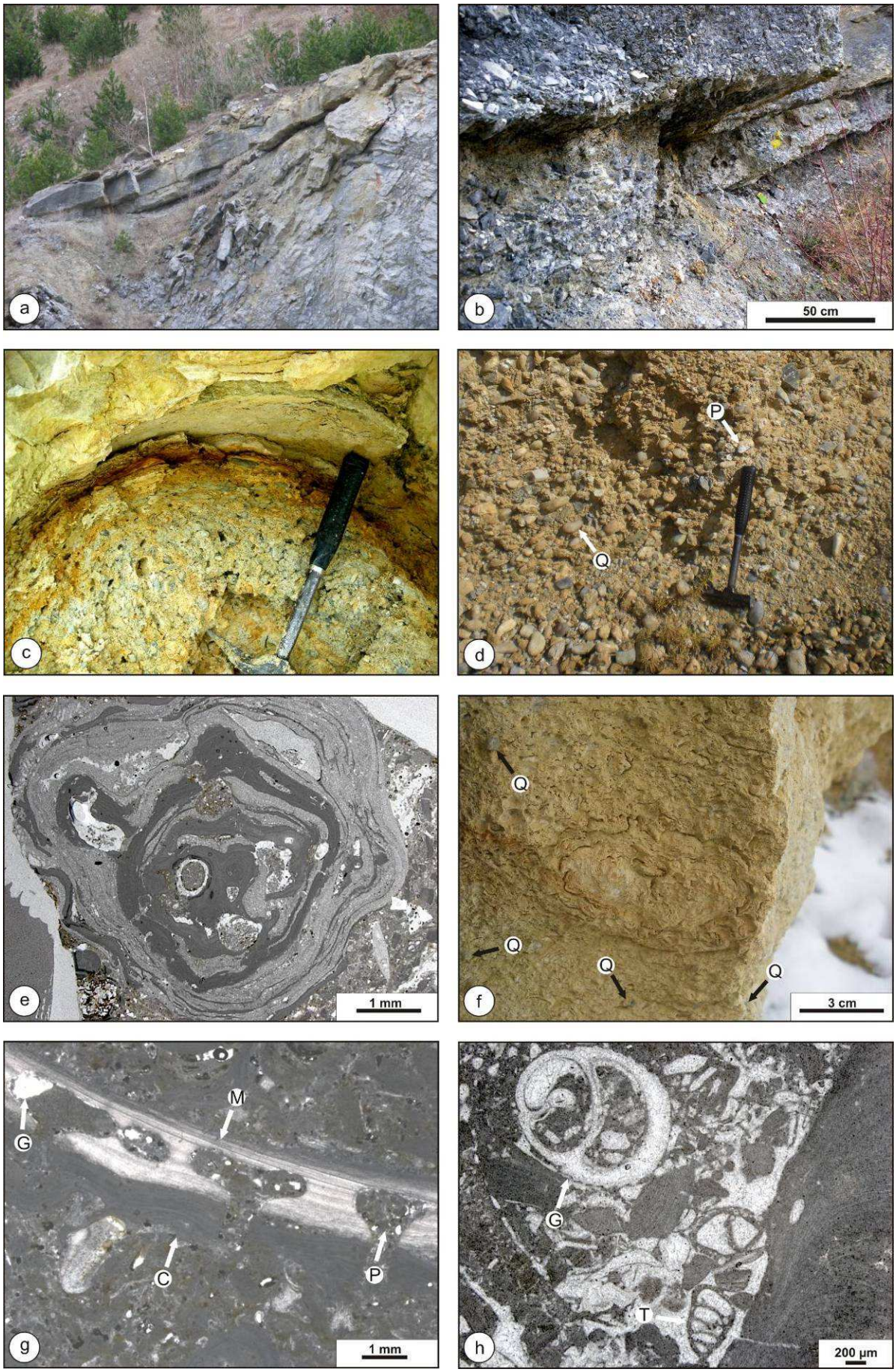
a
b
50 cm
c
P
Q
d
e
1 mm
Q
Q
Q
Q
f
3 cm
M
G
C
P
g
1 mm
G
T
h
200 µm

Fig. 2.7 a-b Basal breccia facies. a Onlap of Badenian dolostone breccias onto Triassic dolostone. b Monomictic dolostone breccia with subangular components (1-20 cm) with internal fining-upward trend. c-d Cross-bedded gravel facies. c Well rounded poorly sorted fine-sand-supported gravel (ca. 5-7 cm) overlain by corallinacean limestone with dome-shaped topography (cupola) inbetween. d Cross-bedded gravel of bed 5 with high amounts of quartz (Q) and paragneiss (P). e-f *Acervulina*-rhodolith subfacies. e *Acervulina*-corallinacean macroid of section II (bed B3). f Corallinacean rudstone (same bed as e) containing ellipsoidal rhodoliths (ca. 7 cm length) and quartz grains (Q). g-h Mollusc subfacies. g Encrusting red algae developed around a calcitic bivalve shell (M) which was bored and filled with peloids (P) after encrustation, showing geopetal fabrics (G). h Corallinacean packstone containing gastropods (G) and textulariids (T).

2.5.6 *Amphistegina subfacies*

The *Amphistegina* subfacies (Figs. 2.8a-b) comprises poorly sorted corallinacean rudstones and floatstones dominated by fragments of fruticose (1-3 mm) and thin encrusting growth forms. The interspace between mostly highly fragmented corallinaceans is filled with corallinacean pack- or wackestones. Mass occurrences of *Amphistegina* are name-giving for this facies. Occasionally, *Amphistegina* is associated with *Planostegina*. Biserial textulariids are common; miliolids are rare. Larger bivalves are represented by *Gigantopecten nodosiformis*, *Glycymeris deshayesi*, and *Panopea menardi*. Branched and celleporiform bryozoans occur in low amounts. Regular and irregular echinoids are rare. The facies is developed in the lower part of bed 13 of section I, in bed C4 of section II and in the beds which onlap onto the dolostone. It is associated with the bryozoan subfacies.

Interpretation - The *Amphistegina* subfacies is similar to the *Pinna* subfacies and *Pholadomya* subfacies in its microfacies but is characterized by the very common occurrence of *Amphistegina*. Recent *Amphistegina* inhabits the tropical to subtropical belt in shallow waters down to 70-80 m (Larsen 1976) where it is primarily attached to macrophytes with high densities (Fujita et al. 2009). Its presence implies a minimum water temperature of 17°C (Adams et al. 1990; Betzler et al. 1995). Some living *Planostegina* inhabit commonly water depths between 15 and 45 m, while others have highest abundances below this depth (cf. Hohenegger 2000; Renema 2006 and further references therein). A typical bivalve of this facies is the deep-burrowing *Panopea menardi*, which occurs in life position (e.g. section II). Modern representatives of *Panopea* live in sandy and muddy substrates preferring shallow subtidal habitats down to 20 m, burrowing between 0.6 and 2 m depth into the sediment (Yonge 1971; Ludbrook and Gowlett-Holmes 1989). A similar facies is present in Badenian corallinacean limestones of Croatia (Basso et al. 2008).
In summary, the *Amphistegina* subfacies has been formed in a shallow, sublittoral environment with a depth range of ca. 20-30 m between the bryozoan subfacies and the mollusc subfacies (Fig. 2.4).

2.5.7 Bryozoan *subfacies*

The bryozoan subfacies (Figs. 2.8c-d) consists of poorly sorted, densely packed rudstones and floatstones. They are dominated by debris of fruticose and encrusting corallinaceans (ca. 3-5 mm). Branched or celleporiform bryozoan colonies (in general ca. 2 mm) are abundant. The bryozoans often form bryoliths of 30-50 mm in diameter, occasionally encrusted by *Acervulina*. Interspaces are filled with bioclastic pack- or wackestones. Rare echinoids are highly fragmented. *Thalassinoides* burrows are common. Foraminifers are represented by common biserial textulariids, miliolids (*Triloculina*), rotaliids (*Amphistegina*) and very rare globigerinids. Molluscs are represented by *Modiolus*, *Gigantopecten nodosiformis*, and ostreids. The facies is developed in section I (bed 5 and 13) and section II (bed C3 and C5). The facies is associated with the *Pholadomya* subfacies and the *Amphistegina* subfacies.

Interpretation - The bryozoan subfacies is similar to the algal-bryozoan facies of Studencki (1988, 1999) but Studencki's facies contain a rich bivalve and brachiopod assemblage. The formation of bryoliths is comparable to that of rhodoliths (James et al. 2006) and similar hydrodynamic conditions can be assumed. The sphericity in bryoliths is thought to be in part related to the turning frequency (Rider and Enrico 1979); Barbera et al. (1978) interpreted similar sediments as shallow deposits with sufficient water energy for rhodolith movement. A depth estimate of ca. 30 m is given by Studencki (1988). Modern analogues are found on the Apulian shelf along the shore in ca. 10-30 m water depth (Sarà 1969; Toscano and Sorgente 2002). The bryozoan subfacies is associated with the *Amphistegina* subfacies (section I, section II), the *Pholadomya* subfacies (section II), the mollusc subfacies (section I) and the coral debris subfacies (section II). A water depth deeper than that of the mollusc subfacies can be assumed.

2.5.8 Coral debris subfacies

The coral debris subfacies (Figs. 2.8e1-e2) comprises moderately sorted corallinacean-coral rudstones. The corallinaceans are dominated by debris (3-10 mm) of fruticose growth forms but thin encrusting corallinaceans or encrusting foraminifera (*Acervulina*) are also common. The corals are represented by *Porites* and delicate (ca. 3 mm in diameter) branched corals. The corals are usually

fragmented; in situ colonies of *Porites* are less common. Corals are often encrusted by corallinaceans. Foraminifers occur in variable amounts, occasionally dominated by biserial textulariids and miliolids, occasionally by rotaliids (*Amphistegina*). The associated bivalve fauna is dominated by ostreids (mainly *Hyotissa hyotis* and *Ostrea*), pectinids, such as *Gigantopecten nodosiformis*, cardiids (*Cardium*), venerids (*Periglypta miocaenica*), glycymeridids (*Glycymeris deshayesi*) and lucinids (*Codakia*). Gastropods are represented by *Conus* and *Cerithium*. Associated with the corals is the cirriped *Pyrgoma multicostatum*. The facies occurs in section II (bed 2 as small patches, bed 6 and 8) and is associated with the rhodolith facies.

Interpretation - The coral debris subfacies is similar to the mollusc subfacies in its microfacies and is an equivalent of the modern bivalve/coral-communities of Riegl and Piller (2000) and the 'coral-red algal rudstone-floatstone' of Conesa et al. (2005). The latter authors interpret these limestones as deposits in a high- to moderate-energy environment within or near coral patch reefs. The density of the corals within the limestones in the Mannersdorf sections is rather low and the corals, except *Porites*, which is found in situ, are strongly fragmented. However, these colonies and the associated debris are comparable to the 'coral interval 5' of Riegl and Piller (2000), described from the Fenk quarry. This interval was interpreted as a sparse *Porites*-community on a subtidal soft- or firmground, which formed in a depth range from 3-7 metres (Riegl and Piller 2000).
Thus, the coral debris subfacies represents deposits in a shallow high- to moderate-energy environment. Similar to the Fenk quarry, the coral patches of Mannersdorf might have formed in less than 10 m water depth.

2.5.9 *Pholadomya subfacies*

The *Pholadomya* subfacies (Fig. 2.8f) comprises poorly sorted corallinacean rudstones and floatstones. It is dominated by thin encrusting corallinacean growth forms but fruticose growth forms also occur. Branched and celleporiform bryozoans are common, occasionally encrusted by corallinaceans. Foraminifers are represented by biserial textulariids and rotaliids (*Amphistegina*). The facies is characterized by the occurrence of in situ *Pholadomya alpina* (Matheron, 1842) with a total length of 10-15 cm. The associated bivalve fauna consists of *Periglypta miocaenica* and ostreids.

Corals are represented by fragmented delicate branched forms. Echinoids occur as isolated spines or highly fragmented coronae. The facies is developed in section II (bed C2) and is associated with the bryozoan subfacies.

Interpretation - The *Pholadomya* subfacies shows similarities to the *Amphistegina* subfacies and the *Pinna* subfacies in microfacies but is characterized by in situ occurrences of *Pholadomya*. Extant Pholadomyidae are deep burrowing bivalves (Runnegar 1974). Recent *Pholadomya candida* (Sowerby, 1823) burrows in coralline algal sands and seagrass beds (Díaz and Borrero 1995; McIntyre 2010) and was detected in a water depth of 9 to 25 m (Díaz and Borrero 1995).
A *Pholadomya* facies has already mentioned for Bajocian limestone deposits (Lathuilière 1982). Cretaceous counterparts of the *Pholadomya* subfacies, as described by Lazo (2007) and Armella et al. (2007) are indicative of oxygenated waters of shoreface to inner shelf environments with soft to firm, sandy and bioclastic substrates. The in situ shells of *Pholadomya alpina* (Matheron, 1842) indicate insufficient water energy for exhumation. Recent *Pholadomya* are relatively sensitive to sediment disturbance and indicate deeper water (ca. 40-60 m) with low currents (Schneider 2008). A rather calm sublittoral depositional environment in the aforementioned depth can be postulated for the *Pholadomya* subfacies of Mannersdorf. It indicates the deepest setting in the successions.

2.5.10 *Pinna subfacies*

The *Pinna* subfacies (Figs. 2.8g-h) comprises poorly sorted marly corallinacean rudstones with packstone matrix, and small lenses of quartz fine-sand and silty clay horizons. The bioclasts have diameters up to 4 mm. The cementation of the limestones varies from very porous to well cemented. The corallinaceans are dominated by encrusting and fruticose growth forms but thin encrusting growth forms can dominate locally. The packstone matrix comprises bioclasts of corallinaceans, mollusc debris and foraminifers. Foraminifers are dominated by textulariids and rotaliids such as *Amphistegina*; miliolids are generally rare. Local concentrations of *Amphistegina* occur. The mollusc fauna is characterized by *Pinna tetragona*, which commonly occurs in situ. Additional mollusc taxa are *Gigantopecten nodosiformis*, *Aequipecten malvinae* (du Bois de Montpereux, 1831), *Ctena decussata*, *Periglypta miocaenica*, *Glycymeris deshayesi*, *Glans subrudista*, cardiids, and poorly preserved

rissoid gastropods. Regular and irregular echinoid remains occur in variable amounts. Celleporiform bryozoans are locally common. Single branches of *Porites* of 2-3 cm length and *Thalassinoides* burrows are typical. The facies is developed in section I (bed 6-9 and the lower part of bed 10) and is associated with the *Acervulina*-rhodolith subfacies and the mollusc subfacies.

Interpretation - The *Pinna* subfacies is similar to the *Amphistegina* subfacies in its microfacies but is characterized by in situ occurrences of the fan mussel *Pinna tetragona*. Modern pinnids are shallow marine endobyssate suspension-feeders, which are attached by their byssus to the substrate (Richardson et al. 1999). They occur at depths between 0.5 and 60 m within seagrass meadows, half- to mostly embedded in the sediment (Zavodnik et al. 1991; Hofrichter 2002; Rabaoui et al. 2007; Mikkelsen and Bieler 2008). The Recent *Pinna nobilis* (Linnaeus, 1758) is reported in the Mediterranean sea from sandy bottoms in about 3 m water depth, preferentially close to seagrass meadows (Riedl 1983). *Pinna bicolor* (Gmelin, 1791) occurs in South Australia in ca. 7 m water depth (Keough 1984). In sheltered areas, they can also be found in very shallow waters, including intertidal flats (Yonge 1953; Stanley 1970; Butler et al. 1993). The lucinid bivalve *Ctena decussata*, which bears chemosymbiotic bacteria, also prefers shallow seagrass meadows (Taylor and Glover 2000). At Mannersdorf this bivalve is restricted to the *Pinna* subfacies. Modern counterparts of *Codakia* also bear chemosymbiotic bacteria and settle preferentially within seagrass meadows (Schweimanns and Felbeck 1985) but *Porites* can develop small patches within seagrass environments (Riegl and Piller 2000; Wulff 2008). Quartz fine-sand lenses and clay horizons might go back to the baffling of seagrasses (Tucker and Wrigth 1990).
Hence, the *Pinna* subfacies has developed in a very shallow environment (< 10 m) in moderately agitated water within seagrass meadows. Low oxygen conditions in the sediment might be indicated by the abundance of lucinids (Emery and Hulseman 1962). Such conditions can be caused by decomposition of large quantities of organic material (Eyre and Ferguson 2002), mostly seagrass.

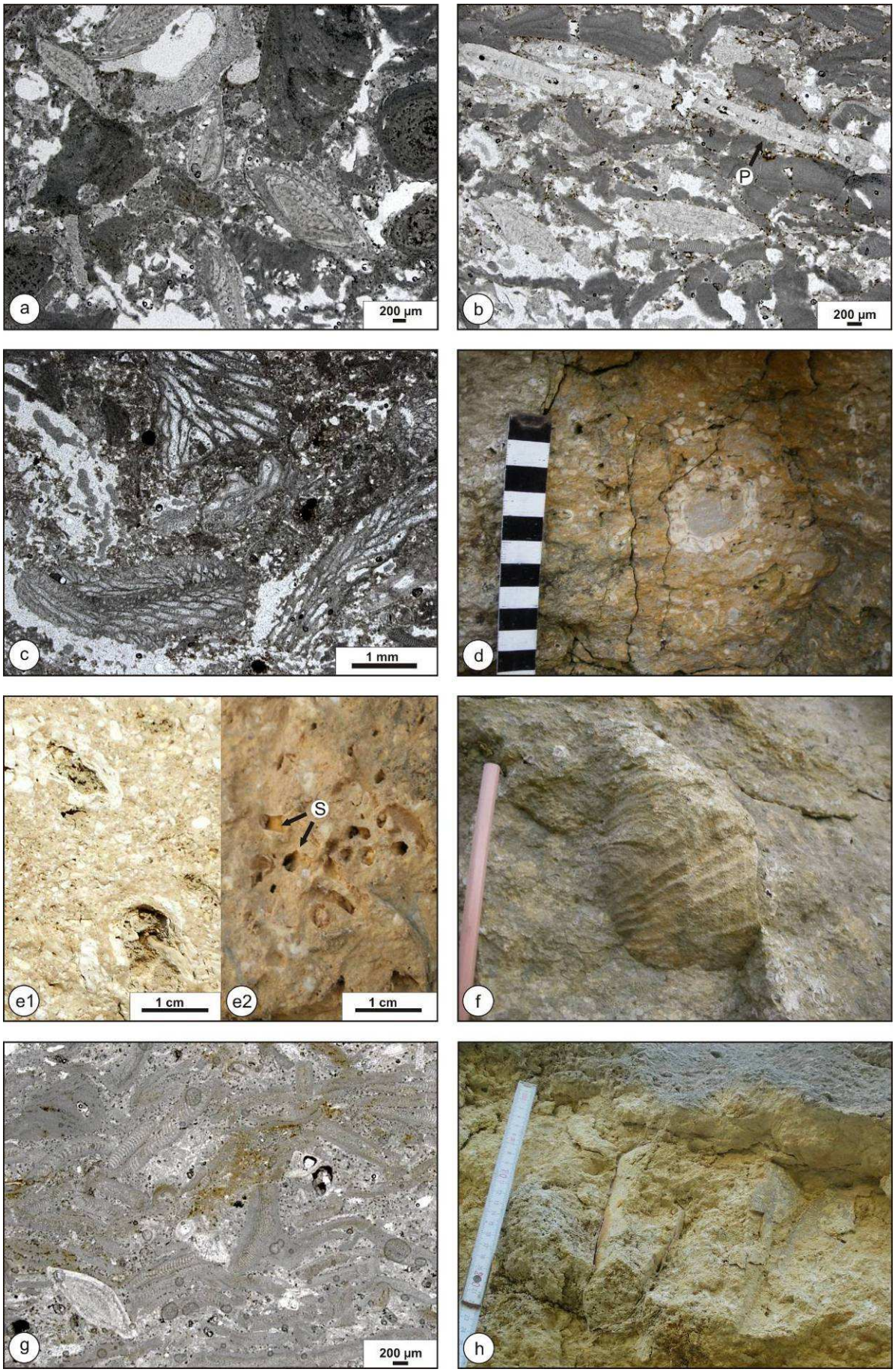
a
200 µm
b
P
200 µm
c
1 mm
d
e1
1 cm
e2
S
1 cm
f
g
200 µm
h

Fig. 2.8 a-b *Amphistegina* subfacies. a Corallinacean rudstone with common *Amphistegina* (A) and corallinacean debris. b Association of *Amphistegina* and *Planostegina* (P) within a corallinacean packstone with common thin encrusting growth forms. c-d Bryozoan subfacies. c Debris of branched bryozoans within a corallinacean packstone. d Corallinacean floatstone with red algae encrusting a celleporiform bryozoan forming a rhodolith. e1-e2 Coral debris subfacies. e1 Corallinacean rudstone containing debris of branched *Porites* encrusted by corallinaceans. e2 Corallinacean rudstone containing debris of *Stylocora*? (S). f *Pholadomya* subfacies. Corallinacean floatstone with in situ *Pholadomya alpina* (pencil for scale). g-h *Pinna* subfacies. g Packstone matrix of a corallinacean rudstone dominated by thin encrusting growth forms. h Shell remains and steinkern of in situ *Pinna tetragona* within a corallinacean rudstone.

2.5.11 Rhodolith facies

The rhodolith facies (Figs. 2.9a-b) is characterized by a poorly cemented corallinacean rudstone dominated by densely packed, mostly spheroidal to ellipsoidal rhodoliths, cm to dm in size, with a warty surface. Interspaces between rhodoliths are filled with clasts of corallinaceans with fruticose and encrusting growth forms. *Acervulina* often encrusts corallinaceans. Other components are formed by molluscs (ostreids) and encrusting bryozoans. Foraminifers are represented by rotaliids (*Amphistegina*) and miliolids (*Triloculina*). The facies is developed in section II (bed C7). It is associated with the coral debris subfacies.

Interpretation - The facies is similar to the rhodolith pavement facies of Dullo (1983) near St. Margarethen. According to Steneck (1986), rhodolith pavements are formed by unattached coralline algae including rhodoliths. A palaeoenvironmental interpretation, based only on rhodolith morphologies, is difficult due to the complex interplay between water movement, transport, substrate type, and bioturbation (Steller and Foster 1995; Marrack 1999; Foster 2001; Bassi et al. 2009). As a rule of thumb, low-energy environments are characterized by open branched rhodoliths, whilst high water agitation is reflected by massive, densely branched or even laminar rhodolith growth forms (Bosence 1979, 1983, 1991; Bosence and Pedley 1982, Studencki 1988).

The shapes of rhodoliths in Mannersdorf fit well with the mainly spheroidal IG-Type of Bassi et al. (2006), which is interpreted to be indicative of moderate to high water turbulence and low substrate stability. However, similar sediments of the Latium-Abruzzi Platform show no indication of high current regimes. These limestones rather indicate low sedimentation rates and biogenically induced periodic turning (Brandano and Piller 2010). This may be induced by crustaceans or foraging fish (Marrack 1999). Hence the rhodolith facies seems to reflect a very shallow water depth with hydrodynamics similar to the *Acervulina*-rhodolith subfacies. This facies is similar to Recent rhodolith accumulations described from the Gulf of California, Ryukyu Islands and Lord Howe Island (Bassi and Nebelsick 2010 and further references therein). Rhodolith belts in the modern Red Sea are adjacent to seagrass meadows and coral zones (cf. Piller and Rasser 1996).

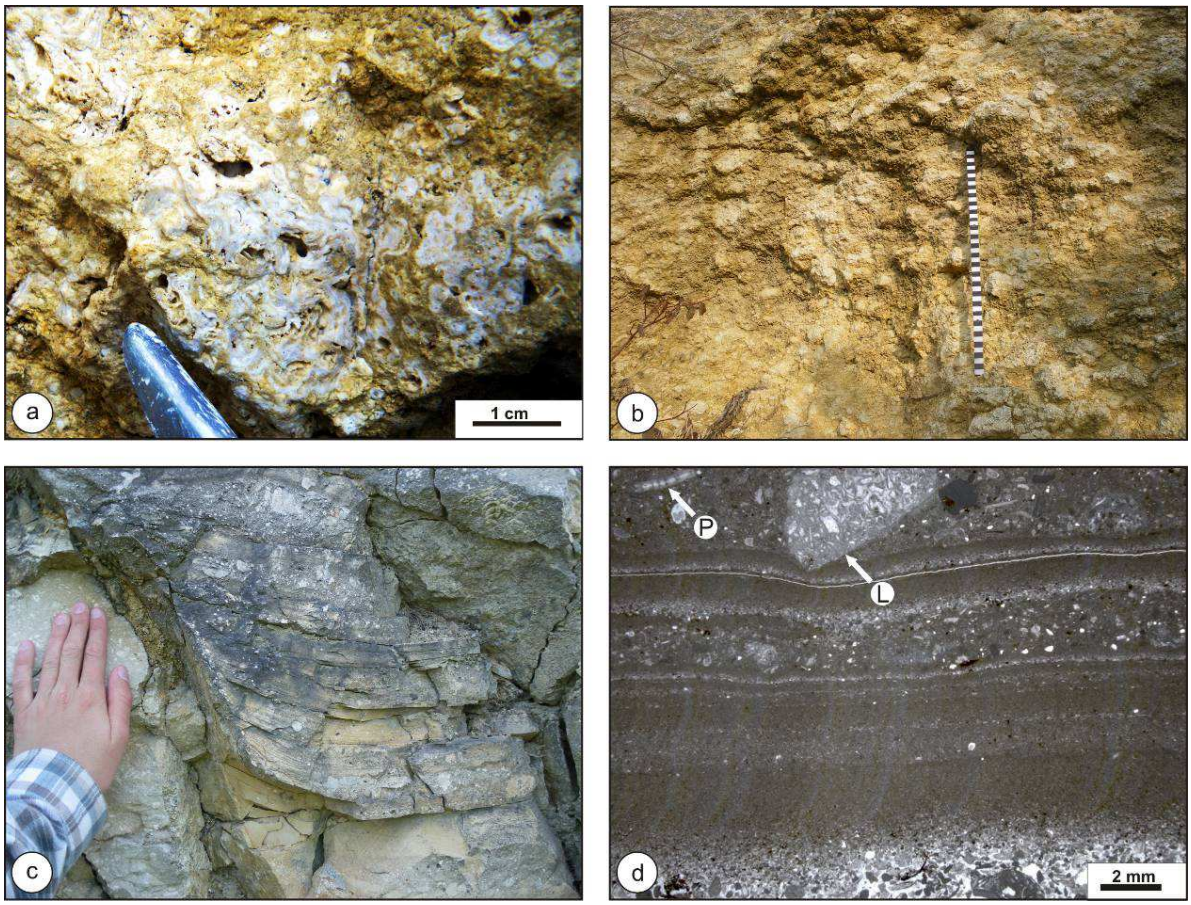

Fig. 2.9 a-b Rhodolith facies. a Ellipsoidal rhodoliths with warty surfaces. b Accumulations of densely packed sphaeroidal to ellipsoidal rhodoliths. c-d Neptunian dyke. c Fissure (hand for scale) filled with well cemented thin mm-layered marly pack-, wacke-, and mudstone. d Reworked clast (L) forming a load cast on laminated layers below, *Planostegina* (P).

2.5 Facies zonations

Combining the results of field observations and microfacies analysis, a facies zonation for the Mannersdorf locality can be developed for the subtypes of the bioclastic corallinacean facies and for the rhodolith facies.

In very shallow settings (<10 m) the *Pinna* subfacies is developed, which represents seagrass meadows baffling sand and mud under moderate water energy. The coral debris subfacies and the adjacent rhodolith facies developed in a similar water depth with higher water energy. The *Acervulina*-rhodolith subfacies, intercalated within gravels or terminating the latter, indicates slight deepening due to marine transgression. The *Acervulina*-rhodolith subfacies is adjoining to the mollusc subfacies, which represents a deeper environment (ca. 20-30 m) with moderate water energy. It is associated with the *Amphistegina* subfacies which again mirrors deeper water with a range of 20 to 30 m. Transitions from the mollusc subfacies to the bryozoan subfacies go along with deeper water (below 30 m) and lower energy levels. The deepest setting is represented by the *Pholadomya* subfacies indicating a water depth of ca. 40-60 m with low water energy. The remaining facies types of Mannersdorf belong to a separate system. The basal breccia facies and the cross-bedded gravel facies represent high energy environments with a few metres of water depth. While the basal breccia facies represents coastal scree onlapping on a cliff, the cross-bedded gravel facies shows characteristics of a prograding delta.

2.6 Facies succession and synsedimentary tectonics

Deposition of the lowermost sediments started during rising relative sea-level with the development of dolostone breccias and river-transported gravels (Fig. 2.5a). A relative sea-level rise is indicated by onlapping of the dolostone breccia onto the dolostone. The limestone bed intercalated within the gravels may reflect a distinct transgressive pulse. It is again overlain by gravels of a prograding river delta. The gravel body is terminated by corallinacean limestones (Fig. 2.10a), which indicate a strong relative sea-level rise by development of the deepest sediments. They are characterized by the common occurrence of *Pholadomya alpina*, which prefers calmer, deeper habitats. Falling relative sea-level (Fig. 2.5b) is indicated by a shallowing-upward trend expressed in facies types deposited in relatively shallower

marine settings. Onsetting tectonic movement divided the area into two independent blocks (Fig. 2.10b). The tectonic movements (Fig. 2.6) verify a normal-fault (south-western block as hanging wall) with dextral strike-slip tectonics due to ENE-WSW and N-S trending extensions. The fault zone shows a normal fault reactivated as a dextral strike-slip fault. A flexure enabled the onlap of sediments. This happened during a relative sea-level fall (indicated by deposition of the *Acervulina*-rhodolith facies in section I). At the same time, a relative sea-level fall led to erosion or non-deposition on the north-eastern block (footwall) indicated by an unconformity in section II. The rapid facies change from the bryozoan subfacies to the coral debris subfacies (bed C5 to C6) also indicates a break in sedimentation. On the south-western block, sedimentation kept up with subsidence and gradually changed from deeper to shallower facies types. With relative rise of sea-level shallow-water carbonates were formed on both blocks (Fig. 2.10c), represented by the coral debris subfacies on the north-eastern block and the *Pinna* subfacies on the south-western block. During tectonic activity also the jointset in section II was formed, which was filled with fine-grained sediments and therefore acted as a neptunian dyke (Fig. 2.5c). With ongoing relative sea-level rise (Fig. 2.10d) the *Amphistegina* subfacies developed on both tectonic blocks, onlapping onto the dolostone in a water depth of ca. 20-30 m. Its deposition indicates tectonic inactivity and burial of the fault.

In comparison with the Fenk quarry at the south-western edge of the Leitha Mountains, which reflects environments similar to the modern Red Sea and the Arabian Gulf (Riegl and Piller 2000), the poor coral fauna and some mollusc assemblages have more similarities to modern environments (such as seagrass meadows) represented in the Florida Keys (e.g., Mikkelsen and Bieler 2008).

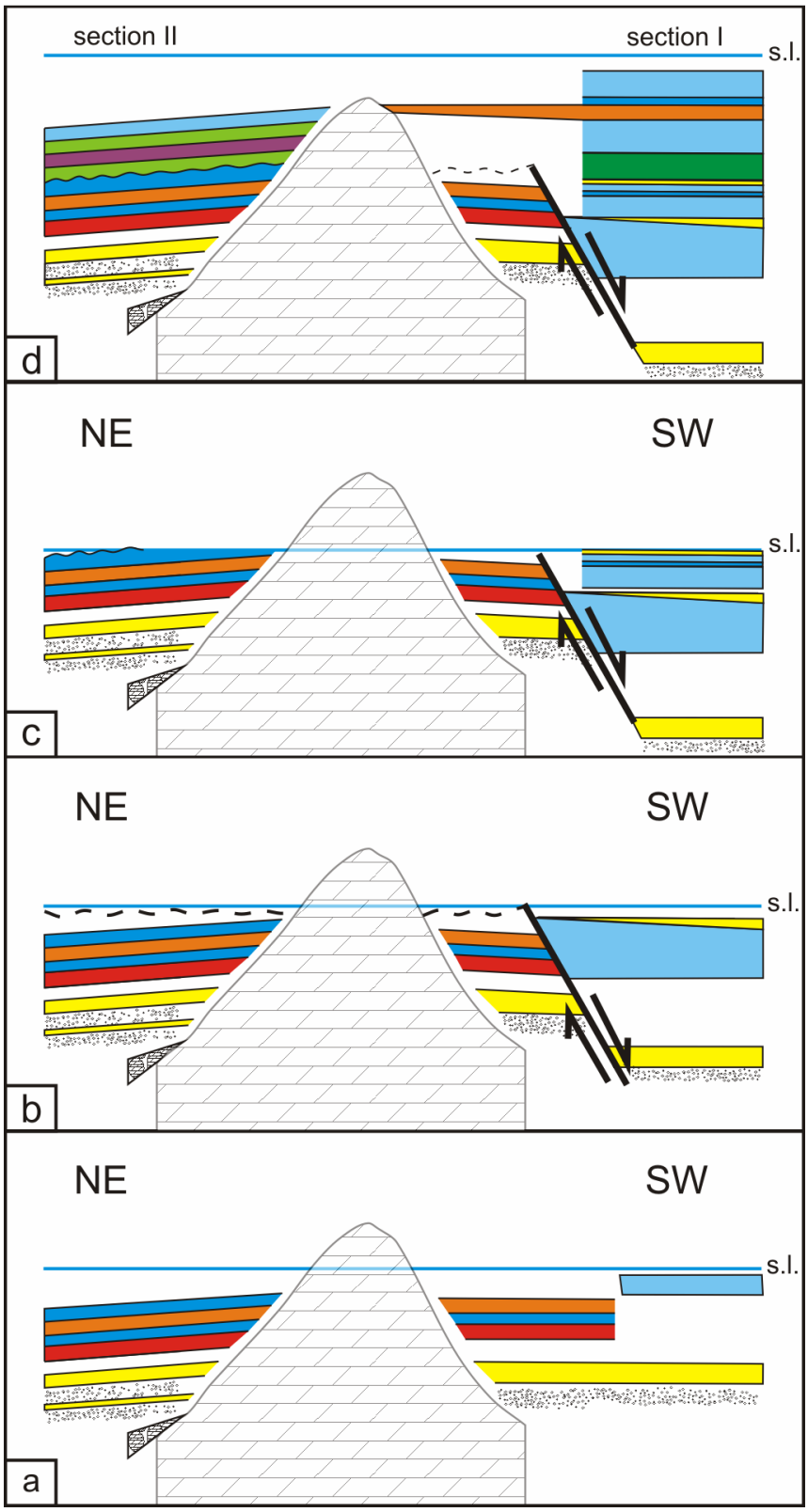

Fig. 2.10 Depositional model illustrating tectonic activity. Arrows show displacement directions during thrusting. Facies types are highlighted with colours (cf. Fig. 3). Starting with undisturbed sedimentation (a), a phase of synsedimentary tectonics (b-c) follows. The last stage is characterized by flooding and undisturbed sedimentation (d).

2.7 Conclusions

The Leitha Limestones of the Mannersdorf quarries (Lower Austria) preserve records of pre-, syn-, and post-tectonical phases of carbonate deposition on a Badenian shallow water carbonate platform in the Vienna Basin with a transition from a siliciclastic to a carbonate depositional environment. The pre-tectonical phase is represented by the flooding of a Mesozoic dolostone during a marine transgression with the development of a coastal slope scree and subsequent progradation of a Gilbert-type fan delta. Facies analyses of the overlying very heterogeneous corallinacean limestones reveals a continuous water depth increase by the vertical transition from the *Acervulina*-rhodolith subfacies to the bryozoan subfacies and the *Pholadomya* subfacies. Subsequently, a fault divided the study area into a northern and a southern tectonic block. Palaeostress analyses verify a normal fault reactivated as a dextral strike-slip fault. This syn-tectonical phase corresponds with a relative sea-level fall. While the northern block was partly eroded, the southern block indicates tectonical movements with onlap of limestones on a tectonic-caused flexure and development of seagrass meadows (*Pinna* subfacies). A post-tectonic phase with renewed marine transgression and onlapping of deeper water carbonates (*Amphistegina* subfacies) on the dolostone is indicated by burial of the fault and development of a neptunian dyke. A facies model comprising corallinacean limestones of both blocks combines the results of field observations and microfacies analysis and illustrates transitions from shallow-water carbonates such as the *Pinna* subfacies to the deepest observed carbonates, represented by the *Pholadomya* subfacies.

2.8 Acknowledgments

This paper was financed by the “NAWI Graz Advanced School of Science” (GASS). Field work was kindly encouraged by the Lafarge-Perlmooser AG; special thanks go to the raw material- and quarry manager Dipl.-Ing. Ralf Baehr-Mörsen for his support. Many thanks go to Dr. Markus Reuter (University of Graz), Dr. Ulrike Exner (University of Vienna) and Dr. Harald Fritz (University of Graz) for constructive discussions. For determination of bivalve remains we would like to thank Dr. Oleg Mandic (Natural History Museum Vienna), for determination of echinoid remains Dr. Andreas Kroh (Natural History Museum Vienna). Thanks also go to Hans Schwengersbauer (Mannersdorf museum of local history) for reports of decades of mining activity. Finally, we thank Dr. Steven J. Weiss (University of Graz) for improving the English of the manuscript. The manuscript benefitted from the constructive comments of the reviewers Dr. Martin Zuschin (University of Vienna) and Dr. James Nebelsick (University of Tübingen), and from the editorial advice of Dr. Franz Theodor Fürsich (University of Erlangen-Nürnberg).

2.9 References

Adams GC, Lee DE, Rosen BR (1990) Conflicting isotopic and biotic evidence for tropical sea-surface temperatures during the Tertiary. Palaeogeogr Palaeoclimatol Palaeoecol 77:289–313

Adey WH (1986) Coralline algae as indicators of sea-level. In: Van de Plassche O (ed) Sea-level research: a manual for the collection and evaluation of data. Geo Books, Norwich, England, pp 229–280

Armella C, Cabaleri N, Leanza HA (2007) Tidally dominated, rimmed-shelf facies of the Picún Leufú Formation (Jurassic/Cretaceous boundary) in southwest Gondwana, Neuquén Basin, Argentina. Cret Res 28:961–979

Barbera C, Simone L, Carannante G (1978) Depositi circalittorali di piattaforma aperta nel Miocene Campano. Analisi sedimentologica e paleoecologica. Boll Soc Geol It 97:821–834

Baskar S, Baskar R, Natuschka L, Kaushik A, Theophilus PK (2008) Precipitation of iron in microbial mats of the spring waters of Borra Caves, Vishakapatnam, India: some geomicrobiological aspects. Environ Geol 56:237–243

Bassi D, Carannante G, Monleau C, Murru M, Simone L, Toscano F (2006) Rhodalgal/bryomol assemblages in temperate type carbonate, channelized depositional systems: the Early Miocene of the Sarcidano area (Sardinia, Italy). In: Pedley HM, Carannante G (eds) Cool-water carbonates. Depositional systems and palaeoenvironmental controls. Geol Soc Spec Publ 255:35–52

Bassi D, Humblet M (2011) Recent ichnocoenosis in deep water macroids, Ryukyu Islands, Japan. Palaios 26:232–238

Bassi D, Nebelsick JH (2010) Components, facies and ramps: Redefining Upper Oligocene shallow water carbonates using coralline red algae and larger foraminifera (Venetian area, northeast Italy). Palaeogeogr Palaeoclimatol Palaeoecol 295:258–280

Bassi D, Nebelsick JH, Checconi A, Hohenegger J, Iryu Y (2009) Present-day and fossil rhodolith pavements compared: Their potential for analysing shallow-water carbonate deposits. Sediment Geol 214:74–84

Basso DM, Vrsaljko D, Grgasović T (2008) The coralline flora of a Miocene maërl: the Croatian "Litavac". Geol Croatica 61(2-3):333–340

Betzler C, Brachert TC, Kroon D (1995) Role of climate for partial drowning of the Queensland Plateau carbonate platform (northeastern Australia). Mar Geol 123:11–32

Bosellini F, Papazzoni C (2003) Paleoecological significance of coral-encrusting foraminifera associations: a case-study from the Upper Eocene of northern Italy. Acta Palaeont Polon 48:279–292

Bosence DWJ (1976) Ecological studies on two unattached coralline algae from western Ireland. Palaeontology 19:365–395

Bosence DWJ (1979) Live and dead faunas from coralline algal gravels, Co. Galway. Palaeontology 22:449–478

Bosence DWJ (1983) Coralline algae from the Miocene of Malta. Palaeontology 26:147–173

Boscence DWJ (1991) Coralline algae: mineralization, taxonomy, and palaeoecology. In: Riding R (ed) Calcareous algae and stromatolites, Springer, Berlin, pp 98–113

Bosence DWJ, Pedley HM (1979) Palaeoecology of a Miocene coralline algal bioherm. Malta. Bull Centr Rech Expl Prod Elf-Aquitaine 3:463–470

Bosence DWJ, Pedley HM (1982) Sedimentology and palaeoecology of a Miocene coralline algal biostrome from the Maltese Islands. Palaeogeogr Palaeoclimatol Palaeoecol 38:9–43

Brandano M, Piller WE (2010) Coralline algae, oysters and echinoids - a liaison in rhodolith formation from the Burdigalian of the Latium-Abruzzi Platform (Italy). In: Mutti M, Piller WE, Betzler C (eds) Carbonate systems during the Oligocene-Miocene climatic transition. Int Assoc Sedimentol Spec Publ 42:149–164

Butler AJ, Vicente N, De Gaulejac B (1993) Ecology of the pterioid bivalves *Pinna bicolor* Gmelin and *Pinna nobilis* L. Mar Life 3:37–45

Cabioch L (1968) Contribution à la connaissance des peuplements benthiques de la Manche occidentale. Cah Biol Mar 9: 493–720

Conesa GAR, Favre E, Münch P, Dalmasso H, Chaix C. (2005) Proceedings of the Ocean Drilling Program (Northeast Australia, ODP Leg 194, Sites 1196 and 1199). In: Anselmetti F, Isern AR, Blum P, Betzler C (eds) Proc ODP Sci Results 194: 1-38

Decker K (1996) Miocene tectonics at the Alpine-Carpathian junction and the evolution of the Vienna basin. Mitt. Ges Geol Bergbaustud Österr 41:33–44

Decker K, Peresson H (1996) Tertiary kinematics in the Alpine-Carpathian-Pannonian system: links between thrusting, transform faulting and crustal extension. In: Wessely G, Liebl W (eds) Oil and gas in Alpidic thrusts and basins of Central and Eastern Europe. Eur Assoc Geosci Eng Spec Publ 5:69–77

Delvaux D, Sperner B (2003) Stress tensor inversion from fault kinematic indicators and focal mechanism data: the TENSOR program. In: Nieuwland D (ed) New insights into structural interpretation and modelling: Geol Soc Lond Spec Publ 212:75–100.

Díaz JM, Borrero FJ (1995) On the occurrence of *Pholadomya candida* Sowerby, 1823 (Bivalvia: Anomalodesmata) on the Caribbean coast of Colombia. J Moll Stud 61:407–408

Dullo WC (1983) Diagenesis of fossils of the Miocene Leitha Limestone of the Paratethys, Austria: An example for faunal modifications due to changing diagenetic environments. Facies 8:1–112

Dunham RJ (1962) Classification of carbonate rocks according to their depositional texture. In: Ham WE (ed) Classification of carbonate rocks–a symposium. Am Assoc Petrol Geol Mem 1:108–121

Embry AF, Klovan JE (1971) A Late Devonian reef tract on Northeastern Banks Island, NWT. Can Petrol Geol Bull 19:730–781

Emery KO, Hulsemann J (1962) The relationship of sediments, life, and water in a marine basin. Deep-Sea Res 8:165–180

Eyre BD, Ferguson AJP (2002) Comparison of carbon production and decomposition, benthic nutrient fluxes and denitrification in seagrass, phytoplankton, benthic microalgal and macroalgal dominated warm temperate Australian lagoons. Mar Ecol-Prog Ser 229:43–59

Fencl M (2005) Sedimentologie der klastischen Miozän-Abfolgen in Mannersdorf am Leithagebirge (Niederösterreich). Unpubl. Diploma Thesis, Univ. Wien

Fodor L (1995) From transpression to transtension: Oligocene-Miocene structural evolution of the Vienna basin and the East Alpine-Western Carpathian junction. Tectonophysics 242:151–182

Foster MS (2001) Rhodoliths: between rocks and soft places. J Phycol 87:659–667

Freiwald A (1994) Sedimentological and biological aspects in the formation of branched rhodoliths in northern Norway. Beitr Paläontol Österr 20:7–19

Freiwald A, Henrich R, Schäfer P, Willkomm H (1991) The significance of high-boreal to subarctic maerl deposits in northern Norway to reconstruct Holocene climatic changes and sea level oscillations. Facies 25:315–340

Fuchs T (1894) Ueber abgerollte Blöcke von Nulliporen-Kalk im Nulliporen-Kalk von Kaisersteinbruch. Z Deutsch Geol Ges 46: 126–130

Fujita K, Osawa Y, Kayanne H, Ide Y, Yamano H (2009) Distribution and sediment production of large benthic foraminifers on reef flats of the Majuro Atoll, Marshall Islands. Coral Reefs 28:29–45

García-García F, Fernández J, Viseras C, Soria JM (2006) High frequency cyclicity in a vertical alternation of Gilbert-type deltas and carbonate bioconstructions in the late Tortonian, Tabernas Basin, southern Spain. Sediment Geol 192:123–139

Häusler H, Figdor H, Hammerl C, Kohlbeck F, Lenhardt W, Schuster R (2010): Geologische Karte der Republik Österreich 1:50.000, Erläuterungen zu Blatt 78 RUST. Geologische Bundesanstalt, Wien

Harzhauser M, Piller WE (2004) The Early Sarmatian–hidden seesaw changes. Cour Forschinst Senckenberg 246:89–111

Harzhauser M, Piller WE (2007) Benchmark data of a changing sea – Palaeogeography, palaeobiogeography and events in the Central Paratethys during the Miocene. Palaeogeogr Palaeoclimatol Palaeoecol 253:8–31

Harzhauser M, Piller WE (2010) Molluscs as a major part of subtropical shallow-water carbonate production - an example from a Middle Miocene oolite shoal (Upper Serravallian, Austria). Spec Publ Int Ass Sed 42:185–200

Herrmann P (1973) Geologie der Umgebung des östlichen Leithagebirges (Burgenland). Mitt Ges Geol Bergbaustud Österr 1973:165–189

Herrmann P, Pascher GA, Pistotnik J (1993) Geologische Karte der Republik Österreich 1.50.000, Blatt 78 Rust. Geol Bundesanstalt, Wien

Hölzel M, Wagreich M, Faber R, Strauss P (2008) Regional subsidence analysis in the Vienna Basin (Austria) - Austr J Earth Sci 101:88–98

Hofrichter R (2002) Das Mittelmeer – Fauna, Flora, Ökologie, Band I: Allgemeiner Teil, Spektrum Akademischer Verlag, Heidelberg, Berlin

Hohenegger J, Wagreich M (2011) Time calibration of sedimentary sections based on isolation cycles using combined cross-correlation: dating the gone Badenian stratotype (Middle Miocene, Paratethys, Vienna Basin, Austria) as an example. Int J Earth Sci (Geol Rundsch) doi: 10.1007/s00531-011-0658-y

Hohenegger J, Yordanova E, Hatta A (2000) Remarks on West Pacific Nummulitidae (Foraminifera). J Foram Res 30:3–28

Hottinger L (1983) Neritic macroid genesis, an ecological approach. In: Peryt TM (ed) Coated grains. Springer, Berlin, Heidelberg, pp 37–55

Iryu Y, Nakamori T, Matsuda S, Abe O (1995) Distribution of marine organisms and its geological significance in the modern reef complex of the Ryukyu islands. Sediment Geol 99:243–258

James DW, Foster MS, O'Sullivan J (2006) Bryoliths (Bryozoa) in the Gulf of California. Pac Sci 60:117–124

Jannsen R, Zuschin M, Baal C (2011) Gastropods and their habitats from the northern Red Sea (Egypt: Safaga). Part 2: Caenogastropoda: Sorbeoconcha and Littorinimorpha. Ann Naturhist Mus Wien 113(A):373–509

Keegan BF (1974) The macrofauna of maerl substrates on the west coast of Ireland. Cah Biol Mar 15:513–530

Keferstein C (1828): Beobachtungen und Ansichten über die geognostischen Verhältnisse der nördlichen Kalk-Alpenkette in Österreich-Bayern. – Teutschland geognostisch-geologisch dargestellt 5(3):1–425

Keough MJ (1984) Dynamics of the epifauna of the bivalve *Pinna bicolor*: interactions among recruitment, predation, and competition: Ecology 65:677–688

Klimcouk AB (2007) Hypogene speleogenesis: Hydrogeological and morphogenetic perspective. Nat Cave Karst Res Inst Spec Pap 1:1-102

Konhauser KO, Ferris FG (1996) Diversity of iron and silica precipitation by microbial mats in hydrothermal waters, Iceland: Implications for Precambrian iron formations. Geology 24:323–326

Kröll AW, Wessely G (1993) Strukturkarte Basis der tertiären Beckenfüllung. Geologische Themenkarte der Republik Österreich. Wiener Becken und angrenzende Gebiete 1: 200.000. Geol Surv Austria, Vienna

Lankreijer A, Kovac M, Cloetingh S, Pitonak P, Hloska M, Biermann C (1995) Quantitative subsidence analysis and forward modelling of the Vienna and Danube basins: thin-skinned versus thick-skinned extension. Tectonophysics 252:433–451

Larsen AR (1976) Studies of recent *Amphistegina*, taxonomy and some ecological aspects. Israel J Earth Sci 25:1–26

Laskarev VN (1924) Sur les equivalentes du Sarmatien supérieur en Serbie. Zborník Cvijic, pp 73–85

Lathuilière B (1982): Bioconstructions bajociennes à madréporaires et faciès associés dans l'Île Crémieu (Jura du Sud; France). Geobios 15:491–504

Lazo DG (2007) The bivalve *Pholadomya gigantea* in the Early Cretaceous of Argentina: Taxonomy, taphonomy, and paleogeographic implications. Acta Palaeont Polon 52:375–390

Ludbrook NH, Gowlett-Holmes KL (1989) Chitons, gastropods, and bivalves. In Shepherd SA, Thomas IM (eds) Marine invertebrates of southern Australia, Part II: Government Printer, South Australia, Adelaide, pp 504–724

Marrack EC (1999) The relationship between water motion and living rhodolith beds in the southwestern Gulf of California, Mexico. Palaios 14:159–171

McIntyre AD (2010) Life in the world's oceans. Diversity, distribution, and abundance. Blackwell Publishing Ltd., Oxford

McPherson JG, Shanmugam G, Moiola RJ (1987) Fan-deltas and braid deltas: Varieties of coarse-grained deltas. Geol Soc Am Bull 99:331–340

Mikkelsen PM, Bieler R (2008) Seashells of southern Florida: Living marine mollusks of the Florida Keys and adjacent regions: Bivalves. Princeton University Press: Princeton, NJ (USA)

Papp A, Cicha I (1978) Definition der Zeiteinheit M – Badenien. In: Papp A, Cicha I, Seneš J, Steininger FF (eds) M4 – Badenien (Moravien, Wielicien, Kosovien). Chronostratigraphie und Neostratotypen. Miozän der Zentralen Paratethys. Slowakische Akademie der Wissenschaften, Bratislava, pp 47-48

Perrin C (1994) Morphology of encrusting and free living acervulinid foraminifera: *Acervulina*, *Gypsina*, and *Solenomeris*. Palaeontology 37:425–458

Piller WE, Kleemann K, Friebe JG (1991) Miocene reefs and related facies in Eastern Austria. In: Excursion B4. Guidebook of the VI International Symposium on Fossil Cnidaria including Archaeocyatha and Porifera, International Association for the Study of Fossil Cnidaria and Porifera, Münster

Piller WE, Harzhauser M, Mandic O (2007) Miocene Central Paratethys stratigraphy–current status and future directions. Stratigraphy 4:151–168

Piller WE, Rasser M (1996) Rhodolith formation induced by reef erosion in the Red Sea, Egypt. Coral Reefs 15:191–198

Plan L, Pavuza R, Seemann R (2006) Der Nasse Schacht bei Mannersdorf am Leithagebirge, NÖ (2911/21) – eine thermal beeinflusste Höhle am Ostrand des Wiener Beckens. Die Höhle 57:30–46

Postma G (1990) Depositional architecture and facies of river and fan deltas: a synthesis. Spec Publs Int Ass Sediment 10:13-27

Prager EJ, Ginsburg RN (1989) Carbonate nodule growth on Florida's outer shelf and its implications for fossil interpretations. Palaios 4:310–317

Rabaoui L, Tlig Zouari S, Katsanevakis S, Kalthoum O, Hassine B (2007) Comparison of absolute and relative growth patterns among five *Pinna nobilis* populations along the Tunisian coastline: an information theory approach. Mar Biol 152:537–548

Rasser M, Piller WE (1997) Depth distribution of calcareous encrusting associations in the northern Red Sea (Safaga, Egypt) and their geological implications. Proc 8th Int Coral Reef Symp 1:743–748

Rasser M (2000): Coralline red algal limestones of the Late Eocene Alpine Foreland Basin in Upper Austria: Components analysis, facies and palecology. Facies 42:59–92

Ratschbacher L, Behrmann JH, Pahr A (1990) Penninic windows at the eastern end of the Alps and their relation to the intra-Carpathian basins. Tectonophysics 172:91–105

Ratschbacher L, Frisch W, Linzer HG, Merle O (1991) Lateral extrusion in the Eastern Alps. Tectonics 10:257–271

Reid RP, Macintyre IG (1988): Foraminiferal-algal nodules from the Eastern Caribbean: growth history and implications on the value of nodules as paleoenvironmental indicators. Palaios 3:424–435

Renema W (2006) Large benthic foraminifera from the deep photic zone of a mixed siliciclastic-carbonate shelf off East Kalimantan, Indonesia. Mar Micropaleont 58:73–82

Richardson CA, Kennedy H, Duarte CM, Kennedy DP, Proud SV (1999) Age and growth of the fan mussel *Pinna nobilis* from south-east Spanish Mediterranean seagrass (*Posidonia oceanica*) meadows Mar Biol 133: 205–212

Rider J, Enrico R (1979) Structural and functional adaptations of mobile anascan ectoproct colonies (ectoproctaliths). In Larwood GP, Abbott MB (eds) Advances in bryozoology. Academic Press, New York, pp 297–319

Riedl R (1983) Fauna und Flora des Mittelmeeres. Verlag Paul Parey, Hamburg-Berlin

Riegl B, Piller WE (2000) Biostromal coral facies — A Miocene example from the Leitha Limestone (Austria) and its actualistic interpretation. Palaios 15:399–413

Rohatsch A (1997): Gesteinskunde in der Denkmalpflege unter besonderer Berücksichtigung der jungtertiären Naturwerksteine von Wien, Niederösterreich und dem Burgenland. Unpubl. Habilitation-Thesis, Wien

Rohatsch A (2008) Die Baugesteine des Wiener Stephansdomes. J Alpine Geol (Mitt Ges Geol Bergbaustud Österr) 49:197–200

Royden LH (1985) The Vienna Basin: a thin-skinned pull-apart basin. In Biddle KT, Christie-Blick N (eds) Strike-Slip deformation, basin formation, and sedimentation. SEPM Spec Publ 37:319–338

Runnegar B (1974) Evolutionary history of the Bivalve subclass Anomalodesmata. J Paleont 48:904–939

Sarà G (1969) Research on coralligenous formations: problems and perspectives. Pubbl Staz Zool di Napoli 37:124–134

Schaffer FX (1908) Geologischer Führer für Exkursionen im Inneralpinen Wienerbecken II. Teil. Sammlung geologischer Führer 13, Berlin (Borntraeger)

Schlanger SO, Johnson CJ (1969) Algal banks near La Paz, Baja California - Modern analogues of source areas of transported shallow-water fossils in pre-alpine flysch deposits. Palaeogeogr Palaeoclimatol Palaeoecol 6:141–157

Schmid HP, Harzhauser M, Kroh A (2001) Hypoxic events on a Middle Miocene carbonate platform of the Central Paratethys (Austria, Badenian, 14 Ma). Ann Naturhist Mus Wien 102(A):1–50

Schneider S (2008) The bivalve fauna from the Ortenburg Marine Sands in the well-core “Straß” (Early Miocene; SE Germany) – taxonomy, stratigraphy, paleoecology, and paleogeography. Paläont Z 82:402–417

Schweimanns M, Felbeck H (1985) Significance of the occurrence of chemoautotrophic bacterial endosymbionts in lucinid clams from Bermuda. Mar Ecol Prog Ser 24:113–120

Seifert P (1992) Palinspastic reconstruction of the eastern-most Alps between upper Eocene and Miocene. Geol Carpath 43:327–331

Sohs F (1963) Das Neogen am Westrande des Leithagebirges (zwischen Hornstein und Sommerein). Unpubl. PhD-thesis, Wien

Stanley SM (1970) Relation of shell form to life habits of the Bivalvia (Mollusca). Geol Soc Am Mem 125:1–296

Steininger FF, Rögl F (1984) Paleogeography and palinspastic reconstruction of the Neogene of the Mediterranean and Paratethys. SEPM Spec Publ 17:659–668

Steller DL, Foster MS (1995): Environmental factors influencing distribution and morphology of rhodoliths in Bahía Concepción, B.C.S., México. J Exp Mar Biol Ecol 194:201–212

Steneck RS (1986) The ecology of coralline algal crusts: convergent patterns and adaptative strategies. Annu Rev Ecol Syst 17:273–303

Strauss P, Harzhauser M, Hinsch R, Wagreich M (2006) Sequence stratigraphy in a classic pull-apart basin (Neogene, Vienna Basin). A 3D seismic based integrated approach. Geol Carpath 57:185–197

Studencki W (1988): Facies and sedimentary environment of the Pinczow limestones (Middle Miocene; Holy cross mountains, central Poland). Facies 18:1–26

Studencki W (1999) Red-algal limestone in the Middle Miocene of the Carpathian Foredeep in Poland: facies variability and palaeoclimatic implications. Geol Quat 43:395–404

Taylor JD, Glover EA (2000) Functional anatomy, chemosymbiosis and evolution of the Lucinidae. In: Harper, EM, Taylor JD, Crame JA (eds) The evolutionary biology of the Bivalvia. Spec Publ Geol Soc, London, 177:207–225

Tollmann A (1964): Exkursion II/6. Semmering-Grauwackenzone. Mitt Geol Ges Wien 57:193–203

Tollmann A (1976) Analyse des klassischen nordalpinen Mesozoikums. Deuticke, Wien

Toscano F, Sorgente B (2002) Rhodalgal-bryomol temperate carbonates from the Apulian Shelf (southwestern Italy), relict and modern deposits on a current dominated shelf. Facies 46:103–118

Toscano F, Vigliotti M, Simone L (2006) Variety of coralline algal deposits (rhodalgal facies) from the Bays of Naples and Pozzuoli (northern Tyrrhenian Sea, Italy). In: Pedley HM, Carannante G (eds) Cool-water carbonates: Depositional systems and palaeoenvironmental controls. Geol Soc Lond Spec Publ 255:85–94

Tucker ME, Wright VP (1990) Carbonate sedimentology. Blackwell, Oxford,

Varrone D, D'Atri A (2007) Acervulinid macroid and rhodolith facies in the Eocene Nummulitic Limestone of the Dauphinois Domain (Maritime Alps, Liguria, Italy). Swiss J Geosci 100:503–515

Wagreich M, Schmid HP (2002) Backstripping dip-slip fault histories: apparent slip rates for the Miocene of the Vienna Basin. Terra Nova 14:163–168

Wentworth CK (1922) A scale of grade and class terms for clastic sediments. J Geol 30:377–392

Wessely G (1983) Zur Geologie und Hydrodynamik im südlichen Wiener Becken und seiner Randzone. Mitt Geol Ges Wien 76:27–68

Wessely G (1988) Structure and development of the Vienna Basin in Austria. Am Assoc Petro Geol Mem 45:333–346

Wessely G (2006): Geologie der Österreichischen Bundesländer - Niederösterreich. Geologische Bundesanstalt, Wien

Woelkerling WJ, Irvine LM, Harvey AS (1993) Growth-forms in non-geniculate coralline red algae (Corallinales, Rhodophyta). Aust Syst Bot 6:277–293

Wulff JL (2008) Collaboration among sponge species increases sponge diversity and abundance in a seagrass meadow. Mar Ecol 29:193–204

Yonge CM (1953) Form and habit in *Pinna carnea* Gmelin. Phil Trans Roy Soc Lond, Ser B, Biol Sci 237:335–374

Yonge CM (1971) On the functional morphology and adaptive radiation in the bivalve superfamily Saxicavacea (*Hiatella* (=*Saxicava*), *Saxicavella*, *Panomya*, *Panope*, *Cyrtodaria*). Malacologia 11:1–44

Zavodnik D, Hrs-Brenko M, Legac M (1991) Synopsis on the fan shell *Pinna nobilis* L. in the eastern Adriatic Sea. In: Boudouresque CF, Avon M, Gravez V (eds) Les espèces marines à protéger en Méditerranée. GIS Posidonie publ., Marseille, pp 169–178

Zuschin M, Hohenegger J (1998) Subtropical coral-reef associated sedimentary facies characterized by molluscs (Northern Bay of Safaga, Red Sea, Egypt). Facies 38:229–254

Zuschin M, Janssen R, Baal C (2009) Gastropods and their habitats from the northern Red Sea (Egypt: Safaga). Part 1: Patellogastropoda, Vetigastropoda and Cycloneritimorpha. Ann Naturhist Mus Wien 111(A):73–158

Chapter III

Ecospace variability along a carbonate platform at the northern boundary of the Miocene reef belt (Upper Langhian, Austria)

Thomas Wiedl[1], Mathias Harzhauser[2], Andreas Kroh[2], Stjepan Ćorić[3], Werner E. Piller[1]

[1] Institute of Earth Sciences, Paleontology and Geology, University of Graz, Heinrichstrasse 26, 8010 Graz, Austria, thomas.wiedl@uni-graz.at, werner.piller@uni-graz.at
[2] Natural History Museum Vienna, Burgring 7, 1010 Vienna, Austria, mathias.harzhauser@nhm-wien.ac.at, andreas.kroh@nhm-wien.ac.at
[3] Geological Survey of Austria, Neulinggasse 38, 1030 Vienna, Austria, stjepan.coric@geologie.ac.at

3.1 Abstract

The south-western edge of the Leitha Mountains in the southern Vienna Basin (Austria) exposes parts of an Upper Langhian (Middle Badenian) shallow water (< 30 m) carbonate platform. The study of its ecospace comprises sedimentological and palaeontological data of four up to 36 m thick carbonate sections of the Müllendorf quarries which have been logged and subjected to detailed investigation and sampling. The sedimentary record is dominated by coralline algal debris sands which represent 7 distinct lithofacies (bioclastic coralline algal-mollusc facies, *Hyotissa* facies, *Isognomon* facies, coral facies, rhodolith facies, bryozoan facies). All these facies are described in detail in respect to lithology and biota and are palaeoecologically interpreted. Striking features of these limestone successions are periodical intercalations of coral- and mollusc-rich horizons. Their formation had been triggered by water turbidity and low amplitude changes in relative sea level. These relations are especially interesting as the platform carbonates formed at the northern edge of the Langhian Peri-Mediterranean reef belt. Water turbidity, as ecological

master factor, and depth played the fundamental role in ecosystem and community expression within ecospace. The lateral distribution and the ecological relations between the various facies types allow proposing an ecospace-occupation model.

3.2 Introduction

Each level of organization occupies a specific volume (or functional region respectively) within an ecospace which is e.g. the ecosystem for the community or the niche for the species (Valentine, 1969; Brenchley and Harper, 1998). The term “ecospace” is commonly afflicted with functional meanings (e.g. Bambach, 1983; Novack-Gottshall, 2007) but used here only in sense of spatial (i.e., potential habitat available for the establishment of necessary ecologic interactions) connotation (sensu Buatois and Mágano, 1993). Several physical and chemical factors, which are on the one hand limiting and on the other hand modulating, influence geographical distributions of marine carbonate producing organisms within an ecospace (Brenchley and Harper, 1998).

Typical representatives of these carbonate producing organisms are corals and coralline algae. These were the main constituents of the Miocene carbonate platforms in Europe and also in the area of the Paratethys Sea. Causes for development of either coral reefs (s.s.) or coral bearing coralline algal limestones within the same ecospace are so far not considered for the Central Paratethys. A key location to discuss this problem is the Leitha platform in the southern part of the Vienna Basin. Its limestones, broadly known as Leitha Limestones (sensu Keferstein, 1828), are dominated by coralline algal debris and have been deposited during Langhian and early Serravallian times (corresponding to the Badenian age of the regional Paratethyan stratigraphy; Steininger and Papp, 1978). The coral bearing strata at the south-western rim of the Leitha Mountains (Figs. 3.1ab) are known for a moderately diverse coral fauna (e.g. Reuss, 1871). The former interpretation of these strata as coral reefs (e.g. Schaffer, 1908; Dullo, 1983; Tollmann, 1985) was re-evaluated and it was shown that the term coral carpets (sensu Reiss and Hottinger, 1984) is more appropriate (Piller and Kleemann, 1991; Piller et al.,1996, 1997; Riegl and Piller, 2000). A well studied locality is the Fenk quarry NNW of Grosshöflein (Burgenland province, N 47°50'42.65", E 16°28'36.04"). As type locality of the Badenian Leitha Limestone (Steininger and Papp, 1978) it comprises a ca. 20-m-

thick succession of coralline algal limestones with frame-building coral carpets and non-frame-building biostromal coral communities with horizons of coral debris, in situ coral colonies and oyster/*Isognomon* horizons (Steininger and Papp, 1978; Piller and Kleemann, 1991; Riegl and Piller, 2000). A currently much larger outcrop, exposing a lateral time-equivalent succession of these units, is the Müllendorf quarry (Figs. 3.1cd), well known for its fossil richness (Abel, 1928; Kühnelt, 1931; Reidl, 1937, 1941; Toth, 1950; Kühn, 1963; Schaffer, 1961; Kristan-Tollmann, 1964, 1966; Kleemann, 1982; Schultz, 2001, 2003, 2005; Kroh, 2005). In contrast to other limestones of the Leitha Mountains, these show a soft, chalky appearance, (e.g. Reidl, 1937; Kapounek, 1938), which is caused by post-depositional diagenetic leaching (Dullo, 1983).

The goal of this study is the reconstruction and recognition of environmental factors and their role in modulating a Langhian ecospace within which facies changes are the expression of altered ecospace utilization. Therefore, the sedimentary successions of the south-western part of the Leitha Mountains enable insights into dynamic near-shore environments of a Central Paratethyan carbonate platform where settlement of the sea-floor by corals or specific bivalve associations was limited to narrow niches. In addition, rhythmic bedding of coral and bivalve accumulations is a characteristic feature of these sediments.

3.2.1 Study area

The study area is located at the south-western edge of the Leitha Mountains in the Burgenland province between Hornstein and Großhöflein (Figs. 3.1bc). The Leitha Mountains represent a mountain chain spanning ca. 35 km from southwest to northeast with a maximum width of ca. 17 km (Fig. 3.1b). The Leitha Mountains have a crystalline core dominated by mica schists of the Lower Austroalpine nappe system which is covered by Badenian and Sarmatian limestones (Pascher and Brix, 1994). During the Middle Miocene the Leitha Mountains formed a topographic high or island with extensive carbonate production, giving rise to a carbonate platform (Tollmann, 1955; Dullo, 1983; Riegl and Piller, 2000; Schmid et al., 2001; Strauss et al., 2006; Harzhauser and Piller, 2010). The investigated sections (A: N47°51'29.65", E16°27'22.62", B: N47°51'29.48", E16°27'4.87"; C: N47°51'31.38", E16°27'03.34") are located within and in the south (D: N47°51'20.65", E16°27'5.10") in a more

basinwards position of the active quarry system (Fig. 3.1d) of the Mühlendorfer Kreidefabrik Margit Hoffmann-Ostenhof GmbH. Most of the limestones have a soft, light-coloured, chalky character and underwent a complex diagenetic pathway. They passed through a freshwater phreatic environment, characterized by undersaturated waters flowing rapidly through the sediment, which allowed a leaching without coeval precipitation (Dullo, 1983). They contain high amounts of fossils with calcitic skeletons such as oysters, pectinids, echinoids and cirripedians (e.g. Suess, 1860; Reidl, 1937; Kroh, 2005) while shells of aragonitic skeletons are dissolved and commonly replaced by calcite (Suess, 1860; Kleemann, 1982; Dullo, 1983). These organisms are preserved as molds or steinkerns. The presence of corals, for example, is only documented as voids or sediment-filled corallites.

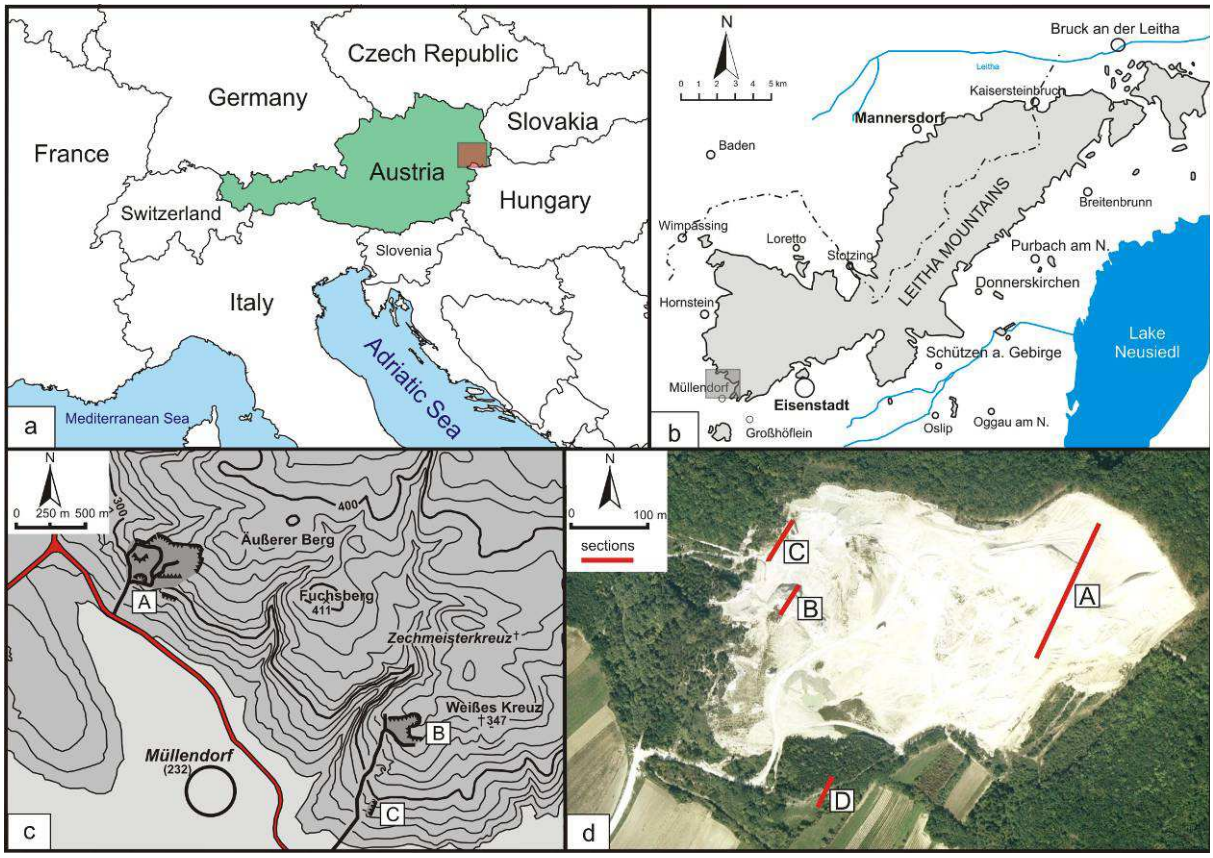

Fig. 3.1 Location of the studied area. **a** Map of Europe with Austria in the centre. The study area is highlighted with a brown rectangle. **b** Geographic map (inset in a) of the Leitha Mountains spanning the border region of Lower Austria and Burgenland provinces. **c** Map with contour lines (metres above sea-level) of the study area. A Müllendorf quarry system, B Upper Fenk quarry system, C Lower Fenk quarry. **d** Satellite image ((C)2010 Google) of the quarry system of the Mühlendorfer Kreidefabrik Margit Hoffmann-Ostenhof GmbH, corresponding to A in Fig 1c. The studied sections are indicated by letters A-D.

3.3 Materials and methods

This study combines sedimentological and palaeontological data. Four sections have been logged and subjected to detailed investigation and sampling within the study area that has an extension of ca. 500 x 500 m and exposes an up to 37-m-thick carbonate succession. Abundances of different taxa were obtained semiquantitatively with categories rare, frequent and dominant. Section A (Figs. 3.1d, 3.2, 3.3a-c) is located ca. 320 m to the E of section B (Figs. 3.1d, 3.2, 3.3a), which is sited ca. 50 m to the SE of section C (Figs. 3.1d, 3.2, 3.3a). Section D (Figs. 3.1d, 3.2, 3.3d) is situated outside of the active mining area ca. 300 m in the SSE of section B. For microfacies analyses 79 thin-sections have been prepared, followed by semiquantitative analyses classifying abundances of taxa with categories rare, frequent and dominant. Furthermore, for nannoplankton analyses three samples had been collected as well as three samples from the marly layers of the Upper Fenk quarry and 8 samples from the marl beds of the Lower Fenk quarry (cf. section of Piller et al., 1996). The carbonate nomenclature follows Dunham (1962) and Embry and Klovan (1971); the classification of siliciclastic sediments is based on Wentworth (1922). The nomenclature of red algae growth forms is based on Woelkerling et al. (1993).

3.4 Sedimentary facies

The studied limestones are composed of coralline algal rudstones with packstone matrix, containing various biota. In some horizons changing amounts of terrigenous sediment occur.

3.4.1 Section A

The section (Figs. 3.1d, 2, 3a-c), starts with platy well-cemented limestones (bed 1) containing few poorly rounded crystalline pebbles. The fauna is represented by the large bivalves *Periglypta miocaenica* and *Spondylus crassicostata* with articulated shells of *Gigantopecten nodosiformis* and regular (*Eucidaris zeamays*) as well as irregular echinoids (*Aliaster cotteauii*, *Clypeaster campanulatus*, *Clypeaster scillae*, *Echinolampas hemisphaericus*, *Schizaster eurynotus*). To the top of bed 1 a fining upward trend concerning the terrigenous material can be observed. In bed 2

crustacean remains are common; to the east shell accumulations of articulated *Gigantopecten nodosiformis* are observed. The amount of quartz fine-sand in bed 3 is higher than in the bed below and increases slightly to the top where encrusting *Porites* (ca. 1 cm thickness) occur. Small rhodoliths are common, occasionally with crystalline pebbles as nuclei. To the east, the bed is characterized by mass occurrences of the bivalves *Isognomon maxillatus* and *Glycymeris deshayesi*. Bed 4, whose base is an erosive surface, starts with a 2-cm-thick marly horizon with pebble sized (∅ 0.2-0.5 cm) poorly rounded quartz and mica schists and highly fragmented mollusc shells; to the top articulated shells of *Gigantopecten nodosiformis* occur and the siliciclastic content decreases. Above an outcrop gap of ca. 1.2 m, limestone bed 5 contains few pebble-sized siliciclastics and *Eucidaris zeamays*. Upsection follows a succession of four beds (15-40 cm thickness) starting with accumulations of the bivalve *Hyotissa hyotis* at the base. These oysters are represented by large (15 cm long, 10 cm thick) articulated specimens, occasionally strongly bored by *Lithophaga laevigata*. The *Hyotissa*-horizon at the base of bed 7 can only be followed over ca. 9 m to the south-east. The amount of siliciclastics is low except for bed 9 where a slight increase can be observed to the top. Within bed 6 additionally many *Isognomon maxillatus* occur randomly dispersed while in bed 7 a horizon with debris of the corals *Porites* and *Tarbellastraea reussiana* (bored by the bivalve *Lithophaga laevigata* and settled by pyrgomatid barnacles) is developed. After a gap of ca. 1.6 m, the limestone (bed 10) contains few coarse grained siliciclastics.

Bed 11 starts with a *Hyotissa*-horizon, followed by a horizon of in situ coral colonies (∅ 10–30 cm) of branching (branch-diameter ca. 7 mm) *Porites* and few small *Tarbellastraea reussiana* colonies (diameter 4–5 cm). The corals are covered by another horizon of *Hyotissa hyotis*. Directly above this *Hyotissa*-horizon in situ *Tarbellastraea reussiana* colonies (∅ 10–30 cm) follow partly settling on the shells. Interspaces between coral colonies and oysters are filled with coralline algal debris. Molluscs are represented by *Cypraea*, *Periglypta miocaenica* and *Acropsis*. Crystalline components are rare in the lower part, but increase to the top. The base of the following bed (12) is characterized by a 60-cm-thick horizon containing up to 40% poorly rounded and sorted pebble-sized siliciclastics (quartz and mica schist). This distinctive horizon can be followed in the quarry over a distance of ca. 320 m to the west and 60 m to the south-east. Its dipping is estimated with ca. 8° to the west. The echinoids *Parascutella gibbercula*, *Clypeaster campanulatus* and *Clypeaster*

calabrus occur in this horizon which is overlain by another *Hyotissa*-horizon. Upsection in bed 12 the siliciclastic content decreases. Again, a *Hyotissa*-horizon is developed ca. 1.8 m from the base. The shells are often affected by *Lithophaga laevigata* borings. Rare thick branched rhodoliths (up to 7 cm in diameter) occur within the bed. Above follows a coralline algal limestone (bed 13) containing many colonies of *Tarbellastraea reussiana* (∅ 10-30 cm) and *Acanthastraea horrida* at the base and ca. 1.8 m from the base. The corals are highly affected by *Lithophaga laevigata* borings. At the top rare fragments of thin branching corals, probably *Stylocora exilis*, occur. Siliciclastics are rare in the entire bed. Similar to bed 12, bed 14 starts with coralline algal limestone containing poorly sorted siliciclastics (up to fine-gravel) in the lower 60 cm. Rhodoliths (∅ 2 cm) occur, often containing subrounded mica schist pebbles as nuclei. The siliciclastics show a fining upward trend (2-3 cm at the base, 5 mm at the top). The amount within the bed fluctuates: 10 % (base), <5 % (middle), 10 % (top). In the upper part of the bed molluscs are very common, represented by many lucinids (e.g. *Codakia*), *Hyotissa hyotis*, double valved *Cardites partschi*, *Megacardita* and *Gouldia*, venerids and rare *Isognomon maxillatus*. A platy poritid colony (60 cm wide, 8 cm thick) occurs associated with the molluscs. Limestones directly above the coral colony are enriched in quartz fine-sand. Just below the top of the bed a *Hyotissa*-coquina including rare *Ostrea lamellosa* is developed. The following bed (15) again shows a high amount (60%) of siliciclastics at the base (poorly sorted pebble to cobble sized). Rhodoliths (∅ 2–3 cm) are common, occasionally with mica schist pebbles as nuclei. The siliciclastic content decreases to ca. 5% at the top. Molluscs such as *Conus*, *Xenophora*, *Periglypta miocaenica* and *Pinna tetragona* commonly occur while highly fragmented *Porites* branches are rare.

The topmost bed (Bed 16: Fig. 3.2) shows fluctuations from 1-5 % in siliciclastic content. In the lower part *Gigantopecten nodosiformis* commonly occurs together with *Periglypta miocaenica*. The rare echinoids are represented by *Clypeaster scillae* and *Parascutella gibbercula*. Sphaeroidal rhodoliths (∅ 5–10 cm) are abundant in the entire bed. They are enriched in a horizon ca. 5.5 m above the base. Above the rhodolith horizon the siliciclastic content decreases to zero to the top.

3.4.2 Section B

Section B (Figs. 3.1d, 3.2, 3.3a) is dominated by a succession of well cemented limestones. The section starts with calcareous pebble-sized gravels (bed 1) characterized by a high content of limonite, followed by a coralline algal limestone (bed 2) with rhodoliths (∅ 2–3 cm) containing mica schist pebbles as nuclei. Single *Clypeaster campanulatus*, *Parascutella gibbercula* and *Clypeaster calabrus* occur. Bed 3 is characterized by a *Hyotissa*-horizon at the base and shell-accumulations ca. 40 cm above. *Acanthastraea horrida* colonies (∅ 10 cm) occur isolated, as well as fragments of *Tarbellastraea reussiana* (∅ < 10 cm). At the base of bed 4, a densely packed *Hyotissa*-bed of ca. 10 cm thickness is developed; the oysters are usually double valved. In situ coral colonies (*Tarbellastraea* and *Porites*, ∅ 10–30 cm) occur in two horizons. Ca. 1 m above the base a horizon with double valved *Hyotissa hyotis* is developed. The gastropod *Cheilea equestris* commonly occurs in the bed. Bed 5 again starts with a *Hyotissa*-horizon, whose shells are often bored by *Lithophaga laevigata*. Nodular bryozoans (∅ 1.5 cm) are enriched directly above the *Hyotissa*-horizon. The following horizon commonly contains in situ *Tarbellastraea*-colonies which are highly affected by *Lithophaga laevigata* and cirripeds, less commonly by *Gastrochaena dubia*. *Porites* and *Acanthastraea horrida* are common too. A fungiid coral with a corallite diameter of ca. 17x16 cm could be detected in this horizon, where quartz fine-sand locally occurs in low amounts. The section terminates with bed 6 which contains common mollusc fragments of *Gigantopecten nodosiformis* and ostreids and steinkerns of gastropods. A horizon containing quartz fine-sand and rare mica schist pebbles (3–4 mm) is developed in the middle of the bed. Small rhodoliths (∅ 1 cm) are common at the top.

3.4.3 Section C

The lowest bed (Fig. 3.2) is characterized by *Porites* debris at its base while molluscs are common upsection. The following bed (2) is dominated by colonies (∅ 20–30 cm) of *Tarbellastraea reussiana* (affected by *Lithophaga laevigata* and settled by pyrgomatid barnacles). Bed 3 contains rare *Amphistegina* and the amount of siliciclastics increases from ca. 5% directly above the corals to ca. 20% towards the top. The bed is terminated by poorly sorted terrigenous coarse sand to fine-gravel (bed 4) containing echinoid remains. The following bed (5) is characterized by

common *Echinolampas manzonii* at the base. It is overlain by a horizon with common steinkerns of gastropods (*Xenophora*, *Conus*, *Cassis*) and a subsequent horizon with crustose *Porites*. It is covered by coralline algal limestone containing quartz fine-sand. Bed 6 starts with a horizon of *Hyotissa hyotis* and *Ostrea lamellosa* followed by a limestone containing ca. 30% siliciclastics. The content of coarse siliciclastics decreases to the top, where residual clay is developed. Bed 7 contains common *Periglypta miocaenica* and small gastropod steinkerns (2-4 mm) and is again covered by residual clay.

Bed 8 (Figs. 3.2) starts with a limestone containing commonly *Periglypta miocaenica* and *Gigantopecten nodosiformis*. A horizon with *Porites* debris is developed ca. 1.7 m from the base. Above this horizon, shells of *Isognomon maxillatus* are common; they are found in situ (double valved) at the top. The bed terminates with a thin layer of residual clay. The top of the section (bed 9) is characterized by common small gastropod steinkerns and shell debris of ostreids. 2.1 m from the base rare *Pinna tetragona* occur in situ together with common large globular rhodoliths (∅ 4–7 cm).

3.4.4 Section D

Section D (Figs. 3.1d, 3.2, 3.3d) consists of massive coralline algal limestones which contain many in situ coral colonies of *Porites* (∅ 10–50 cm), *Tarbellastraea reussiana* (∅ 10–20 cm), and *Acanthastraea horrida* (∅ 10 cm) which are rarely affected by *Lithophaga laevigata*. The space between coral colonies is filled with coralline algal debris and often diffusely bedded (dipping 076/07). The molluscs *Periglypta miocaenica* and *Haliotis* are common within these fine-grained limestones which contain common miliolids (*Spiroloculina*, *Triloculina*) and alveolinids (*Borelis*). Remains of pycnodont oysters and steinkerns of small venerids and gastropods are common as well. Upsection interspaces between coral colonies are commonly filled with *Porites*-rubble. At the top of the section bioclastic grainstones (debris of bivalves, gastropods and echinoids) are developed and the amount of coral colonies (10–15 cm diameter) decreases. Globular rhodoliths occur in the entire bed. The top of the bed is characterized by low amounts of quartz middle- to fine-sand. The uppermost part of the section is unconformably covered by a Sarmatian limestone. It consists of a poorly cemented, well bedded coralline algal rudstone (thickness 6 m) of well rounded and well sorted coralline algal debris with common quartz grains (5-7 mm diameter).

Fig. 3.2 Lithologic columns of sections A-D including sample numbers and GPS coordinates. Colours represent facies types. Three siliciclastic horizons (numbers in square boxes) are used for section correlation.

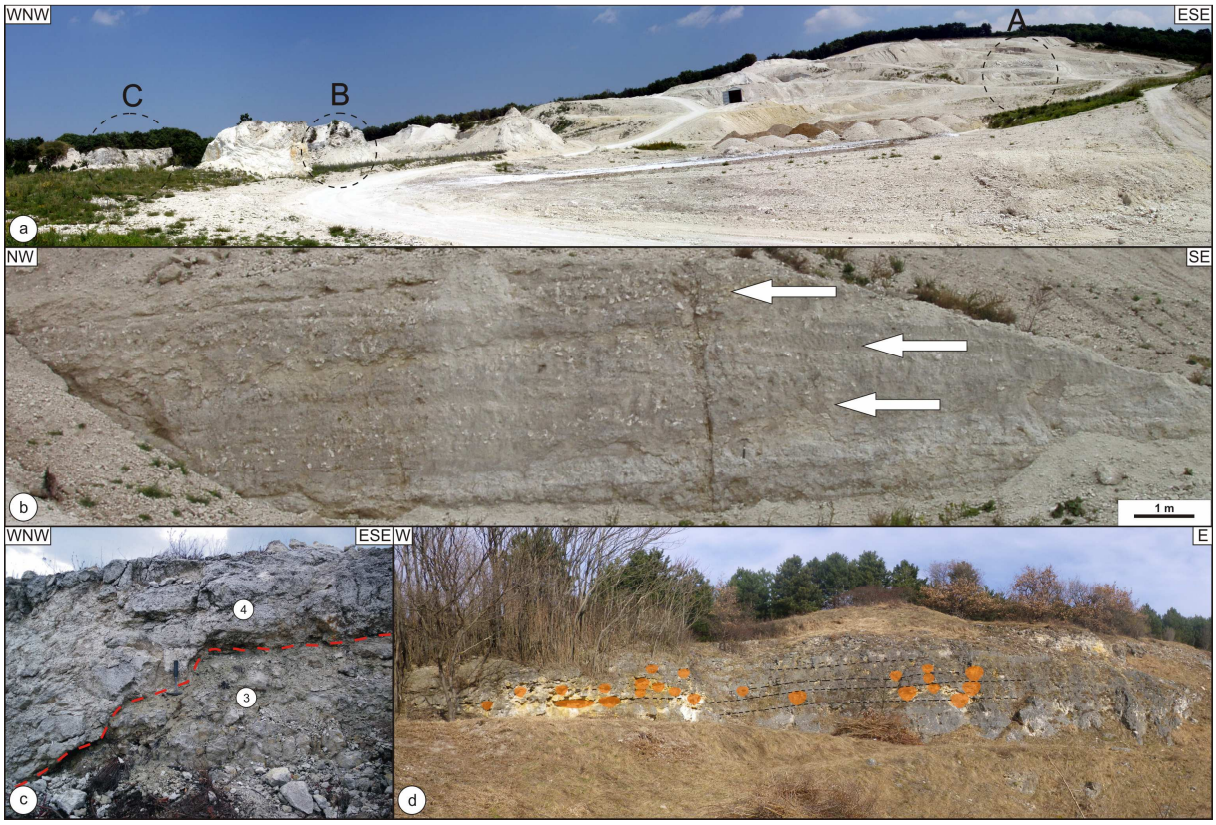

Fig. 3.3 Phototransects of the Müllendorf quarries with geographic orientations. Positions of the sections are indicated in Fig. 1d. **a** Panorama of the active Müllendorf quarry system, display window from the WNW to the ESE ca. 280 m. Stippled circles mark sections A-C. **b** Beds 6-9 of section A. White arrows: *Hyotissa*-horizons. **c** Lower part of section A. The stippled red line traces the unconformable contact between bed 3 and 4. **d** Section D (ca. 30 m in longitudinal extension) showing indistinct bedding indicated with stippled lines. Orange: coral colonies.

3.5 Stratigraphy

Stratigraphic correlation and dating of the coralline algal limestones of the south-western edge of the Leitha Mountains (Fenk and Müllendorf quarries) were based on foraminiferal assemblages. The foraminiferal fauna was first interpreted to correspond to the Upper Lagenidae Zone to *Bulimina-Bolivina* Zone of the regional ecozones (Papp und Turnovsky, 1953; Tollmann, 1955). Later, Steininger and Papp (1978) mentioned a correlation with the *Bulimina-Bolivina* Zone for the Fenk quarry based on uvigerinids. Whilst the later zone would indicate a late Badenian age and a correlation with nannoplankton zone NN6 (Hohenegger and Wagreich, 2012), the original dating could also indicate a middle Badenian age and a correlation with NN5. Herein, a calcareous nannoplankton assemblage from a marly interlayer of the Lower

Fenk quarry (N 47°50'33.96", E 16°28'22.58") was analysed. The assemblage contains *Sphenolithus heteromorphus*, *Calcidiscus leptoporus*, *Coccolithus pelagicus*, *Cyclicargolithus floridanus*, *Geminilithella rotula*, *Helicosphaera carteri*, *Pontosphaera multipora*, *Reticulofenestra gelida*, *Reticulofenestra pseudoumbilicus*, *Sphenolithus moriformis* and *Thoracosphaera saxea*.

The presence of *Sphenolithus heteromorphus* indicates nannoplankton zone NN5 according to Martini (1971) and Young (1998) and excludes a correlation with the *Bulimina-Bolivina* Zone. Additionally, the absence of *Helicosphaera waltrans* excludes the Lower Lagenidae Zone. Therefore, the sediments can be correlated to the Upper Lagenidae and *Spiroplectammina* zones (Fig. 3.4). The thin-bedded limestone-marl sequence of the Lower Fenk quarry represents time-equivalent "basinal" deposits of the Upper Fenk quarry (Piller et al., 1992). Furthermore a time-equivalent development of both locations, the Upper Fenk quarry and the Müllendorf quarries, is very likely as both limestone successions show similar facies successions (Piller and Vavra, 1991) and are situated at the same topographic level (Pascher and Brix, 1994).

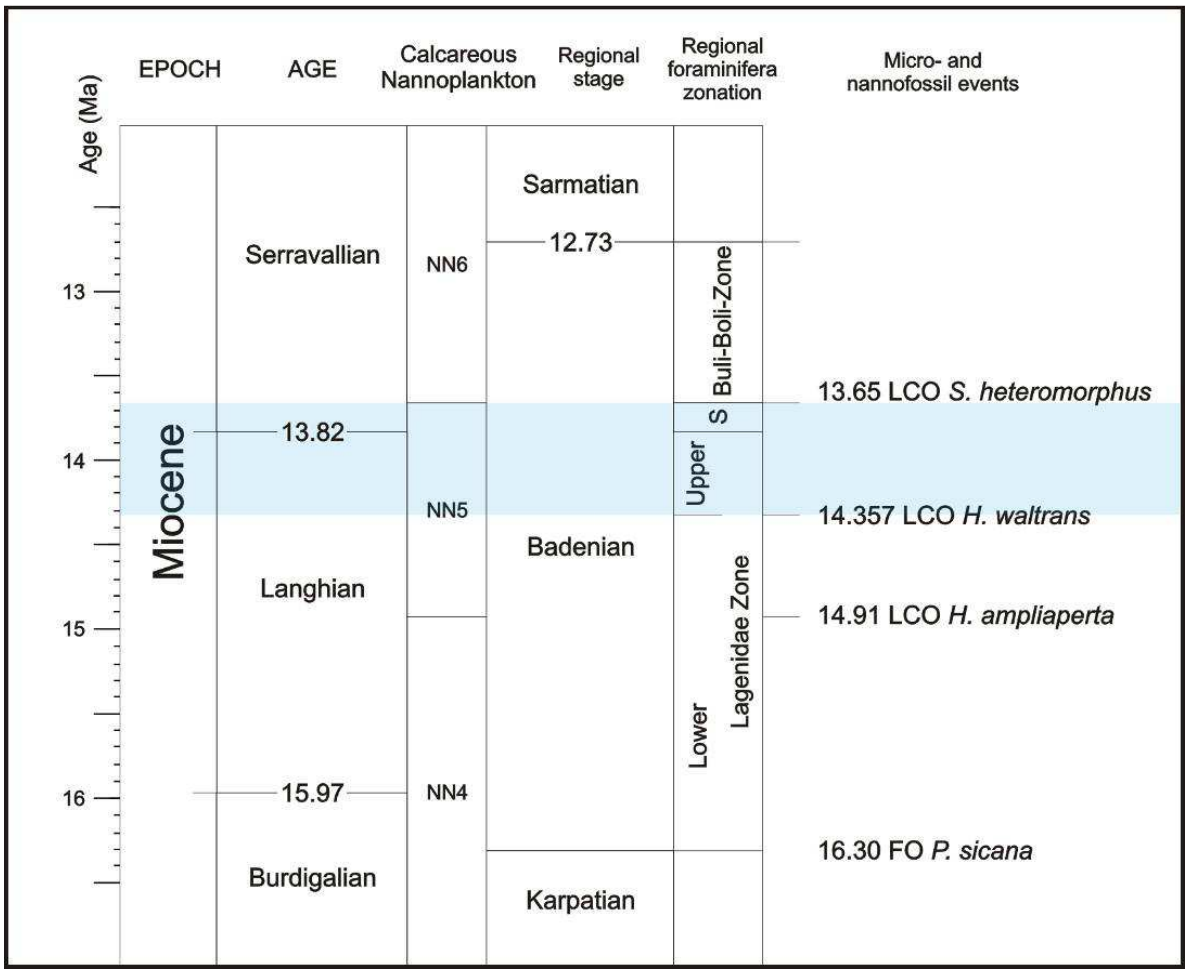

Fig. 3.4 Stratigraphic chart (modified after Hohenegger and Wagreich, 2012) with focus on Badenian geochronology and biozonations of calcareous nannoplankton and Central Paratethyan foraminifera zonations (S: *Spiroplectammina* Zone, Buli-Boli: *Bulimina-Bolivina* Zone). The studied sections are located within nannoplankton zone NN5 (highlighted in blue).

3.6 Facies analysis and interpretation

Combining the results of field observations and microfacies analyses, seven facies types can be distinguished.

3.6.1 Bioclastic coralline algal–mollusc facies

The sediment (Fig. 3.5d) comprises coralline algal rudstones and floatstones with packstone matrix. The facies is marked by high amounts of bivalves and gastropods. Aragonitic shells are completely dissolved and preserved as imprints or steinkerns. Bivalves are represented by very common *Hyotissa hyotis*, common *Gigantopecten nodosiformis*, *Periglypta miocaenica*, *Glycymeris deshayesi*, common Ostrea

lamellosa, *Spondylus crassicosta*, rare *Pinna tetragona* and cardiids and very rare *Pholadomya alpina*. They are usually articulated and randomly distributed within the beds. *Gigantopecten nodosiformis* are often settled by balanids. Gastropods are represented by *Conus*, *Cheilea equestris*, *Cypraea*, *Xenophora* and Turritellidae. Locally (section A, beds 3, 7 and 15; section C, beds 1 and 8), coral debris can be found. *Clypeaster campanulatus*, *Clypeaster calabrus*, *Eucidaris zeamays* and *Parascutella gibbercula* are present. The foraminiferal fauna consists of common biserial textulariids, rare miliolids (*Triloculina*) and alveolinids (*Borelis*) and very rare *Amphistegina*. Celleporiform bryozoans occur in low amounts. The facies is characterized by common bioturbation. Siliciclastics occur in variable amounts within the beds. The facies is represented in section A (beds 1–5, 7–10, 12, 14–16), section B (beds 2–4, 6) and section C (beds 1, 3, 5–9).

Interpretation - The facies is similar to the mollusc subfacies of Wiedl et al. (2012). The common occurrence of *Gigantopecten nodosiformis* is typical for this facies. This bivalve preferentially settled on bioclastic carbonate platforms (Bongrain, 1988) which are occasionally characterized by increased siliciclastic content (Mandic and Piller, 2001). The mineralization of its shells correlates with high metabolic costs and implies favourable climate conditions (Grecian et al., 2000). Comparable to the mentioned mollusc associations are samples from the modern Red Sea (Zuschin and Hohenegger, 1998; Zuschin et al., 2009; Janssen et al., 2011). The apparent dominance of oysters and pectinids is caused by leaching processes which led to these accumulations (Dullo, 1983). *Eucidaris zeamays* is common; extant species of *Eucidaris* are abundant from the intertidal down to 20-30 m (Kier and Grant, 1965; Nebelsick, 1992; Hickman, 1998; Kroh, 2003 and references therein) which fits to the proposed water depth of Wiedl et al. (2012) for the mollusc subfacies.

3.6.2 *Hyotissa* facies

The *Hyotissa* facies (Figs. 3.5ab) is exposed in section A, B and C and is characterized by coralline algal rudstones or packstones with common occurrences of *Hyotissa hyotis*. They are accumulated in horizons of 10 to 40 cm thickness and show, especially within beds 5-9 of section A, repeated occurrences after 1-1.5 m; locally the shells are densely packed. Coarse siliciclastics are rare. Specimens of *Hyotissa* reach dimensions of more than 25 cm length with a shell thickness of more

than 10 cm; often they are articulated and in life position. *Hyotissa* shells are frequently bored by *Lithophaga laevigata* (Fig. 3.5b) or clionid sponges. Specimens of *Hyotissa* < 5 cm are extremely rare. The *Hyotissa* facies, represented in sections A (beds 6–9, 10–12 and 14), B (beds 3–5), and C (bed 6) is predominantly adjacent to the bioclastic coralline algal-mollusc facies.

Interpretation - Gryphaeids are marine and estuarine suspension feeders which are cemented to hard subtidal substrata like rocks or dead corals, generally not being gregarious or reef-forming (Zuschin and Piller, 1997; Slack-Smith, 1998; Bieler et al., 2004; Mikkelsen and Bieler, 2008). The genus *Hyotissa*, commonly associated with corals, is strictly eu- and stenohaline and also stenotherm (Stenzel, 1971). *Hyotissa hyotis* often occurs in subtidal waters down to 30 m (Bieler et al., 2004; Mikkelsen and Bieler, 2008) but dense populations of *Hyotissa*-species commonly occur free lying on the substratum, under intertidal rocks and are commonly attached to dead and degraded coral colonies (Slack-Smith, 1998; Zuschin and Baal, 2007) in water depth <10 m (e.g. Titschack et al. 2010). The geographical extension of extant *Hyotissa hyotis* covers tropical and subtropical waters of the Indo-Pacific (Slack-Smith, 1998; Zuschin and Oliver, 2003; Zuschin and Baal, 2007) and it occurs as neozoon in the Florida Keys (Bieler et al., 2004). High suspension load is very likely the reason for gigantism (up to 30 x 20 cm in dimension) of the specimens in Müllendorf; such phenomena have been observed in recent *Hyotissa hyotis* in the Red Sea where a change in suspension load in the water column induces shifts in bivalve assemblages (Zuschin and Piller, 1997). Furthermore, pioneer assemblages in eutrophic environments are characterized of oysters (as *Hyotissa*) and *Isognomon* (Hendry et al., 2001; Minchinton and McKenzie, 2008; Reuter and Piller, 2011). Similar fossil occurrences of *Hyotissa hyotis* are described from Neogene limestones of the South Florida Platform (Scott, 2001; Missimer, 2002), southwestern Turkey (İslamoğlu and Hakyemez, 2010) and at Gebel Gharra in Egypt (Mandic and Piller, 2001) where – in the two latter cases – *Hyotissa hyotis* is associated with corals too. *Hyotissa*-accumulations within the coralline algal limestones of Müllendorf have biostromal characteristics, composed of shells of almost the same size of which up to 60% are in place. Shell-displacement is very likely caused by water energy. Although *Hyotissa* occurs as well in other localities of the Leitha Mountains (Wiedl et al., 2012), frequent *Lithophaga*-borings in oysters are only reported from the Müllendorf quarry

(Reidl, 1937; Kleemann, 1982). This may be caused by eutrophication of the waters which often stimulates bioerosion by date mussels (Highsmith, 1980). The *Hyotissa* facies is usually adjacent to the bioclastic coralline algal-mollusc facies, which very likely represents a deeper setting (see discussion below). The periodic occurrences of *Hyotissa*-horizons in Müllendorf rather point to high population densities due to increased nutrients than to low sedimentation rates.

3.6.3 *Isognomon* facies

The facies (Fig. 3.5c) is characterized by the common occurrence of articulated shells of *Isognomon maxillatus* (ca. 10 cm in length), which form distinct coquinas within coralline algal rudstones with packstone matrix. They are usually preserved as steinkerns but occasionally remains of the calcitic shell are preserved. *Isognomon maxillatus* is associated with *Glycymeris deshayesi*. Coral debris (*Porites*) occurs as well. *Acervulina*-coralline algal macroids (∅ 0.5–1 cm) are common, as well as small gastropods and celleporiform bryozoans. The amount of siliciclastics is low in this facies. The rare and poorly preserved foraminifers are represented by textulariids and rotaliids. The facies is developed in section A (bed 3 and 6) and C (top of bed 8) and associated with the bioclastic coralline algal-mollusc facies and *Hyotissa* facies.

Interpretation - Isognomonidae are typical shallow-water thermophilic epibionts (Yonge, 1968; Harzhauser et al., 2003). Modern *Isognomon* live in shallow water areas (Wilbur, 1983), even intertidally (Wilk and Bieler, 2009), and settle preferentially along submarine cliffs, on mangroves or even on mudflats (Whorff et al., 1995; Mikkelsen and Bieler, 2008; Printrakoon et al., 2008; Printrakoon and Tëmkin, 2008). Its occurrence within the Upper Fenk quarry is interpreted to indicate a shallow subtidal area with 1–5 m depth range (Riegl and Piller, 2000). *Isognomon* is interpreted as part of a pioneer assemblage in eutrophic habitats (Hendry et al., 2001; Minchinton and McKenzie, 2008; Reuter and Piller, 2011). The high amount of articulated shells, often in life position, indicates that these concentrations are autochthonous (Fürsich et al., 2009). Similar deposits in Spain, consisting of coralline algal-rhodolith rudstones together with *Isognomon*, had been interpreted as low-relief rocky shore deposits of the coastal belt (Braga et al., 2006). Suspension feeding *Isognomon* very likely benefited from nutrients and acted as pioneers in settlement of a shallow sea-floor with coralline algal sands similar to *Hyotissa*.

3.6.4 Bryozoan facies

The bryozoan facies (Fig. 3.5f) consists of densely packed poorly sorted coralline algal rudstones. They are dominated by debris of thin encrusting and fruticose coralline algae. Bryoliths (∅ 1.5 cm) occur in high amounts. Echinoid remains are rare, as well as molluscs except for oysters. Quartz (< 1mm) is rare as are foraminifers. The facies is developed in section B (lower part of bed 5) and associated with the *Hyotissa* facies and the coral facies.

Interpretation – A similar facies (bryozoan subfacies) has been reported by Wiedl et al. (2012) from the Mannersdorf quarries. In contrast to the latter, foraminifers are subordinate and branched bryozoans are missing. In Müllendorf the facies is overlain by the coral facies. Coexistence of coral- and bryozoan-bearing assemblages was explained by variations in the productivity of surface waters (Moisette et al. 2007). A slightly deeper water depth, however, similar to the adjacent facies types, is very likely for this facies in Müllendorf as modern analogues are documented for the Apulian shelf along the shore in ca. 10–30 m water depth (Toscano and Sorgente 2002). Increased nutrient levels probably lead to this heterotrophic-rich association in a lower water depth.

3.6.5 Rhodolith facies

This facies (Figs. 3.5gh) is represented by coralline algal rudstones with packstone matrix containing sub-sphaeroidal laminar rhodoliths with diameters between 2 and 3 cm (sections B and C), sphaeroidal thin-branched rhodoliths between 5 and 10 cm (section A) and sphaeroidal laminar rhodoliths between 5 and 7 cm (section C). It also contains *Acervulina*-coralline algal macroids with diameters of 0.5–3 cm (mostly > 2 cm). Interspaces between rhodoliths and macroids are filled with coralline algal debris. Fruticose and encrusting growth forms dominate coralline algae but thin encrusting growth forms are also common. Foraminifers are represented by rotaliids (*Amphistegina* and *Ammonia*), biserial textulariids and rare miliolids. Bryozoans are rare and commonly encrusted by coralline algae. The facies is represented in section A (beds 1, 4, 7, 13, 16) and section B (beds 4, 6) and section C (bed 9).

Interpretation - The facies has similarities with the rhodolite facies and the *Acervulina*-rhodolith subfacies described by Wiedl et al. (2012) from the north-eastern part of the Leitha Mountains. These authors indicated water depths of 10–20 m for the mentioned facies types, a similar water depth can be therefore assumed for this facies in Müllendorf.

3.6.6 Coral facies

Corals are represented by common in situ massive *Tarbellastraea reussiana* and *Acanthastraea horrida* as well as bushy *Porites* colonies which are embedded in coralline algal rudstones with packstone matrix (Figs. 3.6a-d) dominated by fruticose growth forms. *Stylocora exilis* occurs very rare. One specimen of a large fungiid coral was detected (Fig. 3.6b). In sections A and B platy and encrusting poritids occur in association with coralline algae dominated by thin encrusting growth forms. The corals (in particular *Tarbellastraea*) are bored by *Lithophaga laevigata* (Fig. 3.6c) and *Gastrochaena dubia*. Bivalves are represented by common Lucinidae (as *Codakia*), double valved *Cardites partschi*, *Megacardita*, *Gouldia*, venerids, *Hyotissa hyotis*, *Acropsis*, rare *Periglypta miocaenica* and very rare *Isognomon maxillatus*. Gastropods are represented by *Cheila equestris*, *Cypraea*, *Haliotis* and Turritellidae. Occasionally, the corals settle on *Hyotissa* shells and vice versa (Fig. 3.6d). Echinoid fragments are common. *Acervulina* occurs in low amounts encrusting fragments of *Porites*. Other foraminifers are rare except in section D where high amounts of miliolid foraminifers (*Spiroloculina*, *Triloculina*) occur, as well as biserial textulariids, rotalliids (*Elphidium*) and alveolinids (*Borelis*). *Thalassinoides* burrows (∅ 1–2 cm) are common. Locally quartz fine-sand is enriched; up to pebble-sized siliciclastics are rare. This facies is developed in section A (beds 3, 11, 13, 14), B (beds 3-6), C (beds 2, 5) and D (bed 1) and is associated with the bioclastic coralline algal-mollusc facies, the *Hyotissa* facies, the bryozoan facies and the terrigenous sand facies.

Interpretation - The facies has similarities to coral interval 3 (sand with massive corals, dominated by *Tarbellastraea reussiana*) and coral interval 5 (sand with occasional corals, few *Porites* branches) of Riegl and Piller (2000) described from the Upper Fenk quarry. In section B the facies follows directly above the bryozoan facies, similar to coral interval 5. The corals of interval 5 are interpreted as vestiges of a sparse *Porites* community on a subtidal soft- or firmground, similar to interval 3 of

Riegl and Piller (2000), which represents unstable sandy substrata with individual massive coral colonies. Horizons with oyster-coral associations (section A, bed 11; section B, bed 3) are similar to coral interval 7 (oysterbeds and *Isognomon* alternating with branching corals) of Riegl and Piller (2000). Coral interval 7 has been interpreted as sparse-to-dense non-framebuilding coral community (sensu Geister, 1983) in a shallow subtidal environment alternating with patchy bivalves (Riegl and Piller, 2000). The coral facies has also similarities with the Badenian coralgal facies of the Ukraine (Radwański et al., 2006).

Faviids and poritids are sediment-resistant corals which have advantages in areas of high re-suspension and re-settlement after stormy conditions (Riegl, 1999). Sediment resistance of a coral is mainly determined by growth form and polypar width (Sanders and Baron-Szabo, 2005). While large-polyped corals effectively reject sediment up to fine-gravel size, small-polyped species are more effective in rejection of clay to silt (Bak and Elgershuizen, 1976). Recent Australian *Acanthastraea echinata* show better sediment-rejection rates than poritids and also fungiids are very efficient at cleaning their surfaces (e.g. Hubbard and Pocock, 1972; Stafford-Smith, 1993). Contrary to the Upper Fenk quarry, where *Acanthastraea horrida* is subordinate (Riegl and Piller, 2000), in the Müllendorf area, *Acanthastraea horrida* is very common and probably could better compete with small-polyped corals due to its higher resistance to coarse sediments and smothering. A similar scenario is described for ecological successions of *Porites* and *Tarbellastraea* of Tortonian reefs in Spain showing that *Porites* was able to colonize areas of soft substrate with fine siliciclastic load and also prepares the ground for succeeding *Tarbellastraea* (Martin et al., 1989).

Langhian and Serravallian representatives of *Acanthastraea* in the Gulf of Suez did not occur at depths shallower than 5 m and had been the dominant corals around 10 m; poritids dominated (branching and columnar shallower than massive and domal) in 2.5–6 m and faviids showed their preferential occurrence in the shallowest habitats (Perrin, 2000).

Encrusting growth of corals, observed in sections A-C, is commonly a response to environmental conditions (Riegl and Piller, 2000) and flattening of coral colonies often indicates a decrease in light intensity (Titlyanov and Latypov, 1991) usually caused by high water turbidity. This was probably also the case in the upper part of

bed 14 of section A and in bed 5 of section C, which show increased siliciclastic content and the presence of encrusting corals.

High affection of coral colonies by date mussels often goes along with eutrophication of the waters (Highsmith, 1980) and the nutrient supply for this assemblage of Müllendorf was probably favoured by currents (Kleemann, 1982; Piller and Kleemann, 1991). Most boring organisms are suspension feeders, however, extensive rates of sedimentation are detrimental to organism survival (Perry, 1996), and for example *Lithophaga* is intolerant to even minor amounts of sediment (Bromley and Asgaard, 1993). Other authors suppose that the infestation by bioeroders remains at comparable levels to that found in adjacent clear-water environments (Perry and Macdonald, 2002; Macdonald and Perry, 2003).

The foraminiferal-rich limestones of section D, located in a more basinward position related to the other sections, are characterized by a high density of corals. Due to this fact, the section had been interpreted as reef (Schaffer, 1908; Kapounek, 1935, 1938; Reidl, 1937; Tollmann, 1955) ignoring the fact that the coral colonies are usually isolated within a bedded coralline algal matrix and do not show a frame-building character. The development of grainstone matrices points to increased water energy (Flügel, 2004). Therefore the coral facies at this particular location had been developed in a distal, slightly deeper environment, influenced by increased water energy and hardly affected by terrigenous influx or increased nutrient levels. Summing up, the coral facies in general reflects a shallow subtidal habitat with moderate water energy and nutrient load in a water depth of ca. 5-10 m.

3.6.7 Terrigenous sand facies

The terrigenous sand facies (Fig. 3.5e) comprises three distinct beds dominated by subrounded poorly sorted breccias up to cobble sized mica schists or fine-sands with low amounts of coralline algae or coralline algal limestones with a siliciclastic content > 20 %. Commonly small rhodoliths (∅ 2 cm) occur with lithic nuclei. Echinoids are the predominant larger faunal elements, represented by *Parascutella gibbercula*, *Clypeaster campanulatus*, *Clypeaster calabrus* and *Echinolampas hemisphaericus*. The rare mollusc fauna consists of oyster debris. In thin sections coralline algal debris is characterized by fruticose and thin encrusting growth forms. Foraminifera are rare, locally, however, *Borelis* and textulariids are common. The facies is represented in section A (beds 12, 14, 15), B (bed 1) and C (beds 4, 6) and is

associated with the coral facies, the *Hyotissa* facies and bioclastic coralline algal-mollusc facies.

Interpretation - Poor sorting and subrounding of the lithic components of the terrigenous sand facies indicate a short transport. Echinoids are the dominant faunal elements. The common presence of the large sand dollars *Parascutella* and sea biscuits *Clypeaster* in the Caribbean is linked with mobile sand bottoms where seagrass and filamentous algae are rare or absent (Hendler et al., 1995). The facies is interpreted as the onset of a transgressive pulse after a relative sea-level lowstand, leading to increased reworking of terrestrial material.

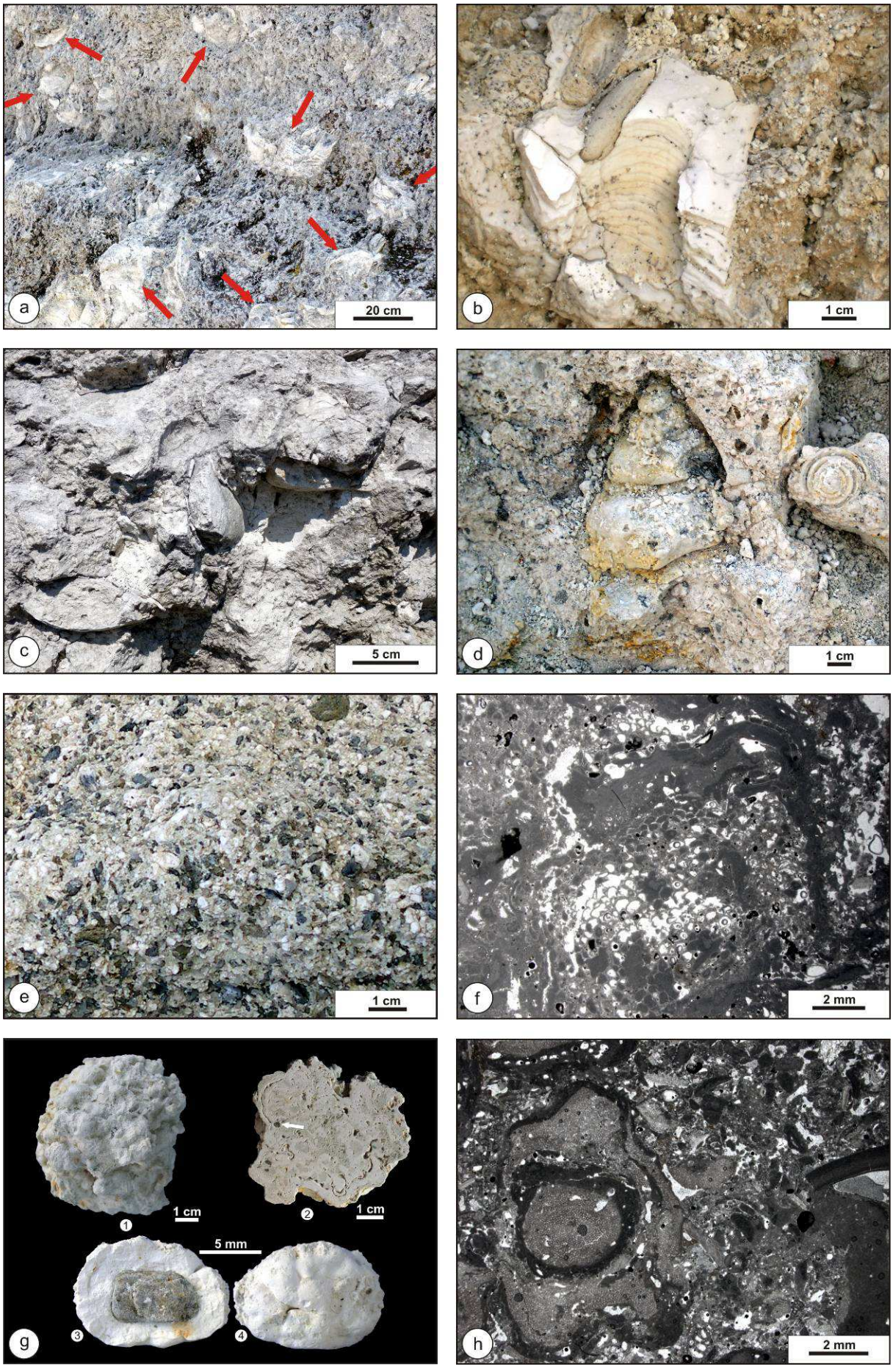
a
20 cm
b
1 cm
c
5 cm
d
1 cm
e
1 cm
f
2 mm
1 cm
1 cm
5 mm
g
h
2 mm

Fig. 3.5 a-b *Hyotissa* facies. **a** Arrows indicate *Hyotissa hyotis* shells within a coralline algal rudstone (section B, base of bed 3). **b** The calcitic shell of *Hyotissa hyotis* bored by two *Lithophaga laevigata* (section A, bed 7). **c** *Isognomon* facies. Shell-accumulation of *Isognomon maxillatus* represented as steinkerns and shell remains; commonly the bivalves are in life position (section A, bed 3). **d** Bioclastic coralline algal-*mollusc* facies. Steinkerns of *Xenophora* and *Conus* within a coralline algal rudstone; the shells are completely dissolved (section C, bed 5). **e** Terrigenous sand facies (section A, bed 12). Coralline algal rudstone with poorly rounded pebble sized mica schists and quartz. **f** Bryozoan facies. Celleporiform bryozoans partly encrusted by red algae (section B, bed 5). **g-h** Rhodolith facies. **g** 1-2 Large sized rhodolith (Rh2): 1 Sphaeroidal laminar rhodolith (section C, bed 9) 2 Section through a sphaeroidal laminar rhodolith (section C, bed 9) binding mica schist grains (white arrow). 3-4 Small sized sub-sphaeroidal laminar rhodoliths of the terrigenous sand facies with a mica schist pebble as nucleus (Rh1, section C, bed 4). **h** *Acervulina*-coralline algal macroid within a coralline algal rudstone (section A, bed 4).

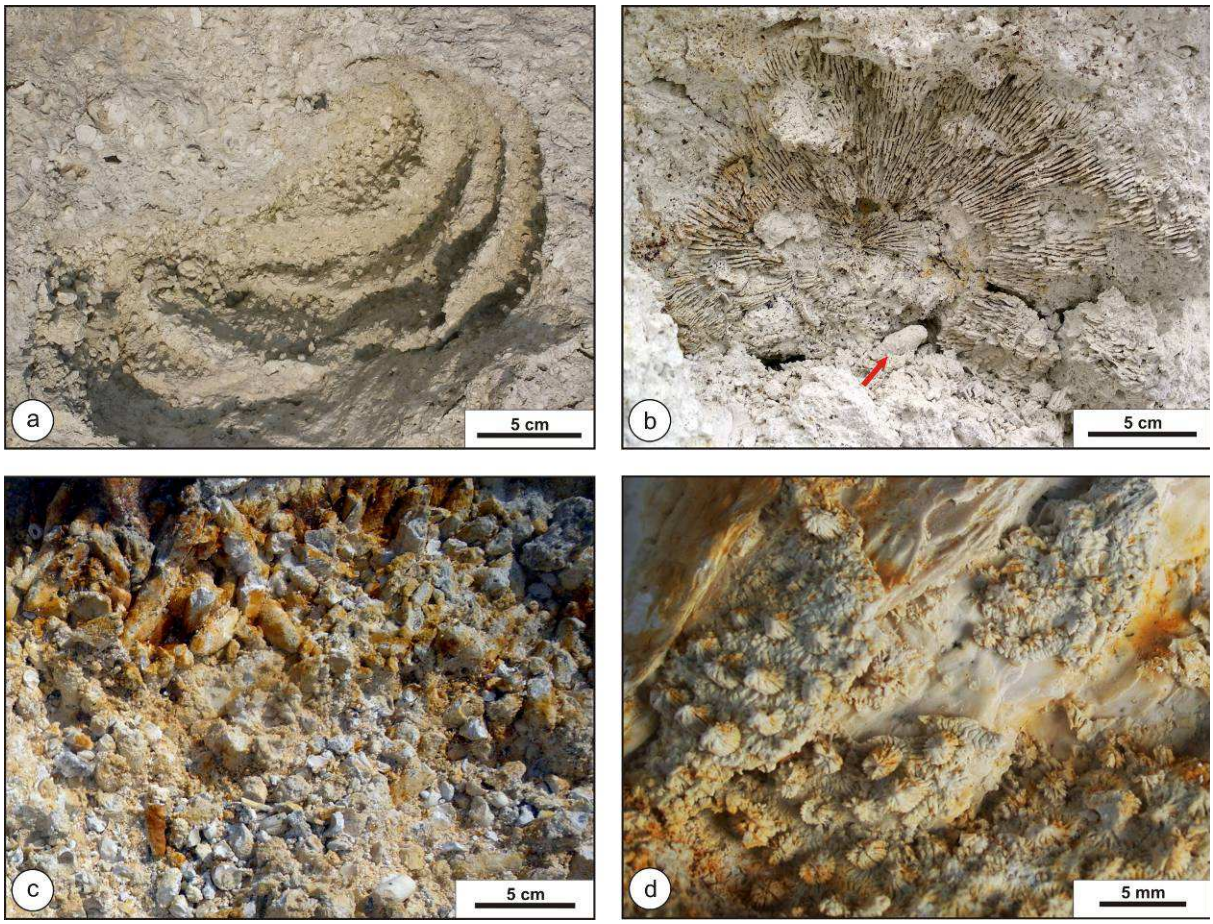

Fig. 3.6 a-d Coral facies. **a** Negative of a dissolved colony of *Tarbellastraea reussiana* with growth lines (section B, bed 3). **b** Negative of a dissolved fungiid coral (section B, bed 5) affected by *Lithophaga laevigata* (arrow). **c** Colonies of *Tarbellastraea reussiana* and *Porites* are often almost beyond recognition due to massive infestation of *Lithophaga laevigata* (section B, bed 5). **d** Coral-oyster association. Infillings of *Tarbellastraea reussiana* corallites on the surface of a *Hyotissa hyotis* shell (section A, bed 11).

3.7 Discussion

The depositional environment of Müllendorf reflects an ecospace along a gently sloping coralline algal-dominated carbonate platform. Recurrent coral (*Tarbellastraea reussiana*, *Acanthastraea horrida*, *Porites* and *Stylocora exilis*) and mollusc biostromes (*Hyotissa hyotis*, *Isognomon maxillatus*) are indicative for shallow subtidal, tropical environments. The limestones are clearly dominated by a coralline algal facies characterized by heterogeneous mollusc assemblages (bioclastic coralline algal-mollusc facies). Coral-rich horizons or monospecific bivalve accumulations (*Hyotissa*, *Isognomon*) are locally present. The occurrence of corals

throughout the successions indicates persistence in ecological parameters within the ecospace as corals are sensitive to changes in temperature, sea-water chemistry or light (e.g. Roberts et al., 1982; Kleypas et al., 1999b; Marubini and Atkinson, 1999; Bergman et al., 2010). Intercalated horizons with terrigenics are interpreted as result of transgressive pulses, expressed in three distinct horizons.

3.7.1 Ecospace modulation – variation under different set-ups

Environmental factors such as light, temperature, nutrients and depth determine the range of organisms and communities within an ecospace (Brenchley and Harper, 1998). For instance, the dominance of coralline algae over corals in tropical environments has been explained as triggered by enhanced trophic resources (Johansen 1981; Littler and Littler, 1984; Halfar and Mutti, 2005). As high nutrient levels had been hypothesized as reasons for mass occurrences of boring organisms in Müllendorf (Kleemann, 1982), this is also supported by accumulations of large-shelled *Hyotissa* and *Isognomon* which point to a beneficial food situation as well (see discussion above). But high nutrient supply has detrimental effects on coral communities as it stimulates plankton growth and as consequence causes increasing water turbidity (Hallock and Schlager, 1986). The common occurrence of large-polyped corals (*Tarbellastraea* and *Acanthastraea*) in Müllendorf, next to common *Porites*, a sediment-resistant coral in areas of high re-suspension (Riegl, 1999), refers to active sediment removal than passive one by increased water energy, which commonly prevents smothering of a reef system (Stafford-Smith, 1992; Jokiel, 2006). As water energy mainly influences sediment composition, accumulation and distribution (Bergman et al., 2010), conspicuous differences in siliciclastic content between the close-by sections B and C (cf. Fig. 3.1d, 3.2) point to a short current driven distribution of siliciclastics. Additionally, corals - representing biostromal coral communities (sensu Riegl and Piller, 2000) - probably caused slight changes in bottom topography and therefore influenced the distribution of siliciclastics, which underwent only a short transport (see above).

Influences of environmental factors on faunal communities within the ecospace of Müllendorf can be deduced from the ecological requirements of this biota discussed in chapter 6 and are best illustrated by a turbidity/water depth diagram (Fig. 3.7). A single parameter change (increased water turbidity) causes displacement of corals by the oyster *Hyotissa* while a change in two parameters, increased water turbidity

and depth, causes the transition to deposits with common shallow-burrowing molluscs (bioclastic coralline algal-mollusc facies) and finally to sediments with common bryozoans (bryozoan facies). The common occurrence of facies formed in very shallow waters shows that water turbidity (determined by nutrient and/or terrigenic values) acted as strongest modulating factor (ecological master factor) in community expression in Müllendorf, followed by influences of water depth regulated by fluctuations in relative sea-level. Other important ecological factors as temperature, which is often documented as ecological master factor (Brett, 1971), had no apparent influence as the sedimentary records shows no indications for temperature changes during the observed time-interval. Based on the observed facies relations, gradations and reconstructed water depths for each facies an idealized ecospace-occupation model (Fig. 3.7) for similar shallow tropical carbonate platforms can be deduced from the Müllendorf case study. It illustrates the position and space of a facies within a depth-turbidity diagram. Facies relationships in multiple directions of the diagram can be produced in this way.

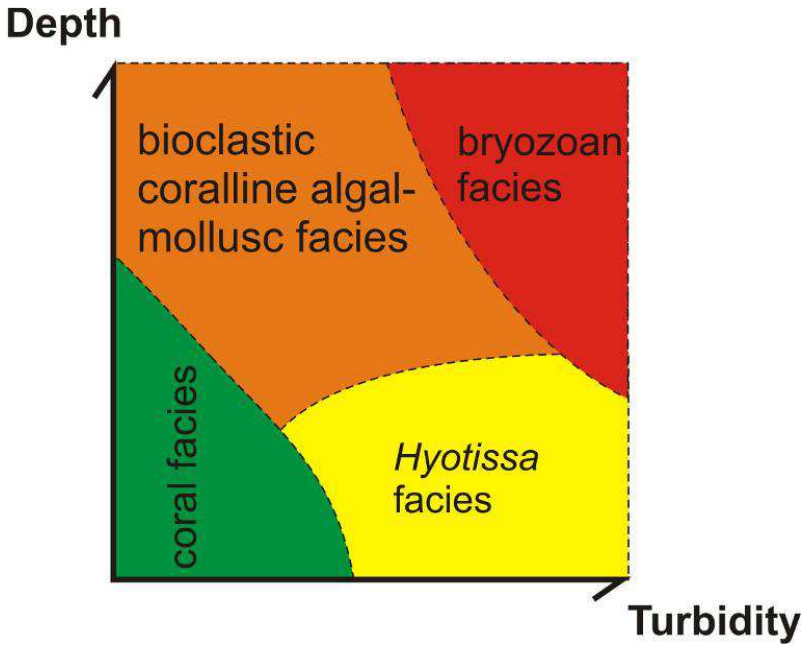

Fig. 3.7 Idealized ecospace-occupation model of depth-turbidity relationships influencing facies distribution (deduced of Fig. 3.8). With increasing depth and turbidity the bryozoan subfacies gains greater importance.

3.7.2 Cyclic sedimentation patterns

Cyclic stacking of sediments is visible in recurring transitions from the bioclastic coralline algal-mollusc facies either to oyster- or to coral-horizons. Such transitions

are tied to low-amplitude relative sea-level oscillations, as the bioclastic coralline algal-mollusc facies has been formed in greater depth than the *Hyotissa*- and coral-horizons (see discussion above), whose individual formation is controlled by turbidity. Therefore these recurring facies changes reflect high frequency shallowing-deepening sequences. However, neither field observations nor thin-section analyses allowed an interpretation whether these sequences reflect shallowing- or deepening-upward cycles. Transgressive-regressive cycles of higher order, bundling the prementioned oscillations, are indicated by changing amounts of siliciclastics.

3.7.3 The northern boundary of the Langhian Peri-Mediterranean reef belt

Coral reefs are typically associated with warm shallow seas (Veron, 1995) and their today's dispersal is restricted to the northern and southern tropics (e.g. Guilcher, 1988; Veron, 2000; Spalding et al., 2001). Nevertheless some coral communities extend beyond the tropics also into higher latitudes (e.g. Florida, Australia, Japan and Southern Africa) between a zone of ca. 30° N to 30° S (Kleypas et al., 1999a) but often fail to form reefs (Veron and Minchin, 1992). The Middle Miocene Climatic Optimum (e.g. Flower and Kennett, 1994; Böhme, 2003) led to an extension of the tropical belt and favoured the wide distribution of coral communities also throughout the Mediterranean and Central Paratethyan seas during Langhian time (Perrin and Bosellini, 2012). During the Langhian the Central Paratethys spanned a zone from ca. 40-47° N (Perrin and Bosellini, 2012). Coral reefs are documented from the entire Mediterranean and from the Central Paratethys up to the southern Vienna and Transylvanian basins (Fig. 3.8). From this distribution pattern of the circum-Mediterranean region a subdivision into two biogeographic areas during Langhian times is possible. The southern area is characterized by coral reefs (s.s.). Its northern boundary can be drawn from the Aquitaine Basin to the Vienna and Transylvanian basins (Esteban, 1996). Further to the north coral occurrences are characterized by coral carpets/assemblages or monospecific coral occurrences (Fig. 3.8). In this context the Leitha platform, which is situated at the edge of the coral reef belt, characterizes the transition zone between coral reefs to non-reefal coral communities – the second biogeographic unit. The development of exclusively non-reefal communities beyond the transition zone is very likely influenced by a distinct climatic north-south gradient well documented by molluscs and echinoids (Harzhauser et al., 2003; Harzhauser and Piller, 2007; Kroh, 2007). Górka (2002) interprets weathered

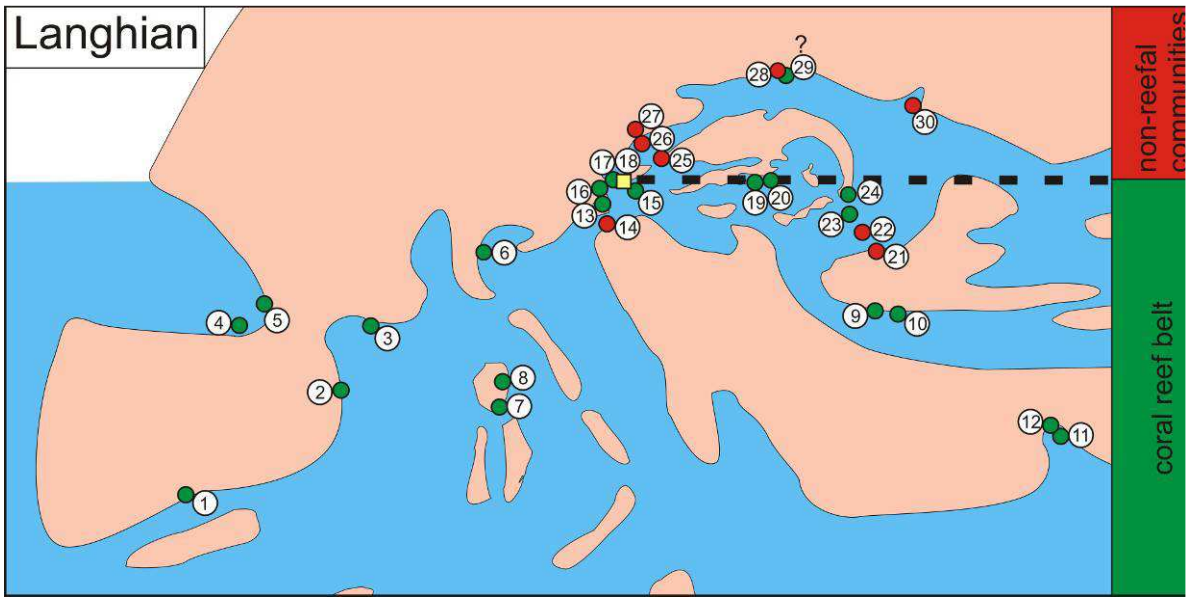

Fig. 3.8 Paleogeographical map of Europe during Langhian time (adapted after Rögl, 1999). The stippled black line shows the northern edge of the coral reef belt. Green dots indicate coral reefs; red dots indicate coral carpets or biostromal coral communities and single coral occurrences. The yellow square highlights the study area. Localities are given by numbers: 1 Murchas (Braga et al., 1996), 2 Sant Pau d'Ordal (Permanyer and Esteban, 1973, Calvet et al., 1994), 3 Hérault (Chevalier, 1961), 4 Saubrigues (Chevalier, 1961), 5 Manciet (Chevalier, 1961), 6 Torino Hills (Chevalier, 1961), 7 Balistra (Pedley, 1996 and further literature), 8 Aléria (Pedley, 1996 and further literature), 9 Ohrid (Okhrid) (Kojumdgieva and Strachimirov, 1960; Kojumdgieva, 1976), 10 Pleven (Kojumdgieva et al., 1978; Budd et al., 1996), 11 Oymapinar (Karabıyıkoğlu et al., 2005), 12 Tepeki and Köprücay (Karabıyıkoğlu et al., 2005), 13 Retznei and 'Tittenbach' quarry (Friebe, 1991; Friebe, 1993; Reuter and Piller, 2011), 14 Duplek (Baron-Szabo, 1997), 15 Fertörákos (Randazzo et al., 1999), 16 Wiesfleck (Kroh, 2007), 17 Sooß-Lindkogel (Piller et al., 1991), 18 Müllendorf/Großhöflein (Dullo 1983; Riegl and Piller, 2000), 19 Budapest area (Oosterbaan, 1990; Randazzo et al., 1999; Saint Martin et al., 2000), 20 Zebegény (e.g. Oosterbaan, 1990; Randazzo et al., 1999), 21 Bahna (Țiță, 2007), 22 Delineşti (Țiță, 1999, 2000), 23 Lăpugiu de Sus (Rus and Popa, 2008), 24 Podeni (Saint Martin et al. 2007; Bucur et al., 2011), 25 Devínska Nová Ves (Švagrovský, 1978), 26 Židlochovice (Cicha, 1978), 27 Borač (Brzobohatý and Cicha, 1978), 28 Korytnica (Bałuk and Radwański, 1977; Roniewicz and Stolarski, 1991; Stolarski, 1991), 29 Grobie (Górka, 2002), 30 Maksymivka (Radwański et al., 2006).

material from an agricultural field at Grobie in Poland as reef core facies of a patch reef. However, in-situ reef-core facies is not documented and, according to the geographical position of other Badenian reefal and non-reefal communities (Fig. 3.8), an affiliation to the latter group is more appropriate. The distribution of corals in the Central Paratethys, being distinctly north of the Holocene tropical zone (Pisera, 1996), is thus clearly linked with the Middle Miocene Climatic Optimum, which

supported the northward shift of tropical elements (Harzhauser et al., 2003). Langhian deposits of the Pannonian basinal system in Hungary, including coral patch reefs, had been interpreted as cool water limestones (Randazzo et al., 1999). But in consideration of the fact that tropical coral assemblages occurred even much further in the north, this interpretation is very unlikely.

3.8 Conclusion

We present a detailed key study on a Middle Badenian (upper Langhian) carbonate platform in the southern Vienna Basin. The investigated parts of the platform formed in a tropical near-shore environment with a maximum water depth of ca. 30 m. Predominant coralline algal limestones represent multiple biofacies, whose distribution was modulated by turbidity and water depth. This relation can be plotted in a depth-turbidity diagram and allows proposing an ecospace-occupation model for Miocene carbonate biofacies of shallow-water carbonate platforms. The sedimentary record, dominated by coralline algal debris sands, reveals stable climatic conditions during the observed time interval where water turbidity and depth acted as ecological master factors in modulating the ecospace. They were therefore responsible for facies changes from accumulations of shallow-water suspension feeding *Hyotissa* and *Isognomon* to coral communities, represented by sediment-resistant taxa (*Acanthastraea*, *Tarbellastraea* and *Porites*). Furthermore, associated changes in water-depth, regulated by fluctuations in relative sea-level, were responsible for development of 7 facies types, represented by the bioclastic coralline algal-mollusc facies (the most common facies), *Hyotissa* facies, *Isognomon* facies, rhodolith facies, bryozoan facies, coral facies and terrigenous sand facies. Cyclic sedimentary patterns point to low-amplitude sea-level fluctuations. The platform was situated at the northern edge of the Langhian Peri-Mediterranean reef belt in the Central Paratethys, where coral reefs (s.s.) and non-reefal coral communities coexisted in the same ecospace while in closeby regions to the north only non-reefal coral communities existed.

3.9 Acknowledgements

This paper was financed by the “NAWI Graz Advanced School of Science” (GASS). Field work was kindly supported by the Mühlendorfer Kreidefabrik Margit Hoffmann-Ostenhof KG by Dr. Peter Hoffmann-Ostenhof, Dipl. Ing. Peter Karlich, Ing. Manfred Lang and the helpful quarry employees. Special thanks go to Gerhard Wanzenböck (Bad Vöslau) for insights in his large collection of fossils and precise information on their proveniences. Many thanks go to Dr. Markus Reuter (Institute of Earth Sciences, University of Graz) for constructive discussions. Finally, we thank Dr. Steven J. Weiss (University of Graz) for improving the English of the manuscript. The manuscript benefited from the constructive comments of two anonymous reviewers and from the editorial advice of Professor Thierry Corrège (Université Bordeaux I).

3.10 References

Abel, O., 1928. Parasitische Balanen auf Stockkorallen aus dem mediterranen Miozänmeer. Paläobiologica 1, 13–38.

Bak, R.P.M., Elgershuizen, J.H.B.W., 1976. Patterns of oil-sediment rejection in corals. Mar. Biol. 37,105–113.

Bałuk, W., Radwański, A. 1977. Organic communities and facies development of the Krytnica basin (Middle Miocene; Holy Cross Mountains, Central Poland). Acta Geol. Polon. 27(2), 85–123.

Bambach, R.K., 1983. Ecospace utilization and guilds in marine communities through the Phanerozoic. In: Tevesz MJS, McCall PL (Eds.), Biotic interactions in Recent and fossil benthic communities. Plenum Press, New York, pp. 719–746.

Baron-Szabo, R.C., 1997. Miocene (Badenian) corals from Duplek, NE Slovenia. Razpr IV Razr Sazu 38(5), 96–115.

Bergman, K.L., Westphal, H., Janson, X., Poiriez, A., Eberli, G.P., 2010. Controlling patterns on facies geometries of the Bahamas, an isolated carbonate platform environment. In: Westphal H, Riegl B, Eberli GP (Eds.), Carbonate depositional systems: assessing dimensions and controlling patterns. The Bahamas, Belize and the Persian/Arabian Gulf. Springer, Dordrecht, Heidelberg, London, New York, pp. 5–80.

Bieler, R., Mikkelsen, P.M., Lee, T., Foighil, D.Ó., 2004. Discovery of the Indo-Pacific oyster *Hyotissa hyotis* (Linnaeus, 1758) in the Florida Keys (Bivalvia: Gryphaeidae). Moll. Res. 24, 149–159.

Böhme, M., 2003. The Miocene Climatic Optimum evidence from ectothermic vertebrates of Central Europe, Palaeogeogr. Palaeoclimatol. Palaeoecol. 195, 389–401.

Bongrain, M., 1988. Les *Gigantopecten* (Pectinidae, Bivalvia) du Miocène Français: Croissance et morphogenèse, paléoécologie, origine et évolution du groupe. Cah. Paléontol. 230 pp.

Braga, J.C., Jimenez, A.P., Martín, J.M., Rivas, P., 1996. Middle Miocene coral-oyster reefs, Murchas, Granada, southern Spain. In: Franseen, E.K., Esteban, M., Ward, W.C., Rouchy, J.M. (Eds.), Models for Carbonate Stratigraphy from Miocene Reef Complexes of Mediterranean Regions. SEPM Concepts Sedimento. Paleontol. 5, 131–139.

Braga, J.C., Martín, J.M., Betzler, C., Aguirre, J., 2006. Models of temperate carbonate depostion in Neogene basins in SE Spain: a synthesis. In: Pedley, H.M., Carannante, G. (Eds.), Cool-water carbonates: Depositional systems and palaeoenvironmental controls. Geol. Soc. Spec. Publ. 255, 121–135.

Brenchley, P.J., Harper, D.A.T., 1998. Palaeoecology. Ecosystems, Environments and Evolution. Chapman & Hall, London (1998). 402 pp.

Brett, J.R., 1971. Energetic responses of salmon to temperature. A study of some thermal relations in the physiology and freshwater ecology of sockeye salmon (*Oncorhynchus nerka*). Am. Zool. 11, 99–113.

Bromley, R.G., Asgaard, U., 1993. Endolithic community replacement on a Pliocene rocky coast. Ichnos. 2, 93–116.

Brzobohatý, R., Cicha, I., 1978. 4. Faziostratotypus: Borač, Karpatische Vortiefe in Mähren, Tschechoslowakei. In: Papp, A., Cicha, I., Senes, J., Steininger, F.F. (Eds.), M_4 – Badenien (Moravien, Wielicien, Kosovien). Chronostratigraphie und Neostratotypen. Miozän der Zentralen Paratethys: Slowakische Akademie der Wissenschaften, Bratislava, pp. 171–173.

Buatois, L.A., Mángano, M.G., 1993. Ecospace utilization, paleoenvironmental trends, and the evolution of early nonmarine biotas. Geology 21, 595–598.

Budd, A.F., Bosellini, F.R., Stemann, T.A., 1996. Systematics of the Oligocene to Miocene reef coral *Tarbellastraea* in the northern Mediterranean. Palaeontology 39, 515–560.

Bucur, I.I., Saint Martin, J.P., Filipescu, S., Săsăran, E., Pleş, G., 2011. On the presence of green algae (Dasycladales, Bryopsidales) in the Middle Miocene deposits from Podeni (western border of the Transylvanian Basin, Romania). Acta Palaeontol. Roman. 7, 69–75.

Calvet, F., Esteban, M., Permanyer, A., 1994. Mid Miocene coral reefs in the Gulf of Valencia, NE Spain. In: Saint Martin JP, Cornee JJ (Eds.), Miocene reefs and carbonate platforms of the Mediterranean. Interim Colloquium R.C.M.N.S., Marseille, 3-6 mai 1994.

Chevalier, J.P., 1961. Recherches sur les Madreporaires et les formations récifales miocènes de la Méditérranée Occidentale. PhD-thesis. Mem. Soc. Geol. Fr. 93

Cicha I., 1978. 3. Faziostratotypus: Židlochovice, Karpatische Vortiefe in Mähren, Tschechoslowakei. In: Papp A, Cicha, I., Senes, J., Steininger, F.F. (Eds.), M_4 – Badenien (Moravien, Wielicien, Kosovien). Chronostratigraphie und

Neostratotypen. Miozän der Zentralen Paratethys: Slowakische Akademie der Wissenschaften, Bratislava, pp. 168–170.

Dullo, W.C., 1983. Diagenesis of fossils of the Miocene Leitha Limestone of the Paratethys, Austria: An example for faunal modifications due to changing diagenetic environments. Facies 8, 1–112.

Dunham, R.J., 1962. Classification of carbonate rocks according to their depositional texture. In: Ham WE (Ed.) Classification of carbonate rocks–a symposium. Am. Assoc. Petrol. Geol. Mem. 1, 108–121.

Embry, A.F., Klovan, J.E., 1971. A Late Devonian reef tract on Northeastern Banks Island, NWT. Can. Petrol. Geol. Bull. 19, 730–781.

Esteban, M., 1996. An overview of Miocene reefs from Mediterranean areas: general trends and facies models. In: Fransen, E.K., Esteban, M., Ward, W.C., Rouchy, J.-M. (Eds.), Models for carbonate stratigraphy from Miocene reef complexes of Mediterranean regions. SEPM Concepts Sedimentol. Paleontol. 5:4–53

Flower, B.P., Kennett, J.P., 1994. The Middle Miocene climatic transition: East Antarctic ice sheet development, deep ocean circulation and global carbon cycling. Palaeogeogr. Palaeoclimatol. Palaeoecol. 108, 537–555.

Flügel, E ., 2004. Microfacies of Carbonate Rocks. Springer, Berlin. 984 pp.

Friebe, J.G., 1991. Middle Miocene Reefs and related facies in eastern Austria. II) Styrian Basin. VI Int Symp Fossil Cnidaria Archaeocyatha Porifera, Excursion Guidebook, Excursion B4, pp 29–47.

Friebe, J.G., 1993. Sequence stratigraphy in a mixed carbonatesiliciclastic depositional system (Middle Miocene; Styrian Basin, Austria). Geol. Rundsch. 82, 281–294.

Fürsich, F.T., Werner, W., Schneider, S., 2009. Autochthonous to parautochthonous bivalve concentrations within transgressive marginal marine strata of the Upper Jurassic of Portugal. Palaeobio. Palaeoenv. 89, 161–190.

Geister, J., 1983. Holocene West Indian coral reefs: geomorphology, ecology, and facies. Facies 9, 173–284.

Górka, M., 2002. The Lower Badenian (Middle Miocene) coral patch reef at Grobie (southern slopes of the Holy Cross Mountains, Central Poland), its origin, development and demise. Acta. Geol. Pol. 52, 521–533.

Grecian, L.A., Parsons, G.J., Dabinett, P., Couturier, C., 2000. Influence of season, initial size, depth, gear type and stocking density on the growth rates and

recovery of sea scallop, *Placopecten magellancius*, on a farm-based nursery. Aquacult. Int. 8, 183–206.

Guilcher, A., 1988. Coral Reef Geomorphology, Wiley, Chichester. 228 pp.

Halfar, J., Mutti, M., 2005. Global dominance of coralline red-algal facies: A response to Miocene oceanographic events. Geology 33, 481–484.

Hallock, P., Schlager, W., 1986. Nutrient excess and the demise of coral reefs and carbonate platforms. Palaios 1, 389–398.

Harzhauser, M., Mandic, O., Zuschin, M., 2003. Changes in Paratethyan marine molluscs at the Early/Middle Miocene transition - diversity, paleogeography and paleoclimate. Acta Geol. Polon. 53, 323–339.

Harzhauser, M., Piller, W.E., 2007. Benchmark data of a changing sea – palaeogeography, palaeobiogeography and events in the Central Paratethys during the Miocene. Palaeogeogr. Palaeoclimatol. Palaeoecol. 253, 8–31.

Harzhauser, M., Piller, W.E., 2010. Molluscs as a major part of subtropical shallow-water carbonate production - an example from a Middle Miocene oolite shoal (Upper Serravallian, Austria). Spec. Publ. Int. Ass. Sed. 42, 185–200.

Hendry, J.P., Perkins, W.T., Bane, T., 2001. Short-term environmental change in a Jurassic lagoon deduced from geochemical trends in aragonite bivalve shells. Geol. Soc. Am. Bull. 113, 790–798.

Hendler, G., Miller, J.E., Pawson, D.L., Kier, P.M., 1995. Sea stars, sea urchins, and allies: Echinoderms of Florida and the Carribean. Smithsonian Institute Press, Washington, DC. 390 pp.

Hickman, C.P., 1998. A field guide to sea stars and other echinoderms of Galápagos. Lexington, Virginia. 83 pp.

Highsmith, R.C., 1980. Geographic patterns of coral bioerosion: a productivity hypothesis. J. Exp. Mar. Biol. Ecol. 46, 177–196.

Hohenegger, J., Wagreich, M., 2012. Time calibration of sedimentary sections based on isolation cycles using combined cross-correlation: dating the gone Badenian stratotype (Middle Miocene, Paratethys, Vienna Basin, Austria) as an example. Int. J. Earth. Sci. (Geol. Rundsch.) 101, 339–349.

Hubbard, J.A.E.B., Pocock, Y.P., 1972. Sediment rejection by recent scleractinian corals: a key to the palaeo-environmental reconstruction. Geol. Rundsch. 61, 598–626.

İslamoğlu, Y., Hakyemez, A., 2010. Oligocene History of the Çardak-Dazkırı Sub-basin (Denizli, SW Turkey): Integrated Molluscan and Planktonic Foraminiferal Biostratigraphy. Turkish. J. Earth. Sci. 19, 473–496.

Janssen, R., Zuschin, M., Baal, C., 2011. Gastropods and their habitats from the northern Red Sea (Egypt: Safaga). Part 2: Caenogastropoda: Sorbeoconcha and Littorinimorpha. Ann. Naturhist. Mus. Wien. (A) 113, 373–509.

Johansen, H.W., 1981. Coralline algae, a first synthesis: CRC Press, Boca Raton. 239 pp.

Jokiel, P.L., 2006. Impact of storm waves and storm floods on Hawaiian reefs. Proceedings of 10th International Coral Reef Symposium, Okinawa, Japan, pp. 390–398.

Kapounek, J., 1935. Geologische Verhältnisse der Umgebung von Eisenstadt. (Vorläufiger Bericht). Anzeiger Akad, Wiss, Wien, Math.-Naturwiss. Kl. 72, 239–241.

Kapounek, J., 1938. Geologische Verhältnisse der Umgebung von Eisenstadt (Burgenland). Jahrbuch der Geol. Landesanstalt 88, 49–102.

Karabıyıkoğlu, M., Tuzcu, S., Çiner, A., Deynoux, M., Örçen, S., Hakyemez, A., 2005. Facies and environmental setting of the Miocene coral reefs in the late-orogenic fill of the Antalya Basin, western Taurides, Turkey: implications for tectonic control and sea-level changes. Sediment Geol 173, 345–371.

Keferstein, C., 1828. Beobachtungen und Ansichten über die geognostischen Verhältnisse der nördlichen Kalk-Alpenkette in Österreich-Bayern. – Teutschland geognostisch-geologisch dargestellt 5(3), 1–425.

Kier, P.M., Grant, R.E., 1965. Echinoid distribution and habits, Key Largo coral reef preserve, Florida. Smiths Misc Collns 149, 1–68.

Kleemann, K.H., 1982. Ätzmuscheln im Ghetto? Lithophaga (Bivalvia) aus dem Leithakalk (Mittel-Miozän: Badenien) von Müllendorf im Wiener Becken, Österreich. Beitr. Paläont. Österr. 9, 211–231.

Kleypas, J.A., McManus, J.W., Menez, L.A.B., 1999a. Environmental limits to coral reef development: where do we draw the line? Am. Zool. 39, 149–159.

Kleypas, J.A., Buddemeier, R.W., Archer, D., Gattuso, J.-P., Langdon, C., Opdyke, B.N., 1999b. Geochemical consequences of increased atmospheric carbon dioxide on coral reefs. Science 284, 118–120.

Kojumdgieva, E., 1976. Paléoécologie des communautés des Mollusques du Miocène en Bulgarie du Nord-Quest. II. Communautés des Mollusques du Badénien (Miocène moyen) en Bulgarie du Nord-Quest: Geol. Balc. 6(2), 63–94.

Kojumdgieva, E., Marinescu, F., Motas, I.C., Popescu, G., 1978. Le Badénien en Roumanie et en Bulgarie. In: Papp, A., Cicha, I., Senes, J., Steininger, F.F. (Eds.), M_4 – Badenien (Moravien, Wielicien, Kosovien). Chronostratigraphie und Neostratotypen. Miozän der Zentralen Paratethys. Slowakische Akademie der Wissenschaften, Bratislava, pp. 105–107.

Kojumdgieva, E., Strachimirov, B., 1960. Les fossiles de Bulgarie VII Tortonien, Sofia. 317 pp.

Kristan-Tollmann, E., 1964. Holothurien-Sklerite aus dem Torton des Burgenlandes, Österreich. Sitzber. Österr. Akad. Wiss., Math.-Naturwiss. Kl., Abt. I, 173, 75–100.

Kristan-Tollmann, E., 1966. Alcyonarien-Sklerite aus dem Torton des Burgenlandes, Österreich. Sitzber. Österr. Akad. Wiss., Math.-Naturwiss. Kl., 175, 129–141.

Kroh, A., 2003. The Echinodermata of the Langhian (Lower Badenian) of the Molasse Zone and the northern Vienna Basin (Austria). Ann. Naturhist. Mus. Wien. (A) 104, 155–183.

Kroh, A., 2005. Catalogus Fossilium Austriae. Band 2. Echinoidea neogenica. Österreichische Akademie der Wissenschaften, Wien. 205 pp.

Kroh, A., 2007. Climate changes in the Early to Middle Miocene of the Central Paratethys and the origin of its echinoderm fauna. Palaeogeogr. Palaeoclimatol. Palaeoecol. 253, 185–223.

Kühnelt, W., 1931. Über ein Massenvorkommen von Bohrmuscheln im Leithakalk von Müllendorf im Burgenland. Paläobiologica 4, 239–250.

Kühn, O., 1963. Korallensteinkerne im österreichischen Miozän. Ann. Naturhist. Mus. Wien 66, 101–112.

Littler, M.M., Littler, D.S., 1984. A relative dominance model for biotic reefs. Advances in reef sciences. Abstracts and Schedule of presentations: a joint meeting of the Atlantic Reef Committee and the International Society for Reef Studies, Miami, Florida, pp. 73–74.

MacDonald, I.A., Perry, C.T., 2003. Biological degradation of coral framework in a turbid lagoon environment, Discovery Bay, north Jamaica. Coral Reefs 22, 523–535.

Mandic, O., Piller, W.E., 2001. Pectinid coquinas and their palaeoenvironmental implications – examples from the early Miocene of northeastern Egypt. Palaeogeogr. Palaeoclimatol. Palaeoecol. 172, 171–191.

Martin, J.M., Braga, J.C., Rivas, P., 1989. Coral successions in Upper Tortonian reefs in SE Spain. Lethaia 22, 271–286.

Martini, E. 1971. Standard Tertiary and Quaternary calcareous nannoplankton zonation. In: Farancini, A. (Ed) Proceedings of the second plankton conference, Rome, 1970, pp. 739–785.

Marubini, F., Atkinson, M.J., 1999. Effects of lowered pH and elevated nitrate on coral calcification. Mar. Ecol. Prog. Ser. 188,117–121.

Mikkelsen, P.M., Bieler, R., 2008. Seashells of southern Florida: Living marine mollusks of the Florida Keys and adjacent regions: Bivalves. Princeton University Press: Princeton, NJ (USA). 503 pp.

Minchinton, T.E., McKenzie, L.A., 2008. Nutrient enrichment affects recruitment of oysters and barnacles in a mangrove forest. Mar. Ecol. Progr. Ser. 354, 181–189.

Missimer, T.M., 2002. Late Oligocene to Pliocene evolution of the central part of the South Florida Platform: Mixing of siliciclastics and carbonate sediments: Tallahassee, Florida Geological Survey Bulletin 65. 184 pp.

Moissette, P., Dulai, A., Escarguel, G., Kázmér, M., Müller, P., Saint Martin J.P., 2007. Mosaic of environments recorded by bryozoan faunas from the Middle Miocene of Hungary. Palaeogeogr Palaeoclimatol Palaeoecol 252, 530–566.

Nebelsick, J.H., 1992. Echinoid distribution by fragment identification in the Northern Bay of Safaga, Red Sea, Egypt. Palaios 7, 316–328.

Novack-Gottshall, P.M., 2007. Using a theoretical ecospace to quantify the ecological diversity of Paleozoic and modern biotas. Paleobiology 33, 273–294.

Oosterbaan, A.F.F., 1990. Notes on a collection of Badenian (Middle Miocene) corals from Hungary in the National Museum of Natural History at Leiden (The Netherlands). Contr. Tert. Quatern. Geol. 27, 3–15.

Papp, A., Turnovsky, K., 1953. Die Entwicklung der Uvigerinen im Vindobon (Helvet und Torton) des Wiener Beckens. Jb. Geol. B.-A. 46, 117–141.

Pascher, G.A., Brix., F., 1994. Geologische Karte der Republik Österreich ÖK 77 Eisenstadt 1:50.000, Geologische Bundesanstalt, Wien

Pedley, M., 1996. Miocene reef distributions and their associations in the central Mediterranean region. In: Fransen, E.K., Esteban, M., Ward, W.C., Rouchy, J.M.

(Eds.), Models for carbonate stratigraphy from Miocene reef complexes of Mediterranean regions. SEPM 5, 73–87.

Permanyer, A., Esteban, M., 1973. El arrecife mioceno de Sant Pau d'Ordal (provincial de Barcelona). Rev. Inst. Inv. Geol. 28, 45–72.

Perrin, C., 2000. Changes of palaeozonation patterns within Miocene coral reefs, Gebel Abu Shaar, Gulf of Suez, Egypt. Lethaia 33, 253–268.

Perrin, C., Bosellini, F.R., 2012. Paleobiogeography of scleractinian reef corals: changing patterns during the Oligocene-Miocene climatic transition in the Mediterranean. Earth.-Sci. Rev. 111, 1–24.

Perry, C.T., 1996. Distribution and abundance of macroborers in an upper Miocene reef system, Mallorca, Spain: implications for reef development and framework destruction. Palaios 11, 40–56.

Perry, C.T., Macdonald, I.A., 2002. Impacts of light penetration on the bathymetry of reef microboring communities: implications for the development of microendolithic trace assemblages. Palaeogeogr. Palaeoclimatol. Palaeoecol. 186, 101– 113.

Piller, W.E., Kleemann, K., 1991. Miocene Reefs and related facies in eastern Austria. I) Vienna Basin. In: Excursion B4. Guidebook of the VI International Symposium on Fossil Cnidaria including Archaeocyatha and Porifera, International Association for the Study of Fossil Cnidaria and Porifera, Münster, pp. 1–28.

Piller, W.E., Decker, K., Haas, M., 1996. Sedimentologie und Beckendynamik des Wiener Beckens: Sediment 96, 11. Sedimentologentreffen, Exkursion guide, Geologische Bundesanstalt, Wien. 41 pp.

Piller, W., Kleemann, E. [sic], Steininger, F., 1992. STOP No. 1/3. In: Sauer, R., Seifert, P., Wessely, G. (Eds.), Guidebook to Excursions in the Vienna Basin and the Adjacent Alpine-Carpathian Thrustbelt in Austria. Mitt. Österr. Geol. Ges. 85, 112–118.

Piller, W.E., Kleemann, K., Friebe, J.G., 1991. Miocene reefs and related facies in Eastern Austria. In: Excursion B4. Guidebook of the VI International Symposium on Fossil Cnidaria including Archaeocyatha and Porifera, International Association for the Study of Fossil Cnidaria and Porifera, Münster. 47 pp.

Piller, W.E., Vavra, N., 1991. Das Tertiär im Wiener und Eisenstädter Becken. In Roetzel, R., Nagel, N. (Eds.), Exkursionen im Tertiär Österreichs, Molassezone –

Waschbergzone - Korneuburger Becken – Wiener Becken – Eisenstädter Becken. Österreichische Paläontologische Gesellschaft, pp. 161–216.

Piller, W.E., Summesberger, H., Draxler, I., Harzhauser, M., Mandic, O., 1997. Meso- to Cenozoic tropical/subtropical climates - selected examples from the Northern Calcareous Alps and the Vienna Basin. In: Kollmann, H.A., Hubmann, B. (Eds.), Excursion Guides, Second European Paleontological Congress, Climates: Past, Present and Future, Wien, pp 70–111.

Pisera, A., 1996. Miocene reefs of the Paratethys: a review. In: Fransen, E.K., Esteban, M., Ward, W.C., Rouchy, J.-M. (Eds.), Models for carbonate stratigraphy from Miocene reef complexes of Mediterranean regions. SEPM Concepts in Sedimentology and Paleontology 5, 97–104.

Printrakoon, C., Tëmkin, I., 2008. Comparative ecology of two parapatric populations of Isognomon (Bivalvia: Isognomonidae) of Kungkrabaen Bay, Thailand. Raffles Bull. Zool. 18, 75–94.

Printrakoon, C., Wells, F.E., Chitramvong, Y., 2008. Distribution of molluscs in mangroves at six sites in the upper Gulf of Thailand. Raffles Bull. Zool. 18, 247–257.

Radwański, A., Górka, M., Wysocka, A., 2006. Middle Miocene coralgal facies at Maksymivka near Ternopil (Ukraine): A preliminary account. Acta Geol. Polon. 56, 89–103.

Randazzo, A.F., Müller, P., Lelkes, G., Juhász, E., Hámor, T., 1999. Cool-water limestones of the Pannonian basinal system, Middle Miocene, Hungary. J. Sediment. Res. 69, 283–293.

Reidl, G., 1937. Paläobiologische Untersuchungen im Leithakalkaufschlusz am “Aeszeren Berg” bei Müllendorf im Burgenland. Unpubl. PhD-thesis, Wien. 77 pp.

Reidl, G., 1941. Über eine neue Spatangidenart *Plabiobrissus abeli* nov. spec. aus dem Torton von Müllendorf (ehem. Burgenland). Berichte der Reichsstelle für Bodenforschung 1941, 24–29.

Reiss, Z., Hottinger, L., 1984. The Gulf of Aqaba. Ecological Micropaleontology: Springer-Verlag, Berlin. 454 pp.

Reuss, A.E., 1871. Die fossilen Korallen des österreichisch-ungarischen Miocäns. Denkschr. Kais. Akad. Wiss., Math.-Naturwiss. Cl. 31, 197–270.

Reuter, M., Piller, W.E., 2011. Volcaniclastic events in coral reef and seagrass environments: evidence for disturbance and recovery (Middle Miocene, Styrian Basin, Austria). Coral Reefs 30, 889–899.

Riegl, B., 1999. Corals in a non-reef setting in the southern Arabian Gulf (Dubai, UAE): Fauna and community structure in response to recurring mass mortality. Coral Reefs 18, 63–74.

Riegl, B., Piller, W.E., 2000. Biostromal coral facies - a Miocene example from the Leitha Limestone (Austria) and its actualistic interpretation. Palaios 15, 399–413.

Roberts, H.H., Rouse, L.J., Walker, N.D., Hudson, J.H., 1982. Cold-water stress in Florida Bay and northern Bahamas; a product of winter cold-air outbreaks. J. Sed. Petrol. 52, 145–155.

Rögl, F., 1999. Mediterranean and Parathetys. Facts and hypotheses of an Oligocene to Miocene paleogeography (short overview). Geol. Carpath. 50, 339–349.

Roniewicz, E., Stolarski, J., 1991. Miocene Scleractinia from the Holy Cross Mountains, Poland; Part 2 -Archaeocoeniina, Astraeina and Fungiina. Acta Geol. Polon. 41(1-2), 69–83.

Rus, M., Popa, M.V., 2008. Taxonomic notes on the Badenian corals from Lăpugiu de Sus (Făget Basin, Romania). Acta Palaeontol. Roman. 6, 325–337.

Saint Martin, J.P., Merle, D., Cornée, J.J., Filipescu, S., Saint Martin, S., Bucur, I.I., 2007. Les constructions corallines du Badénien (Miocène moyen) de la bordure occidentale de la dépression de Transylvanie (Roumanie). C.R. Palevol. 6, 37–46.

Saint Martin, J.P., Müller, P., Moissette, P., Dulai, A., 2000. Coral microbialite enviroment in Middle Miocene reef of Hungary. Palaeogeogr. Palaeoclimatol. Palaeoecol. 160, 179–191.

Sanders, D., Baron-Szabo, R.C., 2005. Scleractinian assemblages under sediment input: their characteristics and relation to the nutrient input concept. Palaeogeogr. Palaeoclimatol. Palaeoecol. 216, 139–181.

Schaffer, F.X., 1908. Geologischer Führer für Exkursionen im Inneralpinen Wienerbecken II. Teil. Sammlung geologischer Führer 13, Berlin (Borntraeger). 153 pp.

Schaffer, H., 1961. *Brissus* (*Allobrissus*) *miocaenicus*, eine neue Echinidenart aus dem Torton von Mühlendorf (Burgenland). Sitzungsberichte der Österreichischen

Akademie der Wissenschaften, Math.-Naturwiss. Kl., Abteilung I, 170(3/4), 149–157.

Schmid, H.P., Harzhauser, M., Kroh, A., 2001. Hypoxic events in a Middle Miocene Carbonate Platform of the Central Paratethys (Austria, Badenian, 14 Ma). Ann. Naturhist. Mus. Wien. (A) 102, 1–50.

Schultz, O., 2001. Bivalvia neogenica (Nuculacea – Unionacea). Catalogus Fossilium Austriae, 1/1: XLVIII. Österreichischen Akademie der Wissenschaften, Wien. 380 pp.

Schultz, O., 2003. Bivalvia neogenica (Lucinoidea – Mactroidea). Catalogus Fossilium Austriae, 1/2: X. Österreichischen Akademie der Wissenschaften, Wien. 350 pp.

Schultz, O., 2005. Bivalvia neogenica (Solenoidea – Clavagelloidea). – Catalogus Fossilium Austriae, 1/3: V. Österreichischen Akademie der Wissenschaften, Wien. 520 pp.

Scott, T.M., 2001. Text to Accompany the Geologic Map of Florida, Florida Geological Survey, Tallahassee. 28 pp.

Slack-Smith, S.M., 1998. Order Ostreoida. In: Beesley P.L., Ross G.J.B., Wells A. (Eds.), Mollusca: the southern synthesis. Fauna of Australia. Vol 5. Part A. CSIRO, Melbourne, pp. 268–282.

Spalding, M.D., Ravilious, C., Green, E.P., 2001. World Atlas of Coral Reefs, University of California Press, Berkeley. 424 pp.

Stafford-Smith, M.G., 1992. Mortality of the hard coral *Leptoria phrygia* under persistent sediment influx. In: Proceedings of the 7th International Coral Reef Symposium, Guam, University of Guam Press, Vol. 1, pp. 289–299.

Stafford-Smith, M.G., 1993. Sediment-rejection efficiency of 22 species of Australian scleractinian corals. Mar. Biol. 115, 229–243.

Steininger, F., Papp, A., 1978. Faziostratotypus: Gross Höflein NNW, Steinbruch „Fenk“, Burgenland, Österreich. In: Papp, A., Cicha, I., Seneš, J., Steininger, F.F. (Eds.), M_4 – Badenien (Moravien, Wielicien, Kosovien). Chronostratigraphie und Neostratotypen. Miozän der Zentralen Paratethys. Slowakische Akademie der Wissenschaften, Bratislava, pp. 194–203.

Stenzel, H.B., 1971. Oysters. In: Moore, R.C. (Ed.), Treatise on invertebrate paleontology, part N, mollusca 6, vol. 3. Geological Society of America, Inc., Boulder, CO, USA, pp. 953–1224.

Stolarski, J., 1991. Miocene Scleractinia from the Holy Cross Mountains, Poland; Part 1 – Caryophylliidae, Flabellidae, Dendrophylliidae, and Micrabaciidae. Acta Geol. Polon. 41(1-2), 37–67.

Strauss, P., Harzhauser, M., Hinsch, R., Wagreich, M., 2006. Sequence stratigraphy in a classic pull-apart basin (Neogene, Vienna Basin). A 3D seismic based integrated approach. Geol. Carpath. 57,185–197.

Suess, E., 1860. Sitzung am 10. Jänner 1860: 8. F. Karrer, Suess, die Kalkschalen der Fossilien. Verh. Geol. Reichsanst 11, Sitzungsberichte, pp 9–10

Švagrovský, J., 1978. 8. Faziostratotypus: Devínska Nová Ves-Sandberg bei Bratislava, östlicher Rand des Wiener Beckens, Tschechoslowakei. Blatt: Bratislava-Wien M-33-XXXVI. In: Papp, A., Cicha, I., Senes, J., Steininger, F.F. (Eds.), M_4 – Badenien (Moravien, Wielicien, Kosovien). Chronostratigraphie und Neostratotypen. Miozän der Zentralen Paratethys: Slowakische Akademie der Wissenschaften, Bratislava, pp. 188–194.

Tiță, R., 1999. Biostratigraphical study of the Badenian deposits from Delineşti (Romania). Trav. Mus. Natl. Hist. Nat. Grigore Antipa 41, 473–486.

Tiță, R., 2000. Study on Miocene corals (Scleractinia) from Delineşti. Trav Mus Natl Hist Nat Grigore Antipa 42:373–382

Tiță, R., 2007. Comments on the Badenian fauna (Middle Miocene) from Bahna (Southern Carpathians, Romania). Trav. Mus. Natl. Hist. Nat. Grigore Antipa 50, 543–554.

Titlyanov, E.A., Latypov, Y.Y., 1991. Light dependence in Scleractinian distribution in the sublittoral zone of South China Sea Islands. Coral Reefs 10, 133–138.

Titschack, J., Zuschin, M., Spötl, C., Baal, C., 2010. The giant oyster *Hyotissa hyotis* from the northern Red Sea as a decadal-scale archive for seasonal environmental fluctuations in coral reef habitats. Coral Reefs 29, 1061–1075.

Tollmann, A., 1955. Das Neogen am Nordwestrand der Eisenstädter Bucht. Wissenschaftliche Arbeiten aus dem Burgenland 10, 1–74.

Tollmann, A., 1985. Geologie von Österreich. Band II. Außerzentralalpiner Anteil: Deuticke, Wien. 766 pp.

Toscano, F, Sorgente, B, 2002. Rhodalgal-bryomol temperate carbonates from the Apulian Shelf (southwestern Italy), relict and modern deposits on a current dominated shelf. Facies 46, 103–118.

Toth, G., 1950. Zur Kenntnis des österreichischen Miozäns. Ann. Naturhist. Mus. Wien 57, 163–178.

Valentine, J.W., 1969. Patterns of taxonomic and ecologic struc-ture of the shelf benthos during Phanerozoic time. Paleontology 12, 684–708.

Veron J.E.N., 1995. Corals in space and time: the biogeography and evolution of the Scleractinia. University of New South Wales Press, Sydney. 321 pp.

Veron, J.E.N., Minchin, P.R., 1992. Correlations between sea surface temperature, circulation patterns and the distribution of hermatypic corals of Japan. Cont Shelf Res 12, 835–857.

Veron, J.E.N., 2000. Corals of the World, Volume 1, Australian Institute of Marine Science, Townsville

Wentworth, C.K., 1922. A scale of grade and class terms for clastic sediments. J. Geol. 30, 377–392.

Whorff, J.S., Whorff, L.L., Sweet, M.H., 1995. Spatial variations in an algal turf community with respect to substratum slope and wave height. J. Marine Biol. Assoc. 75, 429–444.

Wiedl, T., Harzhauser, M., Piller, W.E., 2012. Facies and synsedimentary tectonics on a Badenian carbonate platform in the southern Vienna Basin (Austria, Central Paratethys). Facies 58, 523–548.

Wilbur, K.M., 1983. The Mollusca, Ecology, vol. 6, Academic Press, Orlando, Florida. 715 pp.

Wilk, J., Bieler, R., 2009. Ecophenotypic variation in the Flat Tree Oyster, *Isognomon altus* (Bivalvia: Isognomonidae), across a tidal microhabitat gradient. Mar. Biol. Res. 5, 155–163.

Woelkerling, W.J., Irvine, L.M., Harvey, A.S., 1993. Growth-forms in non-geniculate coralline red algae (Corallinales, Rhodophyta). Aust. Syst. Bot. 6, 277–293.

Yonge, C.M., 1968. Form and habit in species of *Malleus* (including the “hammer oysters”) with comparative observations on *Isognomon isognomon*. Biol. Bull. 135, 378–405.

Young, J.R., 1998. Neogene. In: Bown, P.R. (Ed.) Calcareous nannofossil biostratigraphy. Cambridge University Press, pp. 225–265

Zuschin, M., Baal, C., 2007. Large gryphaeid oysters as habitats for numerous sclerobionts: a case study from the northern Red Sea. Facies 53, 319–327.

Zuschin, M., Hohenegger, J., 1998. Subtropical coral-reef associated sedimentary facies characterized by molluscs (Northern Bay of Safaga, Red Sea, Egypt). Facies 38, 229–254.

Zuschin, M., Janssen, R., Baal, C., 2009. Gastropods and their habitats from the northern Red Sea (Egypt: Safaga). Part 1: Patellogastropoda, Vetigastropoda and Cycloneritimorpha. Ann. Naturhist. Mus. Wien. (A) 111, 73–158.

Zuschin, M., Oliver, P.G., 2003. Fidelity of molluscan life and death assemblages on sublittoral hard substrata around granitic islands of the Seychelles. Lethaia 36, 133–149.

Zuschin, M., Piller, W.E., 1997. Bivalve distribution on coral carpets in the northern bay of Safaga (Red Sea, Egypt) and its relation to environmental parameters. Facies 37, 183–194.

Chapter IV

From biologically to hydrodynamically controlled carbonate production by tectonically induced palaeogeographic rearrangement (Middle Miocene, Pannonian Basin)

Thomas Wiedl[1], Mathias Harzhauser[2], Andreas Kroh[2], Stjepan Ćorić[3], Werner E. Piller[1]

[1] Institute of Earth Sciences, Palaeontology and Geology, University of Graz, NAWI Graz, Heinrichstrasse 26, 8010 Graz, Austria, thomas.wiedl@uni-graz.at, werner.piller@uni-graz.at

[2] Natural History Museum Vienna, Burgring 7, 1010 Vienna, Austria, mathias.harzhauser@nhm-wien.ac.at

[3] Geological Survey of Austria, Neulinggasse 38, 1030 Vienna, Austria, stjepan.coric@geologie.ac.at

(Author for correspondence: E-mail: thomas.wiedl@uni-graz.at)

Keywords: Miocene, Serravallian, Badenian, Central Paratethys, Vienna Basin, Danube Basin, depositional systems, basin development

4.1 Abstract

The Leitha Mountains in Austria are a chain of hills separating the southern Vienna Basin and the Danube Basin. The Lower East Alpine basement of the Leitha Mts. is covered by Middle Miocene sediments of the Badenian and Sarmatian regional stages. Close to the north-eastern margin of these hills, upper Badenian successions are exposed, which are part of a coralline algal dominated carbonate platform with hydrodynamically influenced sediments. Six sections have been logged and subjected to detailed investigation and sampling. They are characterized by inclined beds (foresets) which have been formed by unidirectional transport of sediments. Large-scale asymmetrical ripples indicate strong currents affecting shallow topset deposits. Generally, this hydrodynamically controlled sedimentation, documented by seven facies types, is reflected in a strongly reduced diversity of facies and biota, contrary to the older facies-rich middle Badenian sediments. This change from biologically to hydrodynamically controlled sedimentation led to a reduction in diversity of facies and biota. Sediment transport, however, caused secondary mass occurrences of echinoids or foraminifers derived from seagrass meadows. This study unravels the distribution and differences of middle and upper Badenian deposits of the Leitha Mountains and the influence of tectonic activity. Changes in hydrodynamics on the Leitha Platform are linked to the formation of the Danube Basin starting in the middle Badenian when a new seaway to the southeast has started to form.

4.2 Introduction

The evolution of the Pannonian Basin System and associated intramontane basins during the Miocene was largely controlled by stress-generated lithosphere subduction and continental collision (Horváth and Cloetingh 1996).

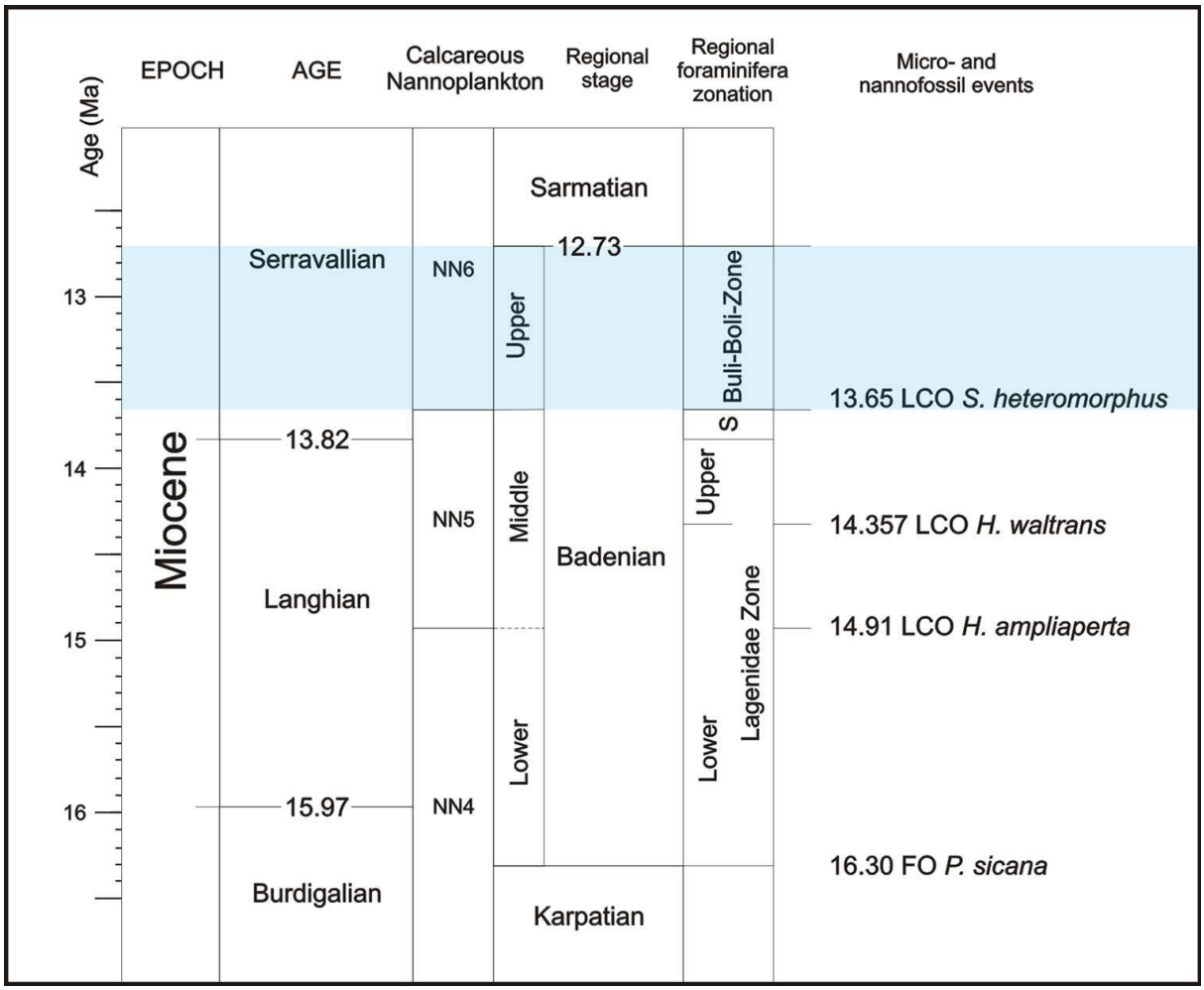

Fig. 4.1 Stratigraphic chart (modified after Hohenegger and Wagreich 2012) with biozonations of calcareous nannoplankton and Central Paratethyan foraminifera zonations (S: *Spiroplectammina* Zone, Buli-Boli: *Bulimina-Bolivina* Zone). The Winden sections are located within nannoplankton zone NN6 (highlighted in blue).

The sedimentary record of the Pannonian Basin indicates major tectonic phases between 17.5 and 14 Ma (Burdigalian to Langhian, Fig. 4.1) with strike-slip and extensional regimes (Horvath 1995; Van Balen and Cloetingh 1995; Mattick et al. 1996; Meulenkamp et al. 1996; Huismans et al. 2001). The end of this process is marked by a middle Badenian (ca. 14 Ma) unconformity (Horvath 1995) with the Eastern Alps and the West Carpathians being affected by eastward escape and

strike slip movements (Huismans et al. 2001 and references therein). The Vienna and Danube basins were formed at the western margins of the Pannonian Basin System. Tectonic activity, normal faulting and extension already began in Burdigalian time in the intra-Carpathian basins (Ratschbacher et al. 1990). While the main extension activity of the Vienna Basin occurred during the early to middle Badenian (Ratschbacher et al. 1990), the onset of extension in the Danube Basin was initiated slightly later (Kováč et al. 1993, 1999; Lankreijer et al. 1995; Kováč 2000). The Vienna Basin was formed by interactive processes of compression, strike-slip movements, extension and lateral extrusion (Ratschbacher et al. 1991; Fodor 1995; Decker and Peresson 1996). In contrast, the Danube Basin was characterized by synrift subsidence controlled by lithospheric extension (Kováč et al. 1999 and references therein).

During Miocene times, the Pannonian Basin was characterized by isolated internal mountains (inselbergs). Examples are the Transdanubian Range or the Mecsek Mountains within the Intra-Carpathian Basin (Csontos and Vörös 2004) or topographic highs in the Vienna Basin that formed islands, shoals, and small platforms with extensive carbonate production (e.g., Dullo 1983; Riegl and Piller 2000; Schmid et al. 2001; Harzhauser and Piller 2010). One of these small carbonate platforms is the Leitha Platform, situated at the southern border of the Vienna Basin (Schmid et al. 2001). Despite the literal translation, the Leitha Mountains are not mountains as such but rather low lying hills. During the Badenian, platform sediments of the Leitha Mountains were formed in shallow subtropical near-shore environments dominated by coralline algal debris (Dullo 1983; Riegl and Piller 2000; Wiedl et al. 2012, 2013). This platform was situated at the northern edge of the Middle Miocene Peri-Mediterranean reef belt in the Central Paratethys (Wiedl et al. 2013).

Up to now, only middle Badenian sediments in the southwestern part of this platform have been studied in detail (e.g. Tollmann 1955; Dullo 1983; Kroh et al. 2003; Wiedl et al. 2012 and references therein; Wiedl et al. 2013). The northeastern part of the platform was studied only to a lesser extent and many localities are only documented in few sentences in the literature (Čžjžek 1852; Karrer and Fuchs 1868; Fuchs 1894; Fuchs 1902; Schaffer 1908; Götzinger 1916; Herrmann 1973; Rohatsch 1996; Häusler 2010). New sedimentological data of upper Badenian deposits from the northeastern part of the Leitha Platform seem to reflect the influence of the structural evolution of the Pannonian Basin System at its western margin. This paper

is part of a series of papers (Wiedl et al. 2012, 2013) dealing with the facies and biota of the Leitha Platform.

4.2.1 Study area and geological setting

The study area (Fig. 4.2) is the central and northeastern part of the Leitha Mountains in the Burgenland province of Austria. This chain of hills between the southern Vienna Basin and the Danube Basin spans ca. 35 km from southwest to northeast with a maximum width of ca. 17 km. Its basement consists of Lower East Alpine units (Dolomite, Semmering-quartzite, sericite-schist, chlorite-biotite-micaschist) which is covered by Badenian and Sarmatian sediments (Herrmann et al. 1993; Häusler 2007; Häusler et al. 2010) which are part of a shallow subtidal carbonate ramp (Piller and Vavra 1991; Piller et al. 1996).

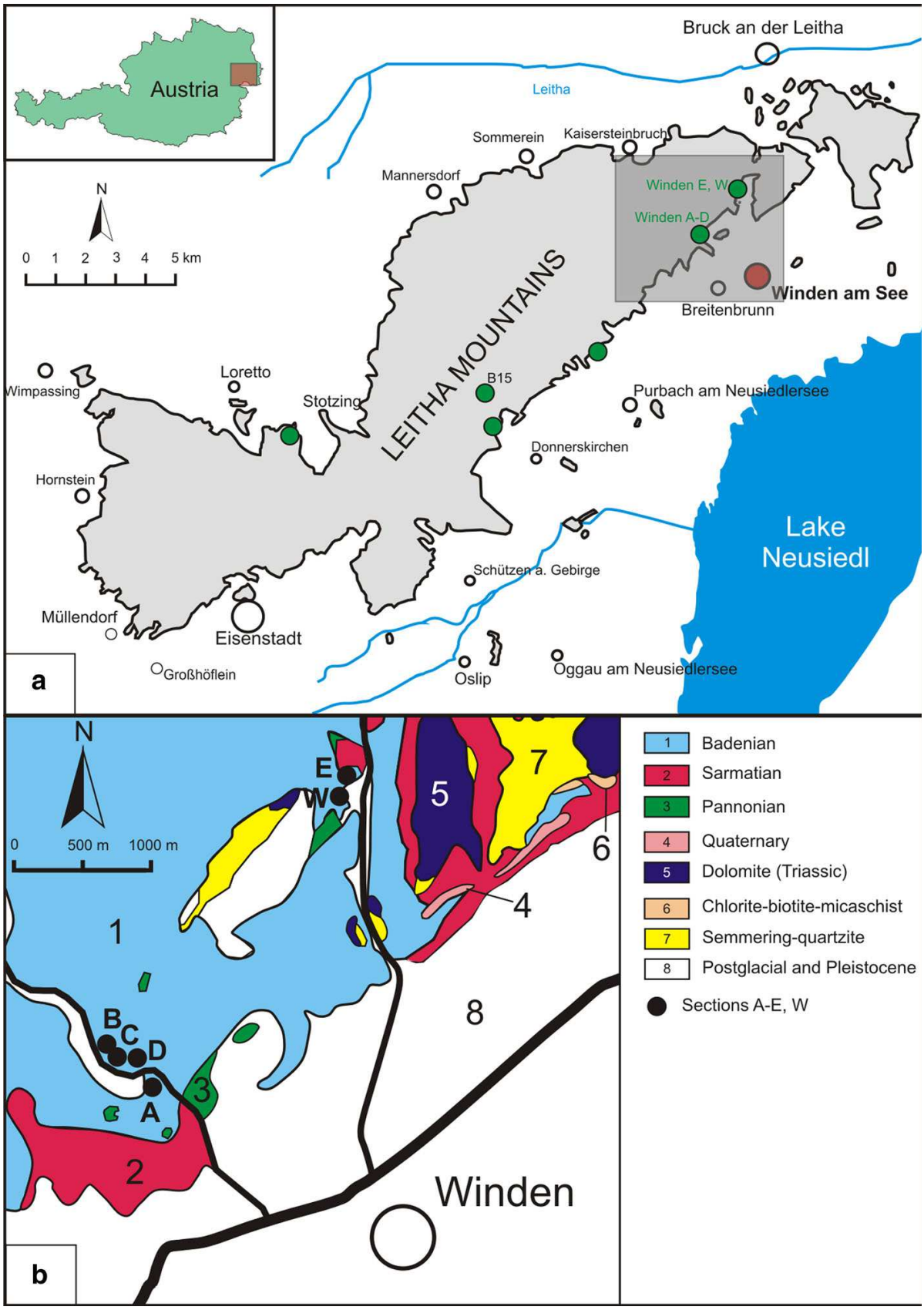

Fig. 4.2 Location of the studied area. **a** Geographic map of the Leitha Mountains (its position within Austria is indicated by the insert). Sections are indicated with green dots. The study area of the Winden sections is highlighted by the rectangle. **b** Geological map of the study area (Häusler et al. 2010) with positions of the sections studied (black dots).

Herein we describe limestone successions exposed in abandoned quarries in the north-eastern part of the Leitha Mountains close to the villages Winden am See and Breitenbrunn am Neusiedlersee (Fig. 4.2). For better understanding of the distribution of the Badenian limestones, also samples were taken close to the road (B15) between Hof am Leithagebirge and Donnerskirchen, as well as in Donnerskirchen, Purbach, Stotzing and Loretto.

4.3 Material and methods

The study combines sedimentological and palaeontological data of six sections, which have been logged and sampled in detail. The thickness and geometry of single beds or horizons were recorded. From each section oriented rock samples were collected for thin-section as well as sieving samples for micropalaeontological analyses. Fossil abundances were recorded semi-quantitatively. Data acquisition of sedimentary units and their geometries in the field were supported by photomosaics. For microfacies analyses, 103 thin-sections were studied. The carbonate nomenclature follows Dunham (1962) and Embry and Klovan (1971). The nomenclature of red algae growth-forms is based on Woelkerling et al. (1993).

To reveal the distribution of Badenian limestones throughout the Leitha Platform, samples for thin-section analyses and investigation of nannoplankton were also collected from Stotzing (N47°54'5.84", E 16°33'0.58") and next to road B15 between Donnerskirchen and Hof (N47°54'17.00", E16°37'32.26") (Fig. 4.2a).

4.4 Stratigraphy

The correlation of the regional Paratethyan stratigraphy to the international stratigraphic standard and the subdivision of the regional Badenian stage is still a matter of debate (e.g., Piller et al. 2007; Lirer et al. 2009; Hohenegger and Wagreich 2012; Hohenegger et al. 2014). The subdivision into lower, middle and upper Badenian as used in this study is based on Steininger and Papp (1978). Stratigraphic correlation and dating of the corallinacean limestones is based on calcareous nannoplankton and pectinid assemblages. The latter are well studied for the Central Paratethys and allow accurate correlations with occurrences from adjacent regions distributed across the NE Atlantic, Mediterranean, and Indian Ocean (Mandic 2004).

The occurrence of *Helicosphaera walbersdorfensis* and *Reticulofenestra pseudoumbilica* and the absence of the NN5 zone-marker *Sphenolithus heteromorphus* in deposits of the Winden sections indicate zone NN6 (Martini 1971; Fornaciari et al. 1996) and CMN8 or CMN9 (Backman et al. 2012) respectively. A middle Badenian age (zone NN5) can also be excluded due to the occurrence of *Aequipecten elegans* (Studencka 1999; Mandic 2004)**.** Therefore, a late Badenian age is proposed for the investigated sections (Fig. 4.1). Furthermore, the ostracod *Carinocythereis carinata* (occurring in sample Winden E/23) indicates the Central Paratethys ostracod-zone NO 10, which again points to a late Badenian age (Jiříček and Riha 1991).

Other localities in the northeastern part of the Leitha Mountains, which are very similar with respect to the facies to the Winden successions, are situated close to Purbach (N 47°55'39.80", E 16°41'26.90") and Donnerskirchen (N 47°53'18.40", E 16°37'40.20") and show common occurrences of *Aequipecten elegans* and *Flabellipecten leythajanus*. Both indicate a late Badenian age (pers. comm. O. Mandic, 2013).

4.5 Sedimentary facies

The studied sedimentary successions (Figs. 4.3-4.6) consist of coralline algal limestones (mainly packstones and rudstones) dominated by debris of predominantly branched growth forms. Section Winden E is characterized by limestone-clay alternations. Winden E and W are unconformably cut by Sarmatian limestone successions, composed of well rounded coralline algal debris.

4.5.1 Winden A

The succession (Figs. 4.3, 4.4a, 4.6) is ca. 13 m thick and composed of inclined beds. The beds pinch out to the southwest. The succession starts with coralline algal limestones (beds 1-5) containing common foraminifers (numerous *Elphidium* and *Asterigerinata* and rare *Planostegina*). Gastropods (< 2 mm) commonly occur, while bivalves (most commonly ostreid fragments) are rare. Echinoids are represented by debris; branched and celleporiform bryozoans are rare. Locally, the beds are internally stratified at cm-scale. A succession with common fragments of bivalves and

gastropods (< 2 mm) follows. At the base of bed 6, a coquina of disarticulated *Gigantopecten nodosiformis* and debris of small pectinids is developed. Rhodoliths, with celleporiform bryozoans as nucleus, are common. Foraminifera (mainly *Elphidium*) are rare. Bed 7 is dominated by rhodoliths (∅ 2-4 cm), while bed 8 contains numerous disarticulated *Flabellipecten*. Up-section, an alternation of foraminiferal-rich coralline algal limestones and intercalated cm-thick marly beds follows containing common echinoid remains and pectinids (*Flabellipecten*) with clionid sponge borings. Mass occurrences of thick-shelled *Spatangus* are documented in bed 15. Bed 16 consists of a well cemented coralline algal limestone containing many branched and celleporiform bryozoans; *Elphidium* and serpulids are also common. The bed is followed by a marly coralline algal limestone (17) in which debris of pectinids and ostreids is very common. The top of the succession consists of a highly weathered coralline algal limestone (bed 18) containing common *Elphidium* and rare *Borelis*. Echinoids and serpulids are also common.

4.5.2 Winden B

The ca. 6.8-m-thick section (Fig. 4.3) starts with a marly coralline algal limestone (bed 1), containing common *Elphidium*. Echinoid remains (*Echinolampas*) also occur while bryozoans are rare. Bed 2 shows high amounts of foraminifers (*Elphidium*, *Asterigerinata*). At the top, a horizon containing echinoid debris (consisting of the regular echinoid *Schizechinus hungaricus* and spatangoids) is developed. Beds 3-5 consist of a coralline algal-echinoid limestone with mass occurrences of *Schizechinus hungaricus* and *Spatangus* fragments and loosely dispersed rhodoliths. The echinoid fragments are flattened and enriched in densely packed horizons (2-3 cm in thickness) intercalated with coralline algal beds with few echinoid remains. Bed 3 locally cuts ca. 30 cm into bed 2. Bed 6 is similar to beds 1-2. The top of the section (bed 7), consists of a porous rhodolith rudstone. Interspaces between rhodoliths (∅ 3-5 cm, laminar) are filled with algal debris. *Aequipecten scabrellus* is common, oyster remains are rare.

4.5.3 Winden C

The section (Figs. 4.3, 4.4b) has a thickness of ca. 6.6 m and consists of coralline algal limestones with high amounts of *Elphidium*. Bryozoans are rare, as are serpulids and ostreids. The top surface of the marly bed 2 is undulated. In beds 3 and 4, bivalve debris is common and single valved *Aequipecten elegans* and oyster remains occur. The uppermost 20 cm of bed 4 consist of marl. Bed 5, which is onlapping on bed 4, is dominated by laminar rhodoliths (∅ 5-6 cm) and wedges out to the east. There follows a succession of coralline algal limestones (beds 6-8) characterized by high amounts of *Elphidium*. Echinoid debris (spatangoids) and serpulids are also common. A thin dark marly bed (9) follows which is covered by a horizon of rhodoliths wedging out to the east, covering bed 10, which contains abundant *Elphidium*. Bed 11 consists of marl. A succession (beds 12-14) with common *Elphidium* and low amounts of echinoids and bryozoans follows.

4.5.4 Winden D

Section D (Figs. 4.3, 4.4c) has a thickness of 3.85 m and starts with a poorly cemented limestone bed of coralline red algae (1) with common *Elphidium*, rare debris of echinoids and pectinids, and few bryozoans. With a thickness of 1.2 m, beds 2a-d show undulated surfaces. Ripples of bed 2a show wave lengths of 1.2 m. Bed 2c is characterized by internal beddings consisting of south-west trending foresets. Bed 2d erosively cuts beds 2b and 2c. Bed 3 shows internal ripple lamination (wave-length 30 cm) and inclined foresets on the stoss side, representing small anti-dunes (Fig. 4.4c). Up-section, the wave length increases to 40 cm and ripples of asymmetrical form are present (steep side in the NW, flat side in the SE, Fig. 4.4c). The ripple trains are transverse sinuous in phase. Towards the top of the bed the ripples are replaced by planar to wavy thin-bedded (2-3 cm) corallinacean limestones. In this part of the section *Thalassinoides* burrows are preserved.

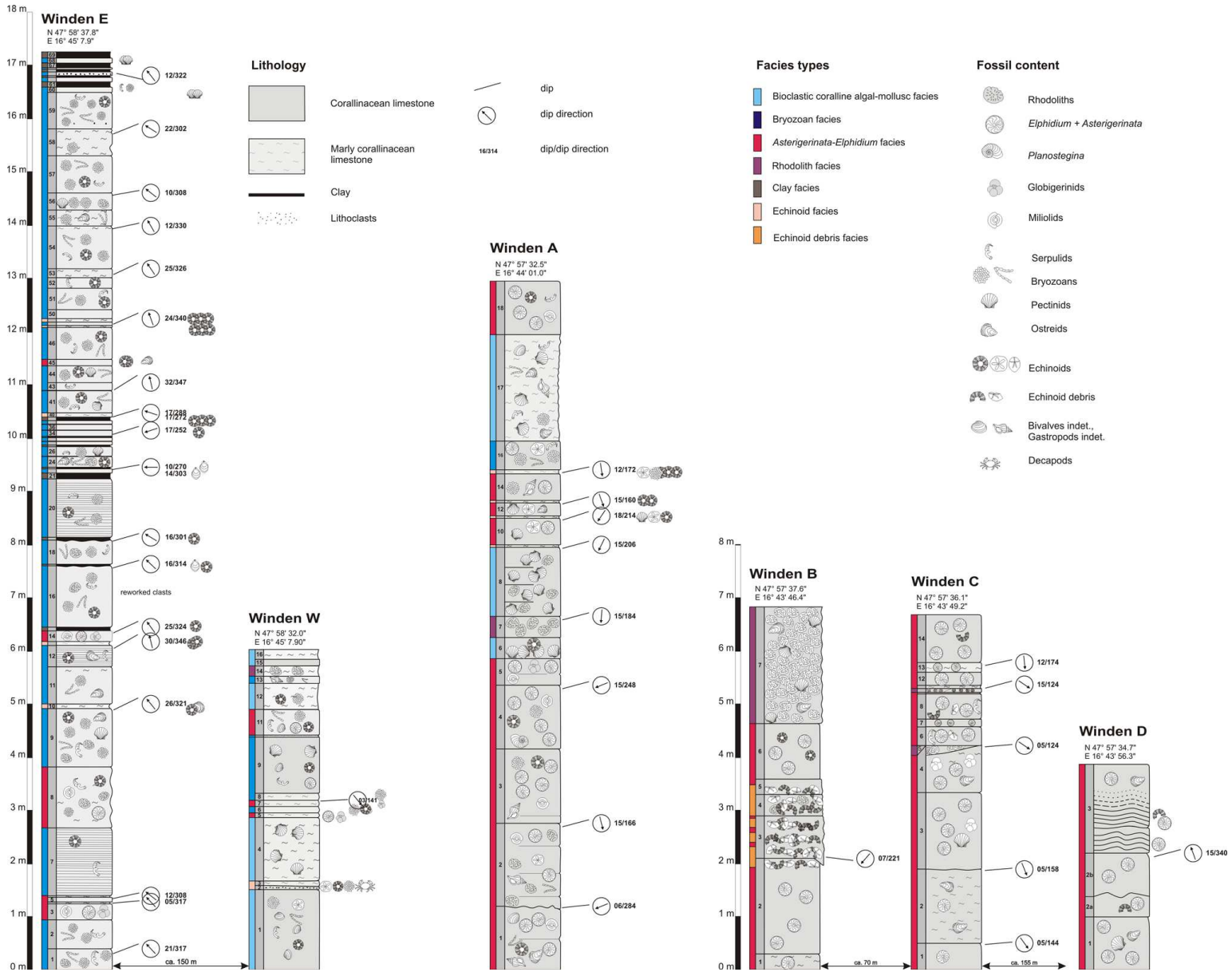

Fig. 4.3 Lithologic columns of sections A-E and W including GPS coordinates. Colours represent facies types. Dip angles and dip directions of single beds are indicated next to the columns.

4.5.5 Winden E

The section (Figs. 4.3, 4.5a, 4.6) has a total thickness of ca. 17 m. The first part (ca. 6.4 m) starts with two porous limestone beds (1-2) containing common celleporiform and branched bryozoans, few rhodoliths, brachiopods (< 1 cm), serpulids and debris of regular echinoids. Foraminifers are dominated by *Elphidium* and *Amphistegina*. Above follows a succession of well cemented beds (3-6) characterized by numerous *Asterigerinata* and *Elphidium*. With bed 7 a change occurs to a well cemented stratified (2-3 cm) limestone (rudstones and packstones). It is covered by a marly bed (8). The well cemented bed 9 contains common celleporiform bryozoans (partly encrusted by coralline algae), common single-valved *Aequipecten elegans* and shell debris of ostreids. Within the marly bed 10, large spines of the echinoid *Stylocidaris*? *schwabenaui* and remains of the oyster *Cubitostrea digitalina* are common. A massive bryozoan-rich bed (11) follows. While bed 12 is similar to bed 7, the marly bed 13 contains numerous cidaroids and spatangoids. It is covered by a foraminiferal-rich bed (14) similar in composition to bed 3.

With a thickness of ca. 4 m, the second part of the succession is represented by limestones with intercalated beds of dark clay (beds 15-39). While the lower two-thirds of the unit are characterized by thick-bedded limestones (0.45-1.2 m), that of the upper part are thin-bedded (2-20 cm) and enriched in branched and celleporiform bryozoans. Small rhodoliths (∅ 1-2 cm) occur. Molluscs are represented by *Gigantopecten nodosiformis* and oyster remains. Serpulids are common, while micromorphic brachiopods are rare. The clay beds are enriched in remains of *Schizechinus hungaricus* and spatangoids, common micromorphic brachiopods and molluscs (single-valved *Aequipecten elegans* and ostreid debris). Foraminifera are represented by common *Elphidium*. Beds 16 and 18 show undulated surfaces at the

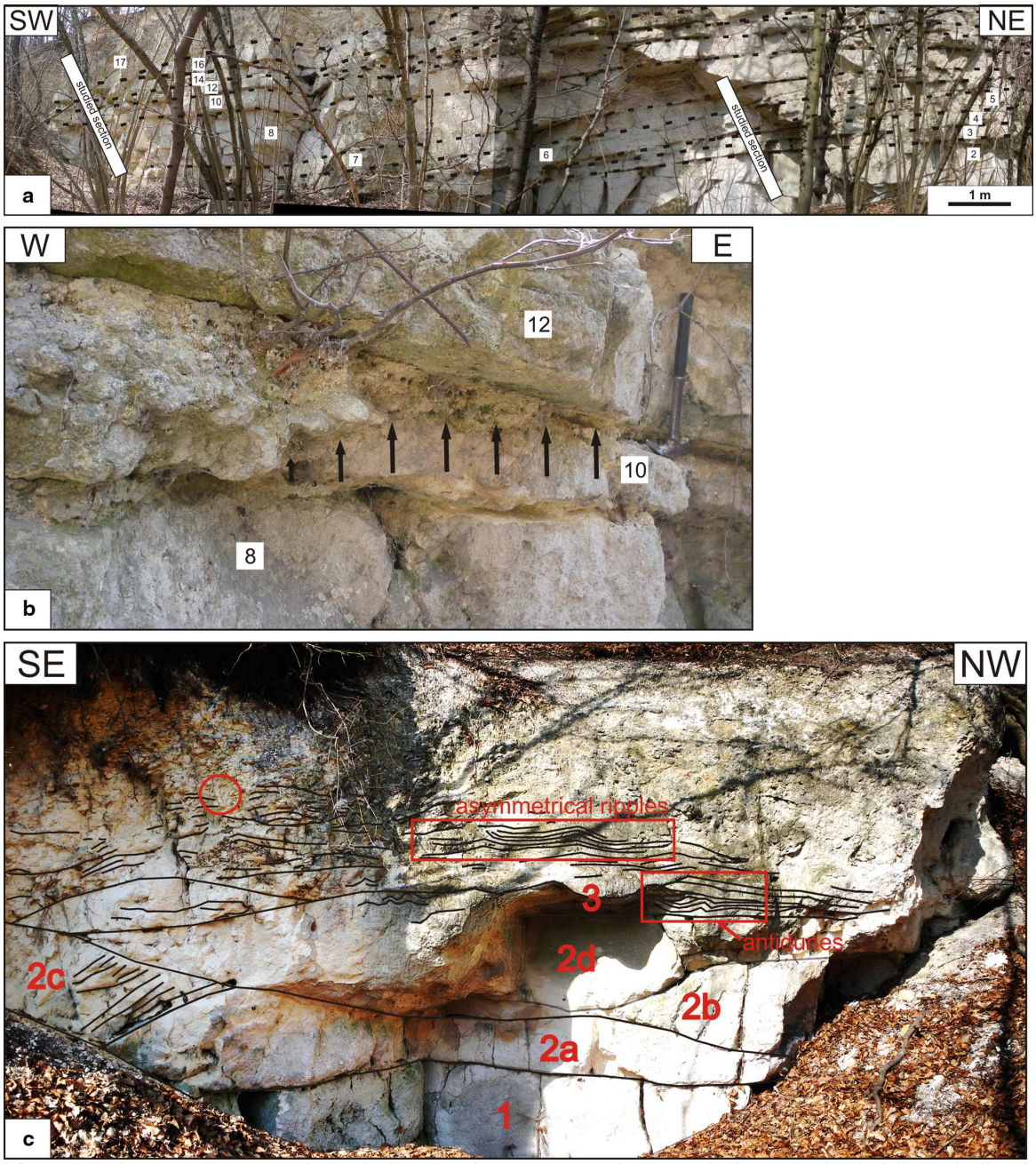

Fig. 4.4. Phototransects of the Winden sections A, C and D. **a** Winden A: stippled lines indicate beds which represent foresets pinching out to the SW. **b** Winden C. Small dune (bed 10, indicated by black arrows) with accumulation of rhodoliths in a small depression (hammer for scale). **c** Winden D: The lower part of the succession (beds 1-2d) shows large-scale asymmetrical ripples. Bed 3 shows small-scale ripples with small antidunes as well as asymmetrical ripples. The red circle indicates *Thalassinoides* burrows.

tops. The very porous limestone bed 20 is internally stratified (rudstones and packstones). Bed 39 is characterized by mass occurrences of *Schizechinus hungaricus*. The third part of the succession (ca. 6.2 m) is similar to the first as it consists of a succession of coralline algal limestones with a single 5-mm-thick clay horizon (42). Branched and celleporiform bryozoans are common. Marly limestones are represented by beds 40, 53-55 and 58. Echinoid remains are very common

(*Schizechinus hungaricus* and spatangoids) in the entire unit; beds 40, 47 and 49 again contain high numbers of *Schizechinus hungaricus*. Bed 45 shows high amounts of rotaliid foraminifers. Small quartz grains (∅ up to 1 mm) occasionally occur; a coarsening-upward trend in coralline algae debris is visible. Serpulids and small pectinids (*Aequipecten elegans*) are locally common, as well as small rhodoliths (∅ 1-2 cm).

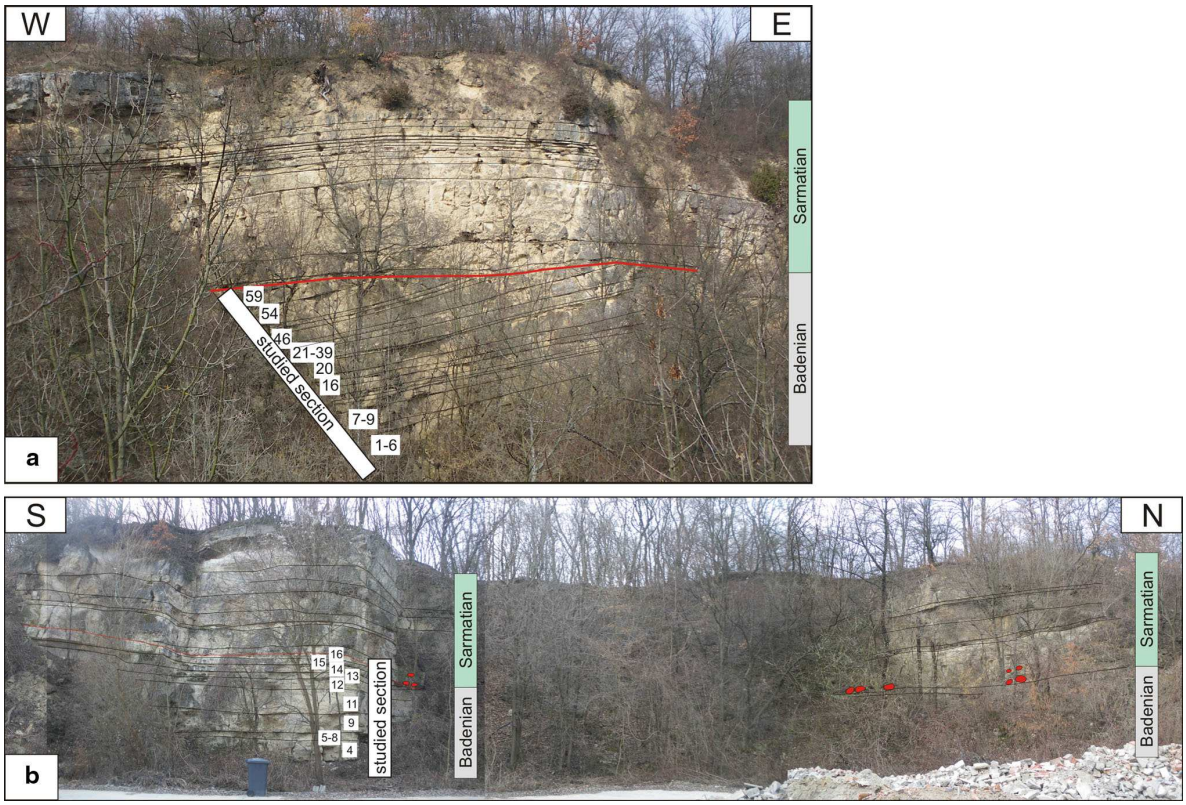

Fig. 4.5 Phototransects of the Winden sections E and W. **a** Winden E: The section is characterized by Badenian limestones showing well developed clinoforms. The succession is erosively truncated (red line) by Sarmatian limestones. **b** Winden W: The upper Badenian succession is erosively truncated (red line) by Sarmatian limestones containing limestone boulders (highlighted in red). Rubbish bin (ca. 1 m in height) for scale.

The uppermost part of the succession (ca. 0.65 m thick) consists of limestone-clay alternations. The limestones are characterized by common branched and celleporiform bryozoans. *Aequipecten elegans* is common, especially at the top of bed 64 and within bed 68. Bed 64 is additionally characterized by common quartz grains (∅ up to 4 mm). The section is unconformably cut by a ca. 15-m-thick Sarmatian limestone succession.

4.5.6 Winden W

The succession (Figs. 4.3, 4.5b) has a thickness of ca. 6 m and is dominated by poorly cemented coralline algal debris limestones (packstones and rudstones). The fauna is composed of common molluscs (ostreids, pectinids) in the lower part (beds 1, 4) while bryozoans (mainly celleporiforms, rarely branched) dominate in the upper part of the section (beds 6, 8-10). Echinoids, represented by *Eucidaris*, *Schizechinus hungaricus*, *Spatangus,* and *Stylocidaris* cf. *schwabenaui*, occur in the entire succession but are especially abundant in beds 2 and 3. Coronae of regular echinoids are filled up with their spines in bed 2, while in the surrounding sediment spines are relatively rare. Foraminifers (*Elphidium*, *Asterigerinata*, *Planostegina*, textulariids) are common in beds 5, 7 and 11. Further faunal elements are represented by rare serpulids and crustacean remains.

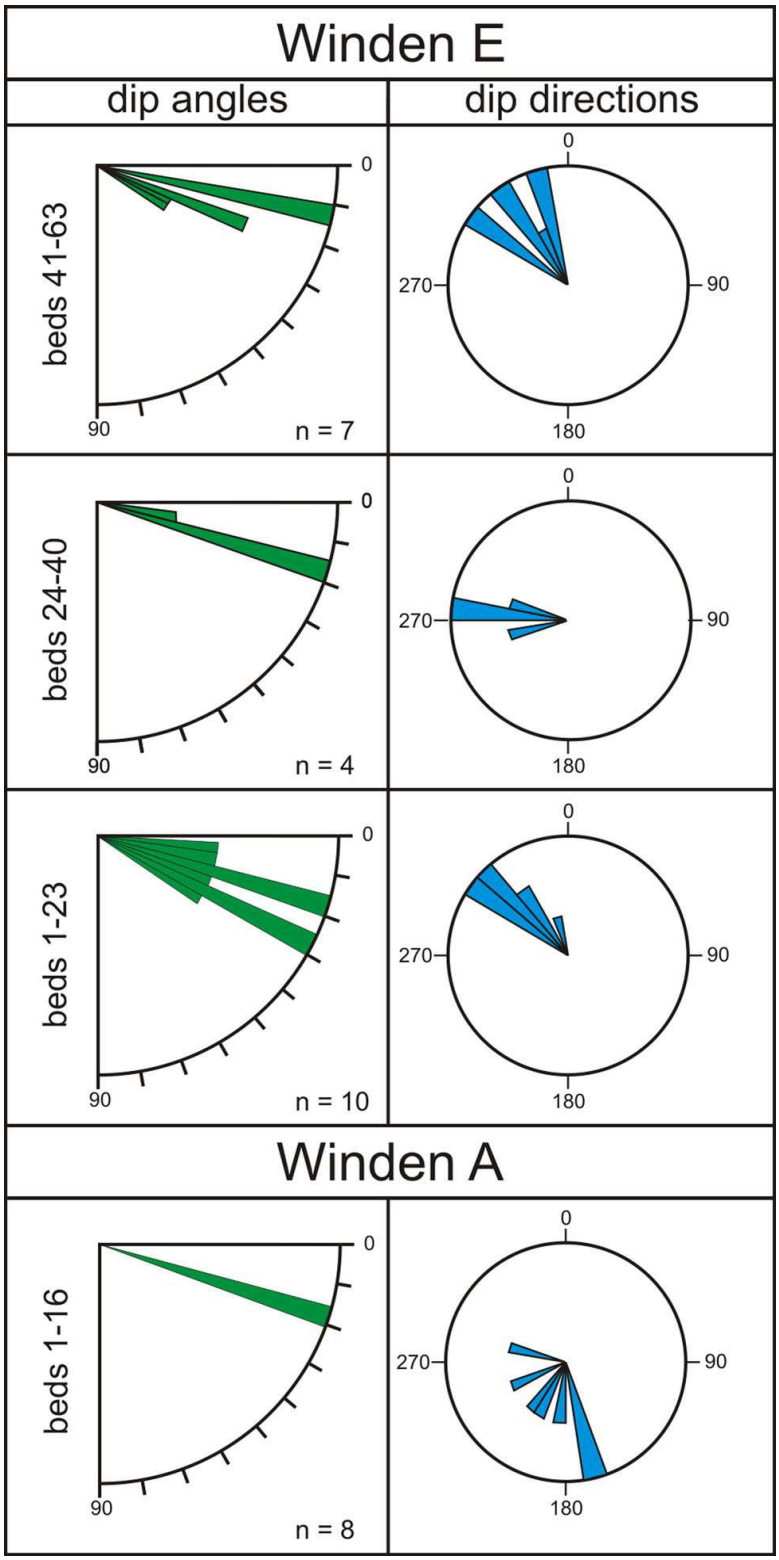

Fig. 4.6 Rose diagrams illustrating dip angles and dip directions (n = number of measurements) of beds within sections Winden A and E.

In the lowermost part of the section, the marl content increases from bed 1 to 3 and largely fills interspaces between coralline algal debris in bed 3; in bed 2 rare, well rounded quartz-grains (∅ 1 mm) occur. The coralline algal debris of bed 4 shows a fining-upward trend. The bed is covered by a succession of marly coralline algal limestones (beds 5-8) including a brown mud- to wackestone (bed 7). The following two beds (8 and 9) consist of coarse grained limestones with common oysters (*Cubitostrea digitalina*). Bed 10 consists of a brown fine-sand with high clay content. Beds 11 to 14 show increased clay contents; bed 14 is covered by a very porous marly bed, which contains common globular rhodoliths (∅ 2-4 cm). The succession is erosively truncated by a Sarmatian limestone succession of ca. 8 m.

4.6 Facies

Six facies types can be distinguished based on field observations and microfacies analyses. They generally consist of coralline algal limestones with additional components used for further differentiation. Three facies types are similar to already established facies types by Wiedl et al. (2012, 2013).

4.6.1 Bryozoan facies

The bryozoan facies (Fig. 4.7a) consists of poorly sorted corallinacean rudstones to packstones with common colonies of branched or celleporiform bryozoans (ca. 2-5 mm). Rare bivalves are represented by pectinid (*Gigantopecten nodosiformis*, *Aequipecten elegans*) and ostreid (*Cubitostrea digitalina*) shells. The foraminiferal fauna consists of common biserial textulariids, miliolids (*Triloculina*) and *Elphidium*; occasionally globigerinids are also common. The facies highly dominates section Winden E and is subordinate in A and W (Fig. 4.3); it is associated with all other facies types described in this paper.

Interpretation - A similar bryozoan facies has already been reported from Mannersdorf (Wiedl et al. 2012) and Müllendorf (Wiedl et al. 2013). There, it is either indicative of slightly deeper water or increased nutrient levels leading to heterotrophic-rich associations in shallower water. A similar situation to Mannersdorf

and Müllendorf but additionally influenced by strong currents can be assumed for the Winden area.

4.6.2 Bioclastic coralline algal-mollusc facies

The bioclastic coralline algal-mollusc facies (Fig. 4.7b) comprises coralline algal packstones and rudstones with a mollusc-fauna characterized by common pectinids and ostreids. Within section Winden A, coquinas of disarticulated *Gigantopecten nodosiformis* and *Flabellipecten* occur. Further elements are common small gastropods (< 2 mm), rare bryozoans (celleporiform and branched forms) and serpulids. Locally, the limestones show increased clay content. The facies is associated with the bryozoan facies, the rhodolith facies, the *Asterigerinata-Elphidium* facies and the echinoid facies.

Interpretation - The facies is similar to the mollusc subfacies reported from Mannersdorf by Wiedl et al. (2012) and to the bioclastic coralline algal-mollusc facies reported from Müllendorf by Wiedl et al. (2013). In comparison to these facies types, the limestones of the Winden quarries show a less diverse mollusc fauna as especially infaunal taxa are rare.

4.6.3 Echinoid debris facies

The echinoid debris facies (Fig. 4.7c) consists of echinoid rudstones containing debris of red algae. The fauna is represented by *Eucidaris*, *Schizechinus*, *Stylocidaris* cf. *schwabenaui,* and *Spatangus.* The echinoids are highly fragmented and constitute a considerable proportion of the sediment (e.g., in Winden B; Fig. 4.7c).

Interpretation - Transport can be assumed for the echinoid coquinas of highly fragmented specimens in section Winden B. The fact that rather delicate regular echinoids are present suggests a special type of transport mechanism. To interpret this mechanism, more data is needed concerning the size distribution of the echinoids, taphonomic details, and associated sedimentological features. Such mass occurrences, often tied to high population densities, are found within shoreface

sequences where concentration processes include winnowing by higher water energy (Moffat and Bottjer 1999; Kroh and Nebelsick 2010; Belaústegui et al. 2012; Mancosu and Nebelsick 2013).

4.6.4 Echinoid facies

The echinoid facies (Fig. 4.7d) is expressed within Winden W, as well as in sections A and E. It consists of marly corallinacean rudstones to packstones with accumulations of well preserved echinoid coronae (Winden E, W, A). The partly diagenetically flattened echinoids (*Schizechinus hungaricus* and *Spatangus* sp.) show spines which accumulated within the interior of the coronae (Fig. 4.7d).

Interpretation - Similar associations of *Spatangus* and *Schizechinus hungaricus* are known from St. Margarethen in Burgenland (Schmid et al. 2001). Extant *Spatangus* is known as a shallow burrower or ploughing the sediment surface in medium to coarse sandy environments at a depth between 10 and 55 m (Schmid et al. 2001). Habitats of extant *Spatangus purpureus* are characterized by muddy sand bottoms adjacent to coralline algal sands (Riedl 1983). This depositional environment fits well with the presence of *Spatangus* in the Winden area which is very abundant in clay or limestone beds with increased clay content. *Schizechinus hungaricus*, co-occurring with *Spatangus*, probably preferred a similar environment. The occurrence of tests filled with spines indicates phases of post-mortem current transport. The transport mechanism is still unclear.

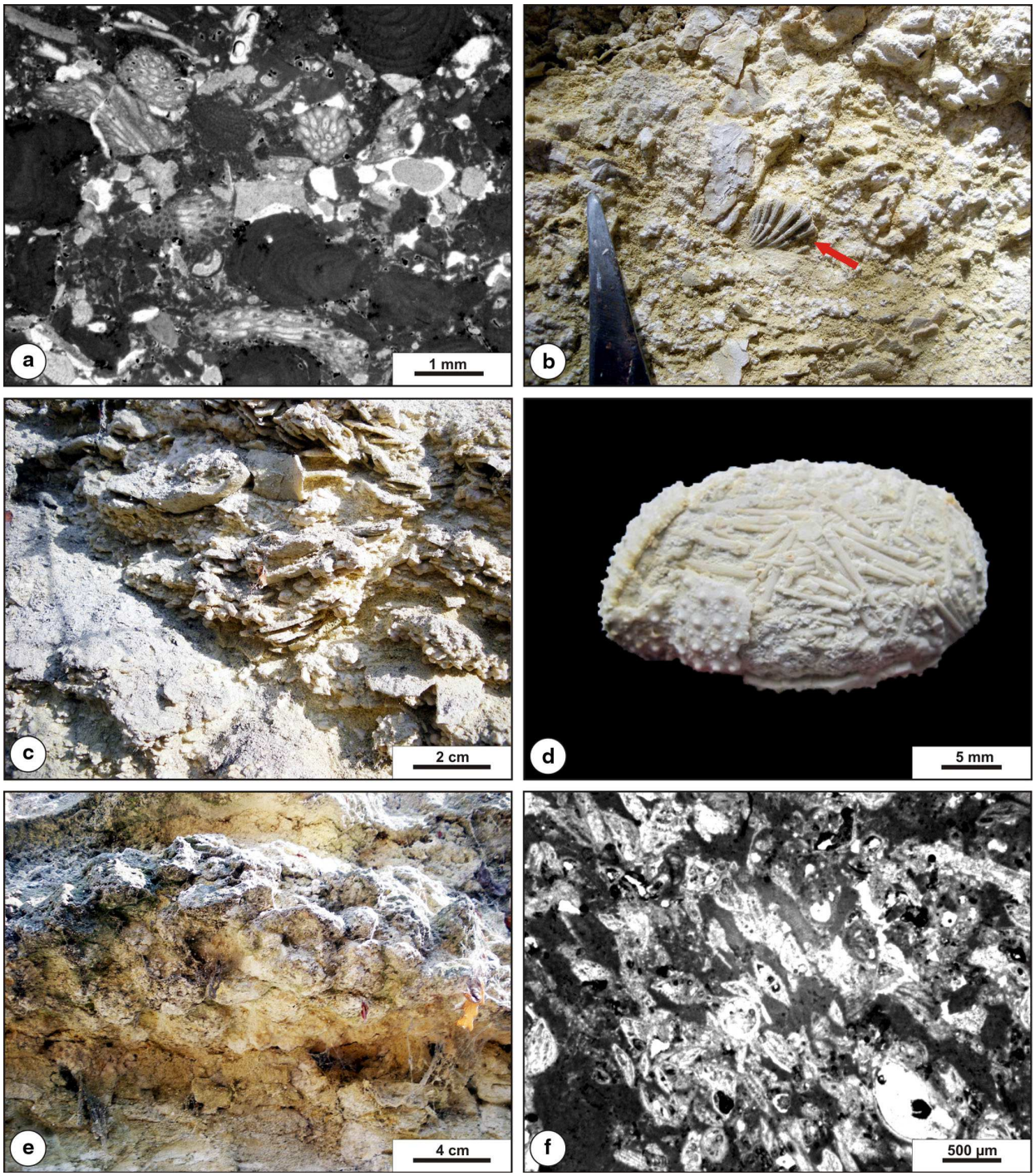

Fig. 4.7 a Bryozoan facies. Debris of celleporiform and branched bryozoans within a red algal packstone (section E, bed 7). **b** Bioclastic coralline algal-mollusc facies (section C, bed 3) with oyster remains and *Aequipecten elegans*. **c** Echinoid debris facies (section B, bed 4). Echinoid rudstone consisting of highly fragmented *Schizechinus* and *Stylocidaris* (Winden B, bed 3). **d** Echinoid facies. Corona of *Schizechinus hungaricus* filled with echinoid spines. **e** Rhodolith facies: Sphaeroidal-laminar rhodoliths (section C, bed 5). **f** *Asterigerinata-Elphidium* facies. *Asterigerinata* and *Elphidium* packstone (section B, bed 5).

4.6.5 Rhodolith facies

The rhodolith facies (Fig. 4.7e) is characterized by coralline algal rudstones containing many sphaeroidal laminar rhodoliths (∅ 2-4 cm) in section Winden A, as well as rhodolith rudstones (sections Winden B and C) of laminar subsphaeroidal rhodoliths (∅ 3-6 cm). Interspaces between rhodoliths are filled with red algal debris. The facies is associated with the bioclastic coralline algal-mollusc facies, the bryozoan facies and the *Asterigerinata-Elphidium* facies.

Interpretation - The facies is identical to the rhodolith facies of Wiedl et al. (2012) described from Mannersdorf. It is interpreted to reflect dynamic shallow waters 10-20 m in depth. The occurrence of rhodoliths (see discussion) within section C indicates that they accumulated in small depressions between dunes of corallinacean debris.

4.6.6 *Asterigerinata-Elphidium* facies

The *Asterigerinata-Elphidium* facies (Fig. 4.7f) is characterized by well preserved accumulations of the name-giving foraminifers within coralline algal rudstones, packstones, grainstones, and floatstones. Further foraminiferal taxa are represented by variable amounts of biserial textulariids and rare rotaliids (*Lobatula*, *Sphaerogypsina*, *Planostegina*), rare miliolids (*Borelis*, *Triloculina*?) and rare planktonic foraminifers (globigerinids). Mollusc remains (mainly pectinids and ostreids) play a minor role, as do serpulids, echinoids, and bryozoans. The facies is developed in all sections and dominates sections Winden C and D.

Interpretation - Recent *Elphidium* and *Asterigerinata* are free living on sand and vegetation (Murray 1991). Common occurrences of Recent *Lobatula lobatula* are typical of seagrass meadows in water depth down to 8 m (Mateu-Vicens et al. 2010). *Asterigerinata* as well as *Lobatula* are typical oxiphilic species (Holcová and Zágoršek 2008). Furthermore, *Asterigerinata* is adapted to high-energy waters with currents and tidal movements (Gonera 2012). The documented foraminiferal association is indicative of seagrass environments. Nevertheless, the rippled beds of section D rather point to high hydrodynamics and therefore to secondary accumulations of seagrass-derived organisms.

4.6.7 Clay facies

The clays of section Winden E are of grey to black colour. They are enriched with partly damaged tests of foraminifers. Common representatives (in alphabetical order) are *Asterigerinata planorbis*, *Cibicidoides* cf. *pseudoungerianus*, *Elphidium crispum*, *Elphidium fichtelianum* and *Lobatula lobatula*. Rare representatives are *Angulogerina* cf. *angulosa*, *?Biapertorbis biaperturatus*, *Cibicidoides* cf. *lopjanicus*, *Globocassidulina* cf. *globosa*, *Gyroidinoides*, *Lenticulina inornata*, *Melonis pompilioides*, *Spiroplectammina pectinata*, *Textularia* cf. *gramen,* and *Uvigerina*. The generally rare ostracods are represented by *Aurila* (*Euarila*) *punctata*, *Bairdoppilata*, *Carinocythereis carinata*, *Cnestocythere truncata*, *Cytheridea acuminata*, *Eucytherura textilis*, *Grinioneis haidingeri*, *Henryhowella asperrima*, *Leptocytheridae*, *Loxocorniculum hostatum*, *Paranesidea*, *Semicytherura* and *Xestoleberis*. Occasionally triaxone sponge spicula are present. Micromorphic brachiopods (*Megerlia*, *Agyrotheca*) are common. Macrofossils are represented by ostreid debris and entire shells of *Aequipecten elegans*, common echinoid debris (*Schizechinus hungaricus*, spatangoids and cidaroids) and rare celleporiform bryozoans.

Interpretation - The clay is interpreted as having been deposited in non-turbulent areas by segregation of different grain sizes. The foraminiferal assemblage is dominated by epifaunal forms such as the free-living *Elphidium*, *Asterigerinata,* and *Lobatula*, extant representatives of which are commonly attached to seagrass (Murray 1991; Langer 1993). The poorly preserved foraminiferal tests indicate abrasion due to transport. Also the documented micromorphic brachiopods indicate post-mortem transport. Fossil *Megerlia* preferred shallow waters in high-energy environments (Bitner and Martinell 2001 and references therein; Bitner and Moisette 2003), similar to *Agyrotheca* which settled in cryptic habitats of firm substrates of the infra- to circalittoral (Dulai 2007).

4.7 Discussion

4.7.1 Environmental interpretation

The *Asterigerinata-Elphidium* facies, the echinoid debris facies and the rhodolith facies are characterized by large-scale asymmetrical ripples in sections Winden B, C, and D. These facies types formed in current-dominated regimes where rhodoliths accumulated in small depressions of deposits composed of transported organisms. The echinoids originally dwelled in shallow subtidal environments and had been transported and concentrated by winnowing processes. The foraminiferal assemblages are indicative of seagrass meadows. The sediments in section Winden A, E, and W represent facies types (bryozoan facies, bioclastic coralline algal-mollusc facies, echinoid facies) which are widely missing in sections B, C, and D. Although these sediments have also been formed in current-driven regimes and also show post-mortem transport of organisms, the mollusc assemblages and bryozoans indicate slightly deeper environments along foresets and clinoforms.

The foresets of Winden A, E, and W sections (Figs. 4.4, 4.5) are composed of carbonate sands intercalated with clay or marl beds. Currents are the driving forces of the sedimentation regime. Sediments have been transported into deeper waters and the alternations of sands and clays or marls are very likely the result of current-driven segregation of different grain sizes. Similar brief reworking and re-sedimentation of material is also reported from Central Paratethyan deposits of Croatia (Vrsaljko et al. 2006; Martinuš et al. 2012). The measured bed orientations document a highly dynamic flow system where current directions differ strongly: north-west directed in section Winden E and to the south in Winden A. These differences can be attributed to local influences of bottom topography (e.g., of the dolomitic basement illustrated in Fig. 4.2b).

Large-scale asymmetric ripples, attaining heights of several decimetres, are developed in section Winden D (beds 2a-b). These ripples, called dunes or sand waves in the literature (Allen 1968), are formed in flow regimes with stream velocities of at least 0.8-2.8 m/s (Williams 1970) represented in, e.g., shallow tidal channels (Sternberg 1967) or surf zones of sandy coasts (Gallagher et al. 1998). Up-section, a shallowing is indicated by the occurrence of antidunes (Fig. 4.4c), characterized by inclined beds on the stoss side of the ripples. Antidunes are usually common bed forms of the upper flow regime, where standing and breaking waves of the water

surface are in phase with the bed forms; resistance to flow is low while sediment transport is large (Simons et al. 1965). The antidune forms migrate up-flow even though the sediment is moving with the flow (Davis 1992). Geometries at the base of bed 3 therefore indicate a migration to the SE (Fig. 4.4c). Rare but well preserved *Thalassinoides* burrows within the thin-bedded wave ripples in the uppermost part of section Winden D indicate their immediate infilling by mobile substrates (Wanless et al. 1988).

The Winden successions A, E, and W are characterized by clinoforms. Beds in Winden B and C are nearly horizontal but in Winden D large-scale asymmetrical and small-scale symmetrical ripples are developed. These geometries can be assigned to a classical depositional model (Fig. 4.8) consisting of clinothems and undathems (sensu Friedman et al. 1992). Thicknesses of the foresets range from ca. 0.2–1.6 m in section A and similarly from 0.1–1.3 m in section E where the limestones are separated by cm-thick marly beds or clays. While the dip angles of the beds are very constant in section A (Fig. 4.6), dip directions show a range between SSE and WSW. Dip angles of section E vary between 5 and 32° (Fig. 4.6) and dip directions change from NW to W and up-section turn back to NW.

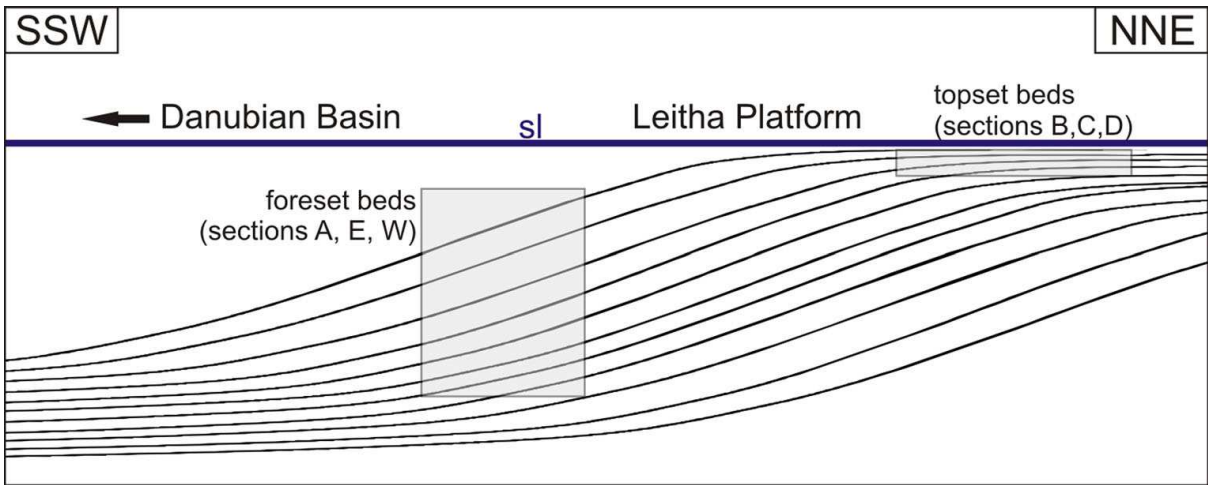

Fig. 4.8 Figure illustrating bed geometries as documented in the Winden sections. Topset beds are represented by sections Winden B-D, while sections A, E and W represent foresets. sl = sea level.

Foresets of Winden A can be seen as depositional equivalents to Winden W and E. Therefore, sections Winden A, E, and W are part of clinothems. Winden B, C, and D are interpreted as topset beds and parts of an undathem. Due to the short distances between sections A, B, C, and D (Fig. 4.2b) as well as between sections W and E, they are interpreted to be part of the same sedimentary body, respectively. This means that two sediment bodies are represented: sections Winden B, C and D

are the topset beds of the clinoforms of section Winden A and section Winden W represents the topset beds of the clinoforms of section Winden E.

4.7.2 Facial and stratigraphic distribution of sediments on the Leitha platform – a matter of tectonics

Middle Badenian sediments are exposed in altitudes up to 440 m (Kirchner quarry = Kürschnergrube) in the western part of the Leitha Mountains (Roth-Fuchs 1926; Bobies 1958; Decker 1996). Successions of the Kirchner quarry are represented by coral- and mollusc-rich limestones (Kittl 1882). Due to similarities in faunal content, they are interpreted as lateral equivalents of the middle Badenian successions at the Fenk and Müllendorf quarries (Bobies 1958), which are located at an altitude between ca. 300-390 m. They, in turn, are equivalents of middle Badenian coral-bearing successions of the Mannersdorf quarries situated at altitudes up to 310 m (Wiedl et al. 2013), to Stotzing (altitude up to 310 m), and the locality B15 (N 47°54'17.00", E 16°37'32.26") between Donnerskirchen and Hof am Leithagebirge (altitude: 240 m).

Late Badenian limestones, however, are not documented from the southwestern part of the Leitha Platform. Limestones of this age are exposed at altitudes of around 230-160 m in the northeast, at the southeast-facing slopes of the Leitha Mountains, while middle Badenian sediments are restricted to the southwest and crop out at an altitude of 440-240 m. These differences in elevations can be explained by vertical tectonics, which was already discussed by Tollmann (1955) and Bobies (1958). Additionally, the occurrence of Sarmatian limestones, covering middle Badenian limestones in the southwest (Wiedl et al. 2013) and upper Badenian limestones in the northeast (this study), indicates tectonic displacement during the late Badenian.

The distribution and elevation of middle and upper Badenian limestones (Fig. 4.9) shows that a N-S trending fault line between Sommerein and Donnerskirchen seems to be especially important for explaining the above mentioned differences. It separates the higher elevated middle Badenian limestone successions in the southwest from less elevated upper Badenian limestone successions in the northeast

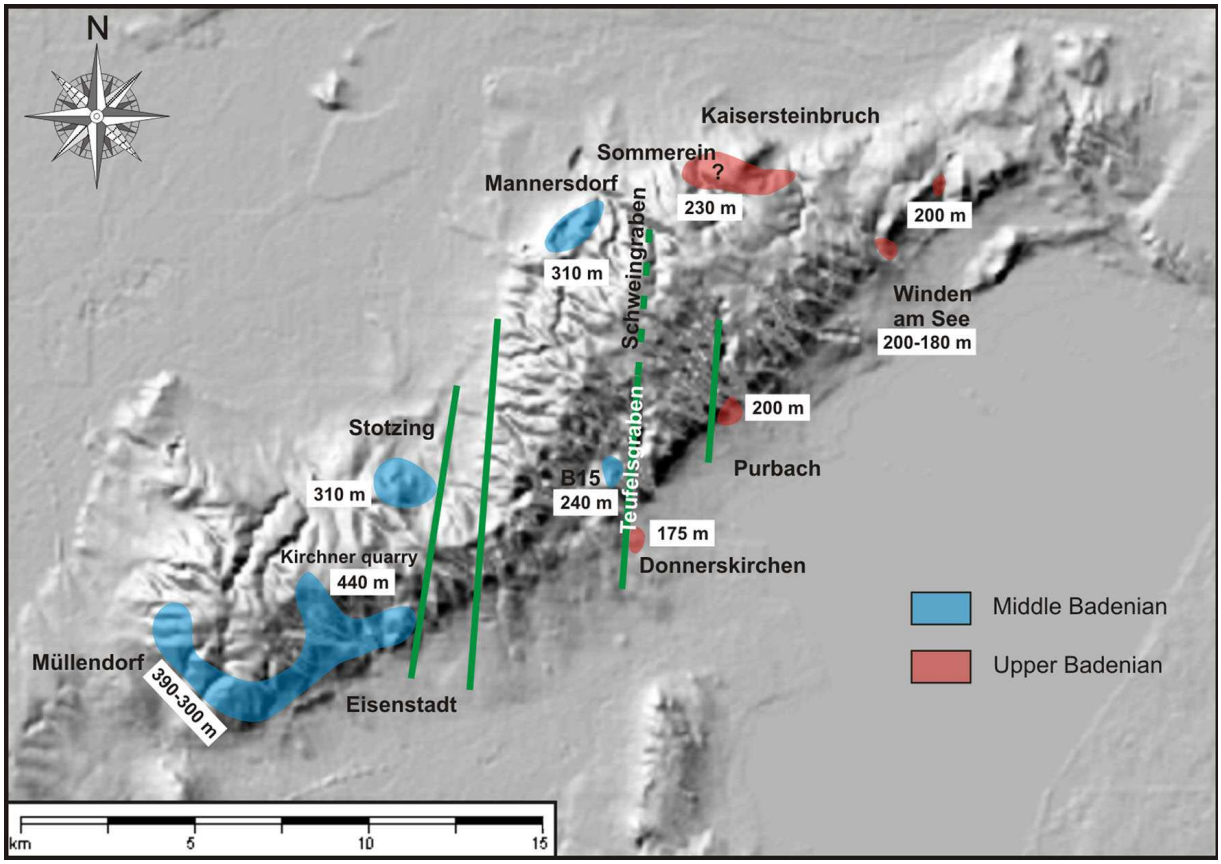

Fig. 4.9 Relief map of the Leitha Mountains including altitudes of outcrops. Blue: Middle Badenian (NN5). Red: Upper Badenian (NN6). Green lines indicate fault lineaments described by Buchroithner (1984). The stippled green line highlights a proposed continuation of one fault lineament.

(Fig. 4.9). A fault line for the Teufelsgraben valley at Donnerskirchen has already been proposed by Čžjžek (1852) and Buchroithner (1984). Therefore, the southern Schweingraben valley, dividing the Mannersdorf and Sommerein area in the north, is a likely candidate for the northward continuation of the Teufelsgraben fault (Fig. 4.9). Today's topography and the distribution of Badenian and Sarmatian sediments on the Leitha Platform very likely reflect a series of horst and graben structures from west to east caused by N-S trending faults (Fig. 4.9). Further lineaments and faults affecting the Leitha Mountains and adjacent areas have been demonstrated by Schmid (1962), Buchroithner (1984), Horváth et al. (2006), Székely et al. (2009), and Häusler et al. (2010).

4.7.3 Tectonic rearrangement of the Leitha Platform

The opening of the Mikulov Gate during the early Badenian, resulting from the sagging block of the Waschberg Zone, created a connection between the Vienna Basin and the Carpathian Foredeep and induced a flooding of the entire front of the tectonic nappes in this area (Brzobohatý and Stráník 2012). This change in marine pathways resulted in current-dominated regimes in the foreshore areas of the emerging Leitha Platform, which were characterized by heterogeneous environments of mixed siliciclastic and carbonate deposits (Kroh et al. 2003). The water energy apparently was reduced up to the climax of carbonate production during the middle Badenian when subtropical low-energy environments of predominantly biologically controlled sedimentation prevailed. These environments are documented by coral and mollusc associations in more than 20 facies types: They include in situ frame-building coral carpets and non-frame-building biostromal coral communities as well as in situ bivalves dwelling in seagrass meadows or burrowing bivalves in deeper environments, all sensitive to sediment disturbance (Riegl and Piller 2000, Wiedl et al. 2012, 2013).

During the middle Badenian, the Waschberg unit became uplifted and the marine connection between the Carpathian Foredeep and the Vienna Basin was shut down (Brzobohatý and Stráník 2012). At the same time, the Danube Basin started to form under rapid tectonic subsidence (Lankreijer et al. 1995; Kováč et al. 2007). These tectonic movements also affected the Leitha Platform as indicated in the facies pattern of the north-eastern part (Wiedl et al. 2012). The formation of the Danube Basin caused a major change in palaeogeography: south of the Leitha Platform a new seaway became established, fundamentally changing the carbonate factory from biologically determined to hydrodynamically guided. As a consequence facies types, completely different from middle Badenian ones, characterize the upper Badenian Leitha Platform. They indicate a predominantly hydrodynamically controlled depositional system represented by foresets, clinoforms as well as large-scale asymmetrical and small-scale symmetrical ripples. Faunal depletion as well as low variability in upper Badenian facies types is very likely the result of this hydrodynamic change which prevented organism groups sensitive to sediment disturbance to settle.

4.8 Conclusions

The study presents upper Badenian limestone successions of the Leitha Platform, which separates the southern Vienna Basin from the Danube Basin. The successions are part of a coralline algal dominated carbonate platform consisting of clinothems and undathems. Seven facies types, i.e., the bryozoan, the bioclastic algal-mollusc, the echinoid debris, the echinoid, the rhodolith, the *Asterigerinata-Elphidium*, and the clay facies have been documented for the six sections studied. The sedimentary textures show that current-driven transport was the driving force in the formation of foresets consisting of carbonate sands and clays. Current-induced flows transported of large quantities of echinoid tests and formed clinoforms as well as large-scale asymmetrical and small-scale symmetrical ripples. Tectonic activity controlled the distribution of Badenian and Sarmatian limestones on the platform. While middle Badenian limestones are found, at present day, in higher altitudes in the southwestern part of the platform, late Badenian limestones are restricted to lower altitudes in the northeastern part. Different elevation patterns are due to vertical tectonics affecting the Leitha Mountains. Changes in hydrodynamics on the Leitha Platform, which allow insights in lower, middle and upper Badenian environments, can be explained by changing seaways and currents. The development of the platform started with mixed siliciclastic and carbonate systems in the early Badenian, influenced by strong currents which were induced by a new seaway connection between the Vienna Basin and the Carpathian Foredeep. During the middle Badenian, at the climax of carbonate production, the area was characterized by subtropical low-energy environments of predominantly biologically controlled sedimentation with a differentiation into multiple facies types. A transition from middle Badenian low energy environments towards upper Badenian high energy environments is directly linked to the formation of the Danube Basin, initiating a new seaway to the southeast. These changes in basin morphology and currents caused a transition to a hydrodynamically influenced system in the upper Badenian and a depletion of facies types.

4.9. Acknowledgements

Special thanks go to Gerhard Wanzenböck (Bad Vöslau) for insights into, and photographs of, his amazing collection of fossils and his precise information on their provenience. Many thanks go to Oleg Mandic (Natural History Museum Vienna) for determination of pectinids, Martin Groß (Universalmuseum Joanneum Graz) for determination of ostracods, Patrick Grunert (University of Graz) for determination of foraminifers, and to Markus Reuter (University of Graz) and Ulrike Exner (University of Vienna) for constructive discussions. The manuscript benefited from the constructive comments of the reviewers Wolf-Christian Dullo (GEOMAR Helmholtz Centre for Ocean Research Kiel) and James Nebelsick (University of Tübingen), and from the editorial advice of Franz Theodor Fürsich (University of Erlangen-Nürnberg).

4.10 References

Allen JRL (1968) Current ripples: their relation to patterns of water and sediment motion. North-Holland Publishing Co., Amsterdam

Backman J, Raffi I, Rio D, Fornaciari E, Pälike H (2012) Biozonation and biochronology of Miocene through Pleistocene calcareous nannofossils from low and middle latitudes. Newsl Stratigr 45:221–244

Belaústegui Z, Nebelsick JH, De Gibert JM, Domènech R, Martinell J (2012) A taphonomic approach to the genetic interpretation of clypeasteroid accumulations from Tarragona (Miocene, NE Spain). Lethaia 45:548–565

Bitner MA, Martinell J (2001) Pliocene brachiopods from the Estepona area (Málaga, South Spain). Rev. Españ Paleont 16:177-185

Bitner MA, Moissette P (2003) Pliocene brachiopods from north-western Africa. Geodiversitas 25:463-479

Bobies CA (1958) Über die Pedalion-Korallenfazies im Wiener und Eisenstädter Becken. Verh Geol B A 1:38–44

Brzobohatý R, Stráník Z (2012) Paleogeography of the Early Badenian connection between the Vienna Basin and the Carpathian Foredeep. Cent Euro J Geosci 4:126–137

Buchroithner MF (1984) Karte der Landsat-Bildlineamente von Österreich 1:500000. Geologische Bundesanstalt Wien

Csontos L, Vörös A (2004) Mesozoic plate tectonic reconstruction of the Carpathian region. Palaeogeogr Palaeoclimatol Palaeoecol 210:1–56

Čžjžek J (1852) Geologische Verhältnisse der Umgebungen von Hainburg, des Leithagebirges und der Ruster Berge. Jahrb kk Geol Reichsanst 3/4:35–55

Davis RA (1992) Depositional systems: An introduction to sedimentology and stratigraphy. Sedond edition. Prentice Hall, Englewood Cliffs, New Jersey

Decker K (1996) Miocene tectonics at the Alpine-Carpathian junction and the evolution of the Vienna basin. Mitt Ges Geol Bergbaustud Österr 41:33–44

Decker K, Peresson H (1996) Tertiary kinematics in the Alpine-Carpathian-Pannonian system: links between thrusting, transform faulting and crustal extension. In: Wessely G, Liebl W (eds) Oil and gas in Alpidic thrusts and basins of Central and Eastern Europe. Eur Assoc Geosci Eng Spec Publ 5:69–77

Dulai A (2007) Badenian (Middle Miocene) micromorphic brachiopods from Bánd and Devecser (Bakony Mountains, Hungary). Fragm Palaeont Hung 24-25:1–13

Dullo WC (1983) Diagenesis of fossils of the Miocene Leitha Limestone of the Paratethys, Austria: An example for faunal modifications due to changing diagenetic environments. Facies 8:1–112

Dunham RJ (1962) Classification of carbonate rocks according to their depositional texture. In: Ham WE (ed) Classification of carbonate rocks–a symposium. Am Assoc Petrol Geol Mem 1:108–121

Embry AF, Klovan JE (1971) A late Devonian reef tract on Northeastern Banks Island, NWT. Can Petrol Geol Bull 19:730–781

Fodor L (1995) From transpression to transtension: Oligocene- Miocene structural evolution of the Vienna basin and the East Alpine-Western Carpathian junction. Tectonophysics 242:151–182

Fornaciari E, Di Stefano A, Rio D, Negri A (1996) Middle Miocene quantitative calcareous nannofossil biostratigraphy in the Mediterranean region. Micropaleontology. 42:37–63

Friedman GM, Sanders JE, Kopaska-Merkel DC (1992) Principles of sedimentary deposits, Macmillan, New York

Fuchs T (1894) Ueber abgerollte Blöcke von Nulliporen-Kalk im Nulliporen-Kalk von Kaisersteinbruch. Z Deutsch Geol Ges 46:126–130

Fuchs T (1902) Über Anzeichen einer Erosionsepoche zwischen Leythakalk und sarmatischen Schichten. Sitzungsber Wiener Akad Wiss math-nat Kl CXI:351–355

Gallagher EL, Elgar S, Thornton EB (1998) Megaripple migration in a natural surf zone. Nature 394:165–168.

Gonera M (2012) Palaeoecology of the Middle Miocene foraminifera of the Nowy Sącz Basin (Polish Outer Carpathians). Geol Quart 56:107–116

Götzinger G (1916) Geologische Beobachtungen im Miocän des nordöstlichen Leithagebirges. Verh KK Geol Reichsanst 9:197–206

Harzhauser M, Piller WE (2010) Molluscs as a major part of subtropical shallow-water carbonate production – an example from a Middle Miocene oolite shoal (Upper Serravallian, Austria). In: Mutti M, Piller WE, Betzler C (eds) Carbonate systems during the Oligo-Miocene climatic transition: Int Assoc Sediment Spec Publ, Wiley-Blackwell, vol 42. pp 185–200

Häusler H (2007) Geologische Karte der Republik Österreich 1:50.000. Erläuterungen zu den Blättern 79 Neusiedl am See, 80 Ungarisch-Altenburg und 109 Pamhagen. Geologische Bundesanstalt, Wien

Häusler H, Figdor H, Hammerl C, Kohlbeck F, Lenhardt W, Schuster R (2010) Geologische Karte der Republik Österreich 1:50000. Erläuterungen zur Geologischen Karte 78 Rust. Geologische Bundesanstalt, Wien

Herrmann P (1973) Geologie der Umgebung des östlichen Leithagebirges (Burgenland). Mitt Ges Geol Bergbaustud 22:165–189

Herrmann P, Pascher G, Pistotnik J (1993) Geologische Karte der Republik Österreich 1:50.000, 78 Rust. Geologische Bundesanstalt, Wien

Hohenegger J, Ćorić S, Wagreich M (2014) Timing of the Middle Miocene Badenian Stage of the Central Paratethys. Geol Carpath 65:55–66

Hohenegger J, Wagreich M (2012) Time calibration of sedimentary sections based on isolation cycles using combined cross-correlation: dating the gone Badenian stratotype (Middle Miocene, Paratethys, Vienna Basin, Austria) as an example. Int J Earth Sci (Geol Rundsch) 101:339–349

Holcová K, Zágoršek K (2008) Bryozoa, foraminifera and calcareous nannoplankton as environmental proxies of the “bryozoan event” in the Middle Miocene of the Central Paratethys (Czech Republic). Palaeogeogr Palaeoclimatol Palaeoecol 267:216–234

Horváth F (1995) Phases of compression during the evolution of the Pannonian Basin and its bearing on hydrocarbon exploration. Mar Petrol Geol 12:837–844

Horváth F, Bada G, Windhoffer G, Csontos L, Dombrádi E, Dövényi P, Fodor L, Grenerczy, G, Síkhegyi F, Szafián P, Székely B, Timár G, Tóth L, Tóth T (2006) Atlas of the present-day geodynamics of the Pannonian basin: Euroconform maps with explanatory text [A Pannon-medence jelenkori geodinamikájának atlasza: Euro-konform térképsorozat és magyarázó]. Magyar Geofiz 47:133–137

Horváth F, Cloetingh S (1996) Stress-induced late-stage subsidence anomalies in the Pannonian basin. Tectonophysics 266:287–300

Huismans RS, Podladchikov YY, Cloetingh S (2001) Dynamic modeling of the transition from passive to active rifting, application to the Pannonian basin. Tectonics 20:1021–1039

Jiříček R, Riha J (1991) Correlation of ostracod zones in the Paratethys and Tethys. Saito Hoon Kai Spec Publ 3:435–457

Karrer F, Fuchs T (1868) Geologische Studien in den Tertärbildungen des Wiener Beckens. Jahrb KK Geol RA 18:269–286

Kittl E (1882) Geologische Beobachtungen im Leithagebirge. Verh kk Geol Reichsanst 15/16:292–300

Kováč M (2000) Geodynamický, paleogeografický a štruktúrny vývoj karpatsko - panónskeho regiónu v miocéne: nový pohlad na neogénne panvy Slovenska. VEDA, Bratislava

Kováč M, Andreyeva-Grigorovich A, Bajraktarević Z, Brzobohaty R, Filipescu S, Fodor L, Harzhauser M, Nagymarosy A, Oszczypko N, Pavelić D, Rögl F, Saftić B, Sliva L, Studencka B (2007): Badenian evolution of the Central Paratethys Sea: palaeogeography, climate and eustatic sea level changes. Geol Carpath 58:579–606

Kováč M, Holcová K, Nagymarosy A (1999) Paleogeography, paleobathymetry and relative sea-level changes in the Danube Basin and adjacent areas. Geol Carpath 50:325–338

Kováč M, Nagymarosy A, Soták J, Šutovská K (1993) Late Tertiary paleogeographic evolution of the Western Carpathians. Tectonophysics 226:401–416

Kroh A, Harzhauser M, Piller WE, Rögl F (2003) The Lower Badenian (Middle Miocene) Hartl Formation (Eisenstadt - Sopron Basin, Austria). In: Piller WE (ed) Stratigraphia Austriaca. Österreichische Akademie der Wissenschaften, Schriftenreihe Erdwissenschaftliche Kommissionen, Vienna, pp 87–109

Kroh A, Nebelsick JH (2010) Echinoderms and Oligo-Miocene carbonate systems: potential applications in sedimentology and environmental reconstruction. In: Mutti M, Piller WE, Betzler C (eds) Carbonate systems during the Oligo-Miocene climatic transition: Int Assoc Sediment Spec Publ, Wiley-Blackwell, vol 42. pp 201–228

Langer MR (1993) Epiphytic foraminifera. In: Langer MR (ed) Foraminiferal microhabitats. Mar Micropaleontol 20:235–265

Lankreijer A, Kováč M, Cloetingh S, Pitonak P, Hloska M, Biermann C (1995) Quantitative subsidence analysis and forward modelling of the Vienna and Danube basins: thin-skinned versus thick-skinned extension. Tectonophysics 252:433–451

Lirer F, Harzhauser M, Pelosi N, Piller WE, Schmid HP, Sprovieri M (2009) Astronomically forced teleconnection between Paratethyan and Mediterranean

sediments during the Middle and Late Miocene. Palaeogeogr Palaeoclimatol Palaeoecol 275:1–13

Mancosu A, Nebelsick JH (2013) Multiple routes to mass accumulations of clypeasteroid echinoids: a comparative analysis of Miocene echinoid beds of Sardinia. Palaeogeogr Palaeoclimatol Palaeoecol 374:173–186

Mandic O (2004) Pectinid bivalves from the Grund Formation (Lower Badenian, Middle Miocene, Alpine-Carpathian Foredeep) taxonomic revision and stratigraphic significance. Geol Carpath 55:129–146

Martini E (1971) Standard Tertiary and Quaternary calcareous nannoplankton zonation. In: Farinacci A (ed) Proceedings of the second plankton conference, Rome, 1970, pp 739–785

Martinuš M, Fio K, Pikelj K, Aščić Š (2012) Middle Miocene warm-temperate carbonates of Central Paratethys (Mt. Zrinska Gora, Croatia): paleoenvironmental reconstruction based on bryozoans, coralline red algae, foraminifera, and calcareous nannoplankton. Facies 59: 481–504

Mateu-Vicens G, Box A, Deudero S, Rodríguez B (2010) Comparative analysis of epiphytic foraminifera in sediments colonized by seagrass *Posidonia ocenaica* and invasive macroalgae *Caulerpa* spp. J Foram Res 40:134–147

Mattick RE, Teleki PG, Phillips RL, Clayton JL, Dávid G, Pogácsás G, Bardócz B, Simon E (1996) Structure, stratigraphy and petroleum geology of the Little Hungarian Basin, northwestern Hungary. AAPG Bull 80:1780–1800

Meulenkamp JE, Kováč M, Cicha I (1996) On Late Oligocene to Pliocene depocentre migrations and the evolution of the Carpathian–Pannonian system. Tectonophysics 266:310–317

Moffat HA, Bottjer DJ (1999) Echinoid concentration beds: Two examples from the stratigraphic spectrum: Palaeogeogr Palaeoclimatol Palaeoecol 149:329–348

Murray JW (1991) Ecology and palaeoecology of benthic foraminifera. Longman Scientific and Technical, Harlow

Piller WE, Decker K, Haas M (1996) Sedimentologie und Beckendynamik des Wiener Beckens: Sediment 96. 11. Sedimentologentreffen, Excursion guide, Geologische Bundesanstalt, Wien

Piller WE, Harzhauser M, Mandic O (2007) Miocene Central Paratethys stratigraphy – current status and future directions. Stratigraphy 4:151–168

Piller WE, Vavra N (1991) Das Tertiär im Wiener und Eisenstädter Becken. In: Roetzel R, Nagel N (eds), Exkursionen im Tertiär Österreichs, Molassezone – Waschbergzone – Korneuburger Becken – Wiener Becken – Eisenstädter Becken. Österreichische Paläontologische Gesellschaft, Wien, pp 161–216

Ratschbacher L, Behrmann JH, Pahr A (1990) Penninic windows at the eastern end of the Alps and their relation to the intra-Carpathian basins. Tectonophysics 172:91–105

Ratschbacher L, Frisch W, Linzer HG, Merle O (1991) Lateral extrusion in the Eastern Alps. Tectonics 10:257–271

Riedl R (1983) Fauna und Flora des Mittelmeeres. Verlag Paul Parey, Hamburg

Riegl B, Piller WE (2000) Biostromal coral facies – a Miocene example from the Leitha Limestone (Austria) and its actualistic interpretation. Palaios 15:399–413

Rohatsch A (1996) Ökologische Aspekte bei Foraminiferenfaunen der kalkigen Randfazies des Wiener Beckens. Mitt Ges Geol Bergbaustud Österr 39/40:55–63

Roth-Fuchs G (1926). Erklärende Beschreibung der Formen des Leithagebirges. Geograph Jb Österreich 13:29–106

Schaffer FX (1908) Geologischer Führer für Exkursionen im Inneralpinen Wienerbecken II. Teil. Sammlung geologischer Führer 13, Borntraeger, Berlin

Schmid H (1962) Das Jungtertiär an der Südostseite des Leithagebirges (zwischen Eisenstadt und Breitenbrunn). Unpubl PhD thesis, Wien

Schmid HP, Harzhauser M, Kroh A (2001) Hypoxic events on a Middle Miocene carbonate platform of the Central Paratethys (Austria, Badenian, 14 Ma). Ann Naturhist Mus Wien 102(A):1–50

Simons DB, Richardson EV, Nordin CF (1965) Sedimentary structures generated by flow in alluvial channels. In: Middleton GV (ed) Primary sedimentary structures and their hydrodynamic interpretation. SEPM Spec Publ 12:34–52

Steininger F, Papp A (1978) Faziostratotypus: Gross Höflein NNW, Steinbruch “Fenk”, Burgenland, Österreich. In: Papp A, Cicha I, Seneš J, Steininger FF (eds) M4–Badenien (Moravien, Wielicien, Kosovien). Chronostratigraphie und Neostratotypen. Miozän der Zentralen Paratethys. Slowakische Akademie der Wissenschaften, Bratislava, pp 194–203

Sternberg RW (1967) Measurements of sediment movement and ripple migration in a shallow marine environment. Mar Geol 5:195–205

Studencka B (1999) Remarks on Miocene bivalve zonation in the Polish part of the Carpathian Foredeep. Geol Quat 43: 467–477

Székely B, Zámolyi A, Draganits E, Briese C (2009) Geomorphic expression of neotectonic activity in a low relief area in an Airborne Laser Scanning DTM: a case study of the Little Hungarian Plain (Pannonian basin). Tectonophysics 474:353–366

Tollmann A (1955) Das Neogen am Nordwestrand der Eisenstädter Bucht. Wiss Arb Burgenld 10:1–74.

Van Balen RT, Cloetingh S (1995) Neural network analyses of stress-induced overpressures in the Pannonian Basin. Geophys J Int 121:532–544

Vrsaljko D, Pavelić D, Miknić M, Brkić M, Kovačić M, Hećimović I, Hajek-Tadesse V, Avanić R, Kurtanjek N (2006) Middle Miocene (Upper Badenian/Sarmatian) palaeoecology and evolution of the environments in the area of Medvednica Mt. (North Croatia). Geol Croat 59:51–63

Wanless HR, Tedesco LP, Tyrell KM (1988) Production of subtidal tubular and surficial tempestites by Hurricane Kate, Caicos Platform, British West Indies. J Sediment Petrol 58:739–750

Wiedl T, Harzhauser M, Piller WE (2012) Facies and synsedimentary tectonics on a Badenian carbonate platform in the southern Vienna Basin (Austria, Central Paratethys). Facies 58:523–548

Wiedl T, Harzhauser M, Kroh A, Ćorić S, Piller WE (2013) Ecospace variability along a carbonate platform at the northern boundary of the Miocene reef belt (Upper Langhian, Austria). Palaeogeogr Palaeoclimatol Palaeoecol 370:232–246

Williams GE (1970) The central Australian stream floods of February-March 1967. J Hydrol 11:185–200

Woelkerling WJ, Irvine LM, Harvey AS (1993) Growth-forms in non-geniculate coralline red algae (Corallinales, Rhodophyta). Aust Syst Bot 6:277–293

Chapter V

The Leitha Mountains carbonate platform – a recorder for transitions of biologically controlled carbonate production to hydrodynamically controlled environments - a synopsis

5.1 Synopsis

This chapter summarizes the results of facies analysis and stratigraphy of various localities of the middle (upper Langhian) und upper Badenian (lower Serravallian) Leitha Platform in the southern Vienna Basin. The study was focused on sediments of a coralline algal dominated carbonate platform exposed close to Mannersdorf in Lower Austria (chapter II), Müllendorf (chapter III) and Winden (chapter IV) in Burgenland. Based on lithological and palaeontological characters, more than 20 facies types have been distinguished. Most of these facies types are dominated by red algal debris but show different kinds of organism groups as for instance corals, molluscs or echinoids.

The middle Badenian sedimentary succession of the Mannersdorf quarries (**chapter II)** shows that influences of sea-level fluctuations and tectonics caused changes from fluvial siliciclastic to marine carbonatic environments. The Mannersdorf quarries preserve records of pre-, syn- and post-tectonic phases of sediment deposition. The pre-tectonic phase is represented by the flooding of a Mesozoic coastal cliff of dolostone, which is overlain by a breccia of the same material. It is followed by a progradation of a Gilbert-type fan delta represented by cross-bedded gravels derived from Lower Austroalpine units. The overlying corallinacean limestones reveal a continuous increase in water depth by vertical transition from *Acervulina* and rhodolith bearing facies to a facies containing the deep burrowing bivalve *Pholadomya*. These deposits indicate a calm sublittoral depositional environment and the deepest settings of the Leitha platform represented in the Mannersdorf quarries. A subsequent falling relative sea-level is indicated by a shallowing-upward trend expressed in facies types deposited in relatively shallower marine settings. Subsequently, a normal fault reactivated as a dextral strike-slip fault, divided the area into two tectonic blocks. This syn-tectonic phase corresponds with a relative sea-level fall and the development of shallow water facies containing corals which are restricted to very shallow subtidal soft- or firmgrounds and subsequent partial erosion

of the northeastern block. Instead, on the southwestern subsiding block, sediment deposition kept up in a very shallow setting. The sea-level fall is visible in the development of a shallow water facies containing in situ specimens of the bivalve *Pinna* and other associated molluscs indicating a habitat represented by seagrass meadows. A post-tectonic phase with renewed marine transgression and onlapping of deeper water carbonates on the basement is indicated by the burial of the fault and a filling of a jointset acting as a neptunian dyke.

The coralline algal limestones of the Müllendorf quarries (**chapter III**), which are situated at the southwestern part of the platform, developed approximately at the same time as the limestones of the Mannersdorf quarries. Contrary to the Mannersdorf successions, recurrent coral and mollusc biostromes, indicative for shallow subtidal tropical environments, are a main characteristic of the Müllendorf successions. These coral associations, which occur repeatedly throughout the successions, indicate persistence in ecological parameters within the ecospace as temperature, sea-water chemistry or light. Nevertheless, the formation of the seven lithofacies types in Müllendorf was modulated by ecological parameter changes. For instance, increased water turbidity as a single parameter change causes replacement of corals by the oyster *Hyotissa*, which is adapted to high suspension load and nutrients. A change in two parameters, increased water turbidity and depth, causes the transition to deposits with common shallow burrowing molluscs and finally common bryozoans in relatively deeper settings. In Müllendorf, water turbidity (determined by raised nutrients and/or terrigenics) acted as strongest modulating factor (ecological master factor) in community expression, followed by influences of water depth regulated by low-amplitude sea-level fluctuations and indicated in cyclic sedimentary patterns.

Time-equivalent deposits to Müllendorf are exposed at the close-by Fenk quarry. Both limestone successions show similar facies successions and are situated at the same topographic level. The terrigenous sand facies of Müllendorf, interpreted as the onset of a transgressive pulse after a relative sea-level lowstand, could be a time-equivalent development to marly layers of the Fenk quarry. In addition, a contemporaneous formation of coral-rich horizons is very likely. Former stratigraphic correlations between both localities were based on foraminiferal communities (Papp and Turnovsky 1953, Tollmann 1955). In this study, a dating of sediments of the Müllendorf quarry is based on calcareous nannoplankton from a marly layer of the

Fenk quarry, which shows an affiliation to the Upper Lagenidae and *Spiroplectammina* zones and therefore a middle Badenian age of the limestones.

During the Langhian, the Leitha Platform was situated at the northern edge of the Peri-Mediterranean reef belt in the Central Paratethys, where coral reefs (s.s.) and non-reefal coral communities coexisted in the same ecospace while in closeby regions to the north only non-reefal coral communities existed. In summary, the sedimentary record of Müllendorf and Mannersdorf indicates stable climatic conditions during the observed time interval and goes along with the mid-Miocene climatic optimum (Harzhauser and Piller 2007).

During early Serravallian (late Badenian) time the sedimentary regime on the Leitha Platform showed different patterns than during the late Langhian (middle Badenian) **(chapter IV)**. The sedimentary environment, represented by limestone - clay or - marl successions close to the village Winden am See in Burgenland, shows a coralline algal dominated carbonate platform with sigmoid clinoforms, dunes and wave ripples. Currents had been the driving forces of the sedimentation regime where alternations of sands, clays and marls are very likely the result of current-driven segregation of different grain sizes. The measured bed orientations document a highly dynamic flow system and differences in current directions can be attributed to local influences of bottom topography. Its foresets had been formed by storm induced current driven short-period reworking and subsequent segregation of sediments. The geometries of these beds can be assigned to a classical depositional model consisting of clinothems and undathems. The topset beds of the Winden successions show instead large-scale asymmetric ripples (synonymously used terms are dunes or sand waves), attaining heights of several decimetres. They have been formed in shallow tidal channels or surf zones of sandy coasts. Up-section, antidunes indicate a shallowing upwards and wave ripples are found at the top of the successions, representing the shallowest setting.

Seven distinct facies types document the hydrodynamically controlled sedimentation. The current regime is reflected in a strongly reduced diversity of facies and biota, contrary to the older facies-rich middle Badenian sediments, where currents played a minor role in deposition. Sediment transport, however, caused secondary mass occurrences of echinoids or foraminifers derived from seagrass meadows.

A change in hydrodynamics on the Leitha Platform with a transition from Langhian low-energy environments towards Serravallian high-energy environments is directly

linked to the formation of the Danube Basin. It initiated a new seaway connection to the Vienna Basin within the Pannonian Basin and therefore changed the local current system. This tectonically induced transition from biologically to hydrodynamically controlled sedimentation led to reduction in diversity of facies and biota on the Leitha Platform.

5.2 References

Harzhauser M, Piller WE (2007) Benchmark data of a changing sea – Palaeogeography, palaeobiogeography and events in the Central Paratethys during the Miocene. Palaeogeogr Palaeoclimatol Palaeoecol 253:8–31

Papp, A., Turnovsky, K., 1953. Die Entwicklung der Uvigerinen im Vindobon (Helvet und Torton) des Wiener Beckens. Jahrbuch Der Geologischen Bundesanstalt 46, 117–141.

Tollmann, A., 1955. Das Neogen am Nordwestrand der Eisenstädter Bucht. Wissenschaftliche Arbeiten aus dem Burgenland 10, 1–74.